MONASH University

CLINICAL INDICATIONS FOR 4D-PET/CT IN LUNG CANCER DIAGNOSIS AND RADIATION THERAPY

Jason Callahan

BAppSci Medical Radiations (Nuclear Medicine)

A thesis submitted for the degree of Doctor of Philosophy at Monash University

Faculty of Medicine, Nursing and Health Sciences

2016

Copyright notice

© The author (2015). Except as provided in the Copyright Act 1968, this thesis may not be reproduced in any form without the written permission of the author.

I CERTIFY THAT I HAVE MADE ALL REASONABLE EFFORTS TO SECURE COPYRIGHT PERMISSIONS FOR THIRD-PARTY CONTENT INCLUDED IN THIS THESIS AND HAVE NOT KNOWINGLY ADDED COPYRIGHT CONTENT TO MY WORK WITHOUT THE OWNER'S PERMISSION.

TABLE OF CONTENTS

ABSTRACT

Over the past decade PET/CT scanning has become an invaluable tool in the evaluation of many oncologic processes. A lesion seen on a PET scan will become blurred if affected by respiratory motion, an effect similar to that created when a person moves while a photograph is taken with a slow shutter speed in low-light conditions. The compounding effects of blurring and mis-registration in whole body PET/CT imaging make accurate characterization of disease in areas of high respiratory motion challenging. A scanning technique known as respiratory gated or 4D-PET/CT scanning is a tool that can control for the effects for respiratory motion. This thesis comprises of a series of studies investigating the clinical application of 4D-PET/CT in lung cancer diagnosis and therapy.

This thesis begins by presenting a review of the literature in chapter two. This chapter is a published review of the literature, performed by the candidate, which encompasses the literature up until the commencement of this thesis. The review is then updated in the second part of chapter two which reports on the progress of 4D-PET/CT in the literature during the preparation of this thesis.

The first stage in the management of lung cancer is a correct diagnosis. The study presented in chapter three investigates the added value of 4D-PET/CT in correctly classifying a lung nodule as either benign of malignant. In a series of 20 patients it was found that an additional 4D-PET/CT scan only influenced the final diagnosis

when the standard whole body scan was of indeterminate aetiology. These results show that use of 4D-PET/CT scanning isn't necessary in every case but that it can be a valuable tool to aid in the timely diagnosis of lung cancer for indeterminate nodules.

The use of 4D-PET/CT scanning in the treatment of known lung cancer is covered in chapters four and five. A malignant lung lesion that is unable to be resected is most likely to be treated with a course of radical radiation therapy. This involves the delivery of a prescribed dose of radiation to a target volume defined on imaging. The delineation of internal target volumes (ITV) in radiotherapy of lung tumours is currently performed using either a free-breathing (FB) FDG-PET/CT or a 4D-CT maximum intensity projection (MIP). In chapter four of this thesis I present our validation of a 4D-PET-MIP, equivalent to a 4D-CT-MIP, for the delineation of target volumes in both a phantom and in patients. In the study comparing 4D-PET and CT MIPs we were able to confirm that a 4D-PET-MIP produces volumes with high concordance with 4D-CT-MIP across multiple breathing patterns and lesion sizes in both a phantom and among patients. This can be achieved without the additional radiation exposure for a separate planning 4D-CT scan.

Chapter five presents our study analysing the consequences of only using 3D-PET/CT for target volume delineation. The purpose was to investigate geographic miss of lung tumours due to respiratory motion for target volumes defined on a standard 3D-PET/CT scan when compared to target volumes defined on a 4D-PET/CT scan. In this study it was found that without any form of motion suppression the current

standard of a 3D- PET/CT and 15mm PTV margin employed for lung lesions has an increasing risk of significant geographic miss in particular when tumour motion increases.

Chapter six presents our study investigating the effects of respiratory motion on VQ-PET/CT scanning and determine if 4D imaging will improve co-registration between PET and CT modalities enabling more accurate ability to quantify regional lung function to allow monitoring of the effect of radiation therapy on the normal lung. In this study we were able to show for the first time that ^{68}Ga-VQ 4D PET/CT is feasible and the blurring caused by respiratory motion is well corrected with 4D acquisition.

The results presented in this thesis show that 4D-PET/CT can have a clinical impact on the management of patients with lung cancer from the point of diagnosis to their treatment and the monitoring of the effects of radiation therapy. The use of 4D-PET/CT is now establishing itself as routine clinical tool that will likely improve outcomes for patient with highly mobile lung tumours.

GENERAL DECLARATION

I hereby declare that this thesis contains no material which has been accepted for the award of any other degree or diploma at any university or equivalent institution and that, to the best of my knowledge and belief, this thesis contains no material previously published or written by another person, except where due reference is made in the text of the thesis.

This thesis includes 5 original papers published in peer reviewed journals. The core theme of the thesis is clinical indications for 4D-PET/CT in lung cancer diagnosis and radiation therapy. The ideas, development and writing up of all the papers in the thesis were the principal responsibility of myself, the candidate, working within the Faculty of Medicine, Nursing and Health Sciences, Monash University under the supervision of A/Prof Michal Schneider, and at the Peter MacCallum Cancer Centre under the supervision of Prof Tomas Kron and Prof Rodney Hicks.

In the case of chapters 2, 3, 4, 5 and 6 my contribution to the work involved the following:

Thesis chapter	Publication title	Publication status*	Nature and extent (%) of students contribution
2	The clinical significance and management of lesion motion due to respiration during PET/CT scanning.	published	80% of concept and 90% of manuscript writing
3	A prospective investigation into the clinical impact of 4D-PET/CT in the characterisation of solitary pulmonary nodules	published	90% of concept, design, data interpretation and manuscript writing, 100% of study conduct, data generation and data collection
4	Validation of a 4D-PET Maximum intensity projection for delineation of an internal target volume.	published	90% of concept, design, data interpretation and manuscript writing, 100% of study conduct, data generation and data collection
5	Geographic miss of lung tumour due to respiratory motion: a comparison of 3D vs 4D PET/CT defined target volumes	published	90% of concept, design, data interpretation and manuscript writing, 100% of study conduct, data generation and data collection
6	High resolution imaging of pulmonary ventilation and perfusion with 68Ga-VQ respiratory gated (4-D) PET/CT	published	90% of concept, design, data interpretation and , data generation and data collection 80% of study conduct and manuscript writing

I have renumbered sections of submitted or published papers in order to generate a consistent presentation within the thesis.

Student signature: [redacted] **Date: 19 February 2016**

The undersigned hereby certify that the above declaration correctly reflects the nature and extent of the student and co-authors' contributions to this work.

Main Supervisor signature: **Date:**

ACKNOWLEDGEMENTS

The completion of this PhD thesis is an achievement that has only come about thanks to the incredibly generous support, encouragement and guidance of my three wonderful supervisors Professor Rodney Hicks, Associate Professor Michal Schneider and Professor Tomas Kron. From the very beginning it was the belief of my supervisors that has made this possible for me. Despite their own tremendous commitments they were always able to make time to meet and discuss my progress and offer invaluable guidance on how to meet each challenge. It is an honour to work alongside such dedicated and talented professionals and I will be forever grateful.

I would also like to sincerely thank all the staff at the Peter MacCallum division of radiation oncology and cancer imaging for their support in all of my studies as well as all the patients who agreed to participate in my studies. In particularly I would like to thank David Binns for giving me the opportunity to pursue this work and for his invaluable technical knowledge and insights along the way. I would also like to thank Dr Sarah Everitt for her support, advice and her patient explanations of the use of PET/CT for the perspective of a radiation therapist. A big thank you for Dr Leon Dunn for the use of his wonderful gating phantom and Dr Nicholas Hardcastle for helping me overcome the many technical obstacles thrown up along the way.

Thank you to the CRC-BID for the scholarship that allowed me to travel overseas to present my results and enable their publication. I also have owe a huge debt of gratitude to all the patients who agreed to participate in our clinical studies to enable us to gain a better understanding of this new technology.

And finally and most importantly I would like to thank my family. To my wife, Christine whose unwavering belief and encouragement always makes me feel anything is possible. To my two beautiful children Mikayla and Jake who joined me during this journey and have reawakened my love of play and appreciation of a good night sleep. And to my amazing parents, Jim and Linda who instilled in me a love of learning and a wonder of the world that still inspires me today.

ABBREVIATIONS

Abbreviation/term	Definition
PET	Positron Emission Tomography
CT	Computed Tomography
SPECT	Single Photon Emission Computed Tomography
FDG	Fluoro-D-deoxyglucose
MR	Magnetic Resonance Imaging
GTV	Gross Tumour Volume
ITV	Internal Target Volume
IGTV	Internal Gross Target Volume
PTV	Planned Target Volume
CTV	Clinical Target Volume
SPV	Solitary Pulmonary Nodule
MAA	Macroaggregated Albumin
VQ	Ventilation / Perfusion
EORTC	European Organization for Research and Treatment of Cancer
SUV	Standardized Uptake Value
MIP	Maximum Intensity Projection
AC	Attenuation Corrected
NAC	Non-Attenuation Corrected
FB	Free Breathing
DIBH	Deep Inspiration Breath Hold
BHCT	Breath Hold Computed Tomography
RPM	Real-Time Position Management
RT	Radiotherapy

Abbreviation/term	Definition
SABR	Stereotactic Ablative Body Radiotherapy
WB	Whole Body
OSEM	Ordered Subset Expectation Maximization
HU	Hounsfield Units
BQ	Becquerel
ICRU	International Commission on Radiation Units
GY	Gray
KCPS	Kilo Counts Per Second
SV	Sievert
68-GE	Germanium-68
68-GA	Gallium-68
99M-TC	Technetium 99m
DC	Dice Co-efficient

LIST OF PUBLICATIONS

1. Callahan J, Kron T, Schneider-Kolsky M, Hicks RJ: **The clinical significance and management of lesion motion due to respiration during PET/CT scanning**. *Cancer Imaging* 2011, **11**:224-236.

2. Callahan J, Kron T, Schneider ME, Hicks RJ: **A prospective investigation into the clinical impact of 4D-PET/CT in the characterisation of solitary pulmonary nodules**. *Cancer Imaging* 2014, **14**(1):24.

3. Callahan J, Kron T, Schneider-Kolsky M, Dunn L, Thompson M, Siva S, Aarons Y, Binns D, Hicks RJ: **Validation of a 4D-PET Maximum Intensity Projection for Delineation of an Internal Target Volume**. *Int J Radiat Oncol Biol Phys* 2013.

4. Callahan J, Kron T, Siva S, Simoens N, Edgar A, Everitt S, Schneider ME, Hicks RJ: **Geographic miss of lung tumours due to respiratory motion: a comparison of 3D vs 4D PET/CT defined target volumes**. *Radiat Oncol* 2014, **9**(1):291.

5. Callahan J, Hofman MS, Siva S, Kron T, Schneider ME, Binns D, Eu P, Hicks RJ: **High-resolution imaging of pulmonary ventilation and perfusion with 68Ga-VQ respiratory gated (4-D) PET/CT**. *Eur J Nucl Med Mol Imaging* 2014, **41**(2):343-349.

LIST OF FIGURES

LIST OF TABLES

CHAPTER 1 - INTRODUCTION

1.1 PET/CT SCANNING

Positron emission tomography-computed tomography or PET/CT is a hybrid imaging modality that acquires both anatomical images through a CT scanner and functional images through a PET scanner in a single session. This device is an evolution of the original PET scanner developed in the 1970s that employs the detection of annihilation photons in co-incidence created by the collision of a positron and an electron (Ter-Pogossian et al., 1975). A limitation of the early PET scanners was the lack of anatomical detail when a PET scan was acquired in isolation. In 1998 the first PET/CT device was described with the clear advantages of improved anatomical correlation and attenuation correction (Kinahan et al., 1998). The PET/CT scanner has now replaced standalone PET scanners as the new standard in PET imaging (Boellaard et al., 2015).

A PET scan involves the administration tracer labelled to a positron emitting radio-isotope, known as a radiopharmaceutical, in order to visualise a physiological system or molecular pathway. The most common radio-isotope used in PET is the Fluorine-18 which is produced in a cyclotron and has a half-life of 110 minutes. In recent years, a commercially available Gallium-68 generator has become available which provides a reliable source of the positron emitting isotope Gallium-68 without the

need for an expensive and complicated cyclotron. The Gallium-68 isotope, with a half-life of 68mins, can be labelled to many different tracers on site and this has opened up a whole new area of tracer research in PET. One such area of research is the substitution of Gallium-68 for Technetium-99m for the scanning on a PET/CT scanner tracers that were previous only able to be visualised on a Nuclear Medicine Gamma Camera (Hofman et al., 2011, Hofman et al., 2015, Breeman et al., 2011).

However the most common radiopharmaceutical employed in PET scanning is 2-deoxy-2-(-18-F) fluoro-D-glucose or FDG. This is a glucose analogue that is taken up by cells by the same metabolic pathway as unlabelled glucose (Tewson et al., 1978). However, unlike unlabelled glucose once FDG is extracted from the circulation it is trapped in the cell through phosphorylation by hexokinase (Tewson et al., 1978). By acquiring a PET scan for a patient administered with FDG the utilisation of glucose by different organs and system can be both visualised and quantified. The same principle is applied to a wide variety of radiopharmaceuticals where a tracer that is known to show a particular physiologic or molecular pathway is labelled and the distribution is visualised on a PET scan. Below is a table of some of the radiopharmaceuticals used in oncology and their method of uptake.

Table 1.1 – Example of some of the radiopharmaceuticals used in oncology.

Radiopharmaceutical	Method of uptake
FET - Fluoroethyl-L-tyrosine	Amino acid to visualise increased protein synthesis in tumours (Wester et al., 1999).
FLT – Fluorothymidine	Incorporated into new DNA to visualise increased cellular proliferation (Shields et al., 1998)
FMISO - Fluoroerythronitroimidazole	Imaging of cellular hypoxia (Yang et al., 1995)
GaTate – Gallium Dotatate	Somatostatin analogue for binding to somatostatin receptors (Kayani et al., 2008).
PSMA – Prostate Specific Membrane antigen	Anti-body that binds to the cell surface protein PSMA (Afshar-Oromieh et al., 2013)
Galligas – Gallium labelled Technegas	Visualisation of lung ventilation through inhalation (Hofman et al., 2011)
GaMAA – Gallium labelled macro aggregated albumin	Visualization of blood flow to the lungs via intravenous injection (Hofman et al., 2011)

1.2 PET/CT IN ONCOLOGY

PET/CT imaging is uniquely placed to provide powerful information to aid in the management of cancer. Unlike anatomical imaging modalities, PET/CT is able to visualise abnormal changes at both a system and cellular level before there are any structural changes that can be visualised by anatomic modalities such as CT or MRI. The use of FDG-PET in oncology exploits a fundamental property of cancer known as the Warburg effect (Kelloff et al., 2005a, Warburg O, 1924). The Warburg effect was an observation made by Otto Warburg that cancer cells have an increase utilisation of glucose compared to normal cells. Therefore any abnormal accumulation of FDG would indicate the presence of cancer. By administering a radioactively labelled form of glucose it is possible with PET/CT to directly measure the rate of glucose metabolism in-vivo and detects areas of abnormal metabolism that would indicate malignancy.

FDG-PET has been used in oncology since it was first described in the 1980s and has been found to have a high overall sensitivity and specificity across a wide range of malignancies (Gambhir et al., 2001). In a number of malignancies, such and lung cancer and lymphoma, PET/CT is now the imaging modality of choice for the staging and monitoring of these cancers (Dunleavy et al., 2010, Akhurst et al., 2015). FDG-PET/CT has also been found to be accurate in the diagnosis on lung nodules found incidentally by anatomic imaging modalities (Cronin et al., 2008). For lung cancer,

FDG-PET/CT is now the recommended imaging modality for planning of radiotherapy treatment (Konert et al., 2015).

1.3 PURPOSE OF THIS THESIS

The main aim of this thesis is to evaluate the clinical application of 4D-PET/CT in clinical practice and establish a role for routine use of 4D-PET/CT in lung cancer diagnosis and radiation therapy. The hypothesis is that 4D-PET/CT has a clinical role that will impact on the management of patients with lung cancer.

This is broken down into four main objectives with the following aims:

AIM 1. DIAGNOSIS/STAGING: The first step in the management of lung cancer is to establish a diagnosis of malignancy. As described above FDG-PET/CT is now a valuable tool in aiding in the characterisation of suspicious lung lesions. The added value of 4D scanning to the standard technique is currently unclear. Therefore the first aim of this thesis is to determine added value of 4D-PET/CT in the characterisation of solitary pulmonary nodules found incidentally on anatomical imaging. This aim has been addressed in chapter three and was published in *Cancer Imaging (Callahan et al., 2014b)*.

AIM 2. TARGET DELINEATION: After a diagnosis of lung cancer the next step in managing these patients is to treat the tumour through either surgical resection or radiation therapy. While standard 3D-PET/CT is now well recognised to play an important part in the delineation of target volumes for radiation therapy the role of 4D-PET is not well established. To this end the second aim is designed to validate the use of 4D-PET in target volume delineation using a new post processing technique, known as a 4D-PET/CT Maximum Intensity Projection, or MIP, to make its clinical application viable for routine use. This aim has been addressed in chapter four and was published in the *International Journal of Radiation Oncology Biology and Physics (Callahan et al., 2013)* .

AIM 3. IMPACT OF TARGET DELINEATION: In many centres where PET/CT is used for target volume delineation the standard 3D-PET/CT is used without any motion correction. It is generally assumed that the slow nature of the 3D-PET/CT scan will take into account any respiratory motion. The third aim of this thesis was designed to test if this assumption was valid to inform clinicians as to whether 4D-PET/CT provides information above what is available in standard 3D-PET/CT scanning. The geographic miss of lung tumours due to respiratory motion was investigated by comparing target volumes defined on a standard 3D-PET/CT scan to target volumes defined on a 4D-PET/CT Maximum intensity projection. This aim has been addressed in chapter five and was published in *Radiation Oncology (Callahan et al., 2014c)*.

AIM 4. ASSESSMENT OF NORMAL LUNG: An important factor affecting a lung cancer patient's quality of life after they have completed their treatment is how much of the normal lung parenchyma is affected by the radiation therapy. A new functional imaging scan, VQ-PET/CT, may enable more accurate quantification of regional lung function to allow monitoring of the effects of radiation therapy to the normal lung. The fourth aim of this thesis was to investigate the effects of respiratory motion on VQ-PET/CT scanning and determine if 4D imaging will improve co-registration between PET and CT. This aim has been addressed in chapter six and has been published in the *European Journal of Nuclear Medicine and Molecular Imaging (Callahan et al., 2014a)*.

CHAPTER 2 – LITERATURE REVIEW

2.1 THE CLINICAL SIGNIFICANCE AND MANAGEMENT OF LESION MOTION DUE TO RESPIRATION DURING PET/CT SCANNING

Jason Callahan[1,3], Tomas Kron[2], Michal Schneider-Kolsky[3], Rodney J Hicks[1]

1. Peter MacCallum Cancer Centre, Division of Radiation Oncology and Cancer Imaging
2. Peter MacCallum Cancer Centre, Department of Physical Sciences
3. Monash University, Department of Medical Imaging and Radiation Science

Cancer Imaging, 2011, 11,224-236

INTRODUCTION

Over the past decade PET/CT scanning has become an invaluable tool in the evaluation of many oncologic processes. The imaging modality of positron emission tomography (PET) uses positron emitting isotopes attached to specific tracers to image metabolic pathways or other biological processes. As PET scanning often interrogates specific biochemical processes involved in substrate utilisation, it is sometimes referred to as metabolic imaging but it can also image a range of molecular targets and physiological processes and therefore is more accurately a form of molecular imaging. The most common tracer used is fluorine-18 fluorodeoxyglucose (FDG), which evaluates the body's utilisation of glucose. Up-regulation of the insulin-independent glucose transporters GLUT-1 and GLUT-3, as well as the initial, rate-limiting enzyme of glycololysis, hexokinase drive the increased glycolytic metabolism, termed the Warburg phenomenon, which is characteristic of most cancer cells (Kelloff et al., 2005b). As changes in cell metabolism precede any change in tumour morphology, PET scanning may detect disease before anatomical changes can be visualised (Hicks et al., 2001). Due to limited spatial resolution and the resulting partial volume effects and apparent spill over of very intense activity into surrounding tissues, molecular imaging is however, less accurate with regard to tumour size than anatomical imaging modalities such as magnetic resonance imaging (MRI) or computerised tomography (CT). In addition, it provides only vicarious anatomical information through the pattern of glucose use in tissues and organs. In order to overcome these limitations, all modern PET scanners now have a CT scanner

attached to the same gantry so that a CT scan can be acquired in the same session. This is termed hybrid imaging. It allows accurate fusion of the powerful metabolic information of a PET scan to the fine anatomical detail of a CT scan. The CT component of the study is also used to provide correction for the attenuation of photons arising from the PET tracer as they pass through the body to the detector, an essential process to provide quantitative PET information.

Because both the PET and CT components of a PET/CT are acquired at almost the same time and in the same geometry, it is expected that images resulting from both modalities will be perfectly aligned. However, this is seldom the case. An inevitable, but not the only, cause of misalignment of the metabolic and anatomical information is normal patient respiration. This is a common source of artefact and can have a profound impact on the ability of a PET scan to detect disease, accurately localise it or provide accurate quantitation of tracer uptake. This is of particular relevance when planning target volumes for radiation therapy. A PET scan is acquired in steps of between two and five minutes duration with the patient breathing freely. A PET-avid lesion will become blurred if affected by respiratory motion, an effect similar to that created when a person moves while a photograph is taken with a slow shutter speed in low-light conditions.

Because the CT scan is acquired sufficiently quickly by most modern scanners to "freeze" this motion for the anatomical component of the study in a random but fixed position of the breathing cycle, misregistration between the PET and co-acquired CT scan can also occur. The compounding effects of blurring and

misregistration in whole body PET/CT imaging make accurate characterization of PET avid disease in areas of high respiratory motion challenging.

There is also an increasing interest in using PET quantitatively to assess disease response in both clinical practice and trials by evaluating tracer uptake before, during and after treatment using a measure known as the standardised uptake value or SUV. The SUV is a semi-quantitative index of tracer uptake normalised by weight and injected activity and is measured by the PET scanner. Currently, PET response criteria such as the EORTC guidelines do not consider the effect of respiratory motion when calculating the SUV (Young et al., 1999). However, both respiratory blurring of activity within a lesion and assignment of inappropriate attenuation correction due to misregistration of the CT and PET data compromise the accuracy and precision of this measure.

There have been a number of different approaches described in the literature to address the issue of respiratory motion in PET/CT scanning (Lupi et al., 2009, Nehmeh and Erdi, 2008, Nehmeh et al., 2002, Nehmeh et al., 2004, Park et al., 2008, Wolthaus et al., 2005). In a recent article Nehmeh and Erdi reviewed a number of different respiratory motion protocols that have been investigated and presented their results concentrating on improvement in image quality and quantitation [4]. They showed in their review that there are a wide range of strategies that can be employed to compensate for the effects of respiratory motion with each having advantages and disadvantages. The present review will concentrate on the clinical significance of lesion movement due to respiration, using examples to illustrate

particular clinical scenarios. It will then discuss the most practical current imaging techniques and approaches to manage the effects of respiratory motion in PET/CT scanning and to optimise the resulting images.

CLINICAL SIGNIFICANCE OF LESION MOTION DUE TO RESPIRATION

The areas most affected by respiratory motion are the lower lungs, liver and upper abdomen. The effect of this motion on a whole body PET scan is to make a PET-avid lesion appear larger but fainter, particularly at its boundaries, which exhibit blurred outlines rather than defined margins. Respiratory motion tends to artificially reduce the SUV (Lupi et al., 2009, Nehmeh and Erdi, 2008, Nehmeh et al., 2002, Nehmeh et al., 2004, Park et al., 2008, Werner et al., 2009). The artefact has the potential to impact on the correct diagnosis of diseases, provide inappropriate planning of target volumes for radiotherapy, impair staging of disease prior to surgery, and may lead to incorrect quantitation in therapeutic monitoring.

Diagnosis of malignancy

The most common parameter used to characterise a lesion is the SUVmax, which is the pixel within a region of interest drawn around a tumour that has the highest SUV. Several studies have advocated the use of SUVmax thresholds for the differentiation of benign from malignant lung nodules. For example, a SUVmax of less than 2.5 is often used to differentiate benign from malignant lesions in the lung (Garcia Vicente et al., 2010, Hubner et al., 1996). An example of a respiratory artefact is shown in Figure 2.1 (page 35). Accurate measurement of the true SUV in a

lesion such as this is not possible. A number of studies have shown consistently higher SUVmax values on a scan corrected for motion compared to a standard whole body acquisition (Lupi et al., 2009, Nehmeh and Erdi, 2008, Nehmeh et al., 2002, Nehmeh et al., 2004, Park et al., 2008, Werner et al., 2009, Garcia Vicente et al., 2010, Larson et al., 2005, Liu et al., 2009). In one case, reported in the study by Lupi and colleagues, the SUV on gated scan was 360% higher than on the un-gated scan. However, the clinical significance of this is not clear in practice. Although the lesion in Figure 2.1 (Page 35) shows a large amount of blurring and misregistration, an experienced physician would still be able to make an accurate diagnosis of malignancy by using the appearance of the lesion on CT as well as knowledge about the effect of motion in this area of the lung when making a diagnosis. Given the complexity of the decision making process required this would make any computer automation or support difficult.

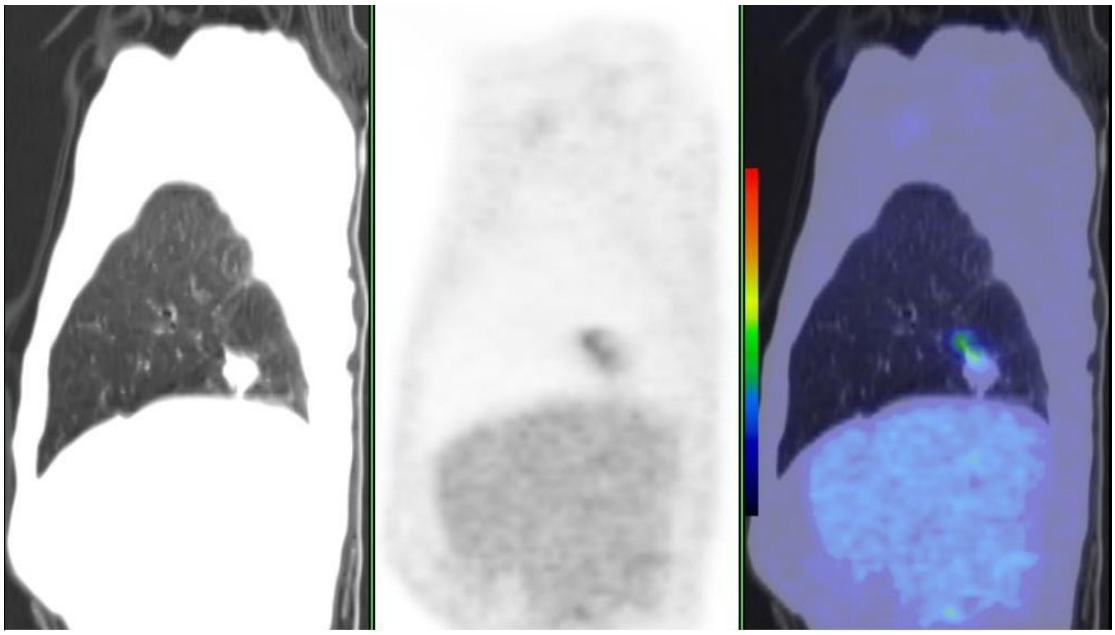

Figure 2.1 - Respiratory motion artefact on a PET/CT scan

Sagittal section of the right lower lobe showing CT (left panel), PET (middle panel), and fused PET/CT (right panel). The PET scan shows significant blurring and misregistration of a malignant lung lesion on the PET scan. The demonstration that the majority of the metabolic abnormality has been attenuated as though arising within normal lung and is elongated in the cranio-caudal dimension compared with the CT lesion indicates substantial respiratory movement of this lesion close to the diaphragm. Accordingly, the combination of radiologic appearances and the assumption that true metabolic activity is significantly underestimated should lead an experienced clinician to strongly suspect a malignant basis for this lesion.

The distance that a lesion moves during respiration determines how severely the PET scan is affected by this artefact (Liu et al., 2009). The greater the motion, the fainter a PET lesion becomes overall and therefore the more difficult it becomes to detect the lesion. When the effect of motion is combined with a small-sized lesion, which is also subject to partial volume effect, then a lesion with uptake of a metabolic tracer can become falsely negative (Figure 2.2 – Page 36). It is in this situation strategies for the management of motion need to be in place.

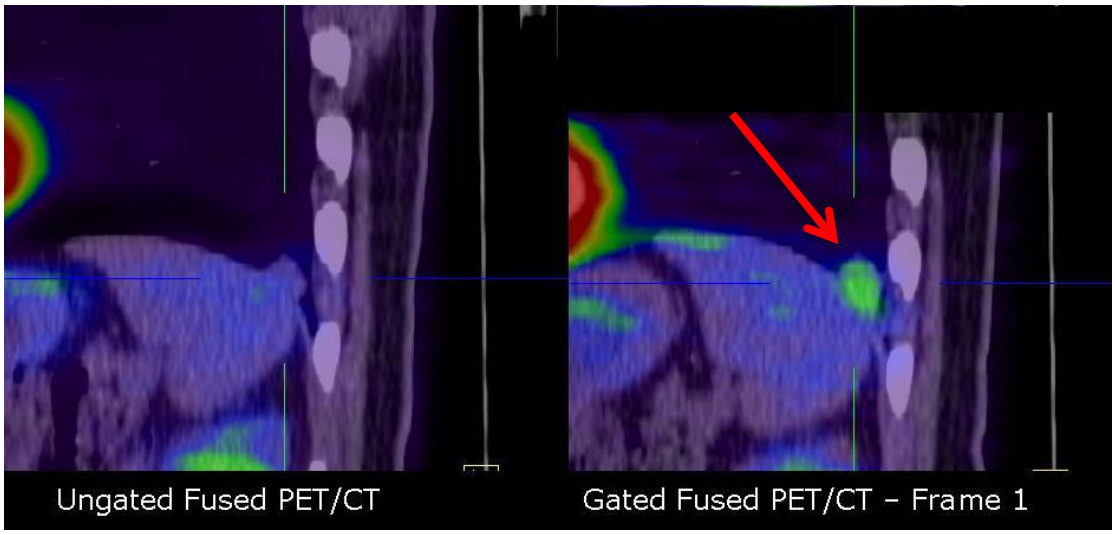

Figure 2.2 – Ungated PET/CT versus Gated PET/CT

Sagittal section of the right lower lobe showing no FDG uptake on the PET scan without respiratory gating (ungated) (left panel) and positive uptake on the best bin1 of the gated PET scan (right panel) indicated by the red arrow. The lesion was found to be malignant on subsequent surgical pathology.

The extent of respiratory motion varies from patient to patient. Diaphragmatic motion was measured in a series of 20 patients who had respiratory gated (4D)-CT scans for radiotherapy planning at the Peter MacCallum PET centre (unpublished data). The median amount of cranio-caudal motion in the right hemi-diaphragm was 21mm (range 8-56mm) and the left hemi-diaphragm was 13mm (range 0-25mm). The wide range of measured movement indicates that the amount of motion from patient to patient is difficult to predict. Figure 2.3 (Page 37) shows an example of a patient with a severely impaired respiratory excursion in the left lung leading to compensation by the right lung producing a large amount of motion. Any lesion in the right lung would likely become falsely negative but the left lung would be unaffected.

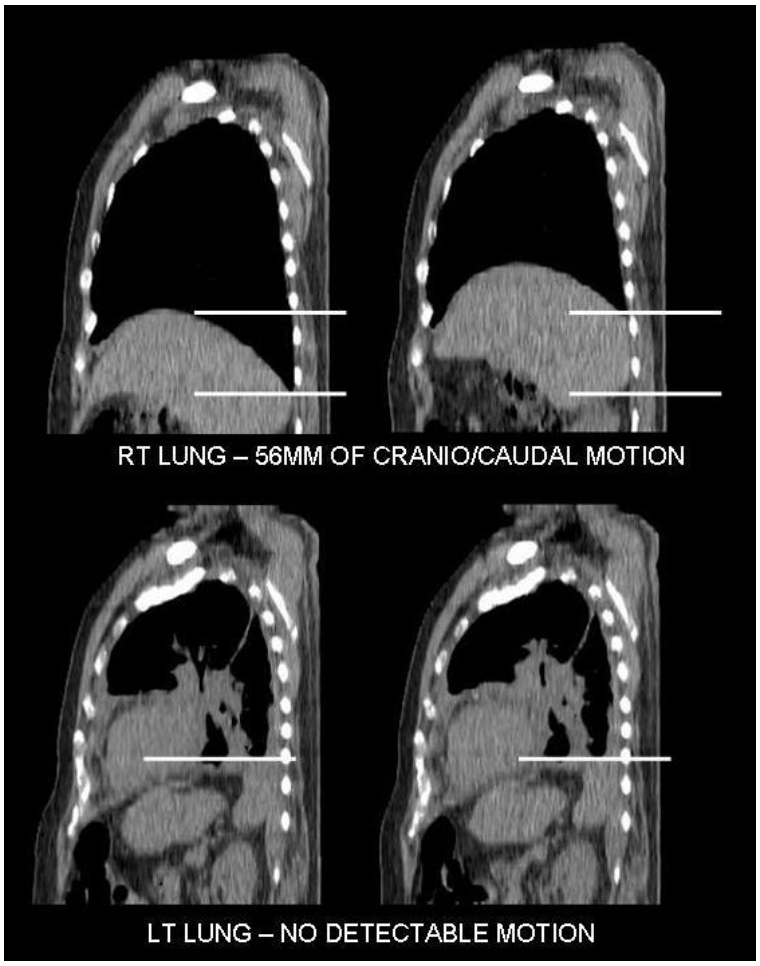

Figure 2.3 – Variable Respiratory motion

Sagittal section of the end-inspiration (left) and end-expiration (right) phases of a 4D CT scan.

Gated or 4D scanning is a scanning technique that enables imaging of the full range of respiratory motion. A 4D-PET or CT scan is performed by acquiring enough data over an area of interest to provide information on the full range of respiratory motion. In both imaging modalities a monitoring device records the subject's respiratory trace during the respective acquisitions. The breathing trace is then used to place data in their respective 'bins' based on its position in the respiratory cycle. For example data acquired when the subject is in full inspiration is placed in the 0% bin. All the data acquired between this point and the next full inspiration is divided evenly between a predetermined numbers of bins based on a percentage of the

respiratory cycle. Then by reviewing all the bins as cine it is possible to observe a lesion through the full range of respiratory motion.

Radiotherapy planning

By using the metabolic information of the PET scan it is easier to accurately determine and therefore often minimise the target volume in the presence of atelectasis or lung collapse (Mac Manus et al., 2006). With the ability of modern radiotherapy practice to deliver highly conformal distributions of dose, the accurate delineation of tumour margins is of the highest importance. The use of PET in the radiotherapy planning process, particularly in lung cancer, is now a well-established practice (MacManus et al., 2009, Mac Manus, 2010).

When using a PET/CT scan to plan radiotherapy target volumes there is an assumption that the blurring effect on a free breathing PET scan will account for motion of the tumour due to respiration (MacManus et al., 2009). A target volume based on the blurred area on the PET scan movement of the tumour due to respiration will be accounted for within the target volume (Figure 2.4 - Page 39). However this assumption may not be valid in some situations. Figure 2.5 (Page 40) shows a lung tumour in the right lower lobe. The top row shows the whole body PET/CT scan and there is little evidence of blurring that would indicate respiratory motion. If this scan alone was used to plan a target volume it is unlikely to include the faint blurring extending into the liver. The second and third rows show the end-expiration and end-inspiration images of a respiratory-gated PET. These two frames

clearly show respiratory motion that was measured to be as high as 15mm. As the CT scan was not gated, inappropriate attenuation correction was applied to the inspiration phase of the gated PET scan leading to inappropriate estimation of true counts within the lesion seen in the third row. If the target volume only included the activity seen on the whole body PET then the lesion would move in and out of the treated area as the patient breathes during treatment.

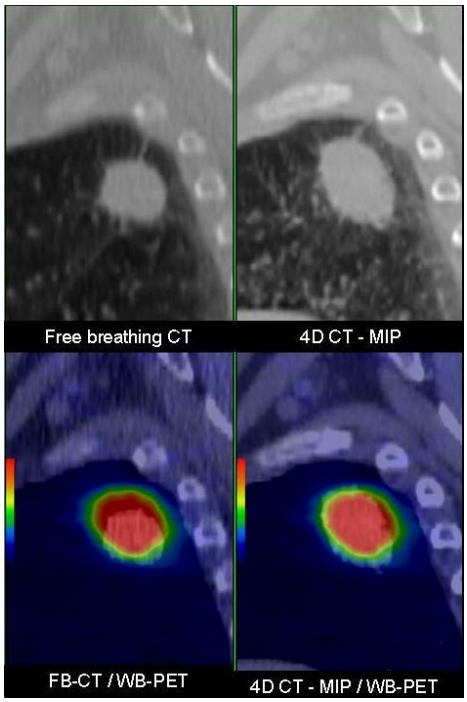

Figure 2.4 – Free breathing PET versus 4D-CT

This figure shows the blurring effect of respiration on ungated whole-body PET imaging. The top left shows the appearance of a lung lesion on a free-breathing CT and the top right shows the lesions when the scan is reconstructed and a MIP reconstruction from a 4D CT. The 4D CT MIP reconstruction is generated by using the maximum pixel values across all 4D CT frames. The bottom left shows the ungated whole-body PET fused with the free-breathing CT and the PET lesion appears larger. Than the CT lesions. However, when the ungated whole-body PET is fused with the MIP reconstruction, there is much better agreement in the lesion size.

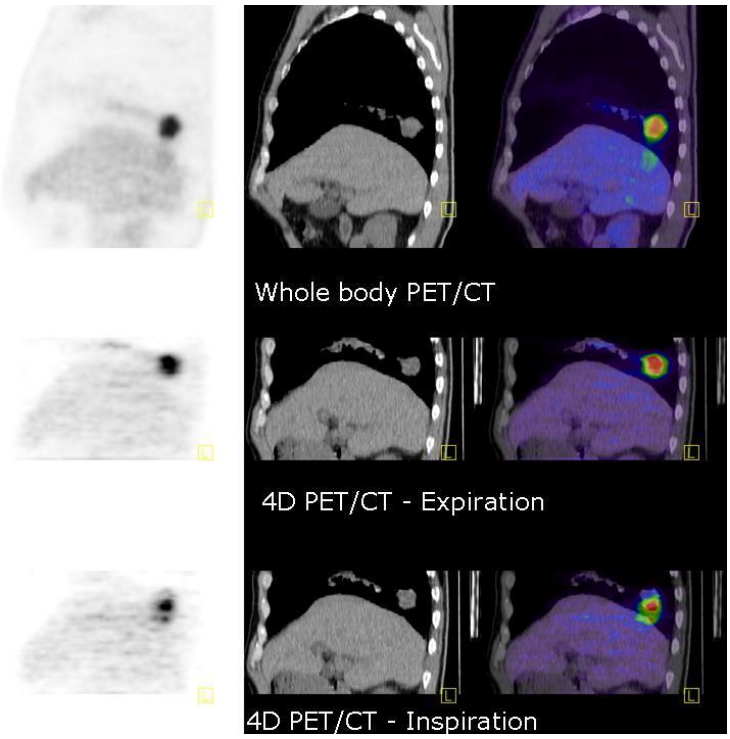

Figure 2.5 – Inspiration versus expiration 4D-PET

Sagittal section of the right lower lobe on the whole-body PET/CT (top row), expiration PET/CT (middle row), and inspiration PET/CT (bottom row).

This was shown in a recent paper by Aristophanous and colleagues analysing the clinical utility of 4D FDG/PET/CT in radiation treatment planning (Aristophanous et al., 2011). In this study they compared the target volumes defined using an ungated PET and an aggregated volume of a 4D PET. They found that the latter was larger than the volume defined on the 3D PET. They concluded that a 4D PET may better define the full physiologic extent of moving tumours when compared to 3D PET. Figures Figure 2.4 and Figure 2.5 provide good examples to illustrate that motion management for PET/CT must consider both imaging modalities and their interaction.

Figure 2.6 (Page 41) shows the effects that different breathing patterns can have on the distribution of activity in an ungated PET scan. A Perspex phantom with four reservoirs of various sizes (5mm, 10mm, 15mm and 20mm) was filled with a solution

containing Fluorine-18. Using a moving phantom (Modus Medical Quasar, London ON Canada) the Perspex insert was driven forward and back 40mm in one direction to simulate respiratory motion. The image in the top row shows the effect on the distribution of activity when the phantom was driven in a sinusoidal pattern. The bottom row simulates the distribution of activity as if there was a pause at the end of the expiration phase, which is not an uncommon breathing pattern. The bottom row shows a dark area with a faint tail of activity compared to top row which shows an evenly distributed area of uptake. The phantom used had no background activity and relatively uniform attenuation, unlike what would be found in the diaphragmatic region where, for example, the liver has significant FDG uptake and markedly different attenuation characteristics than the adjacent aerated lung. If a lesion in or on top of the liver moved with this pattern of movement the faint tail may not be visible as it would fade into the background. This simple experiment shows that the distribution of activity seen on un-gated PET may also be affected by a patient's respiratory pattern.

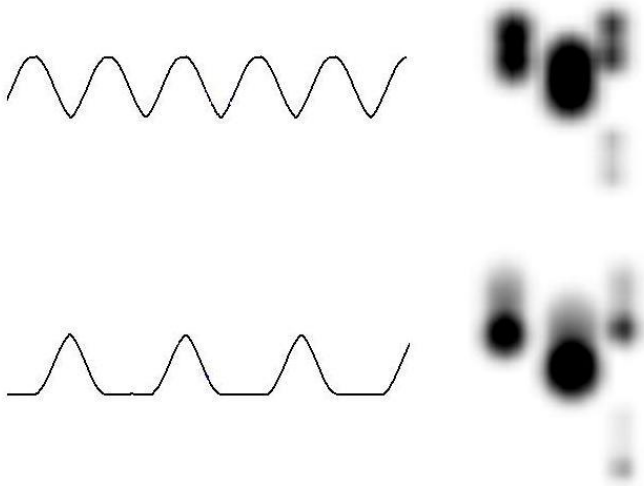

Figure 2.6 - Breathing Patterns and PET

The effect of different respiration patterns on the distribution of activity ungated PET scans in a phantom with no background on four different sized objects (5mm, 10mm, 15mm and 20mm).

These examples illustrate the need to compensate for lesion motion if a PET/CT scan is to be used in radiotherapy planning particularly in areas of high motion such as the lower lobes of the lungs. It is becoming common practice to use a 4D CT scan in the planning of lung cancer patients (Nath et al., 2011, Purdie et al., 2006, Slotman et al., 2006). However, this means that the potential benefits of the FDG PET in delineating the tumour may be lost. An example is a tumour that is situated on top of the liver. A 4D-CT MIP reconstruction is often used to define target volumes for treatment with radiotherapy. A soft tissue lesion positioned on the dome of the liver would merge with the liver on a 4D-CT MIP reconstruction due to respiratory motion. An example of this is shown in Figure 2.7 (Page 42). The inferior margin target volume would be difficult to distinguish from the liver as the Hounsfield units of the liver and a soft tissue tumour would be similar. A 4D-PET with its high tumour uptake when compared to liver would be ideal for defining the tumour margin. Respiratory gated protocols are now being investigated to address this clinical situation and these will be outlined later in this article.

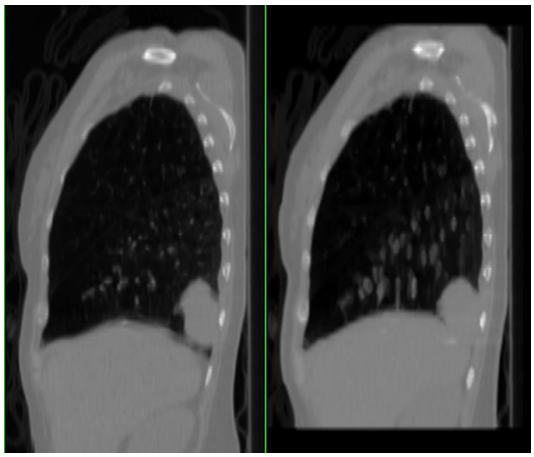

Figure 2.7 – 3D-CT versus 4D-CT

Lower lobe lung lesion on free-breathing CT shows separation between the lesion and liver. However, the lesion on the 4D CT MIP merges the liver making the inferior margin of the tumour difficult to define.

Surgical planning

FDG PET scanning is often used prior to surgery to determine if there is any spread of disease that would require more extensive surgery or alternative therapies. It is possible that due to respiratory motion small lesions particularly in the liver with its high background activity could remain undetected. If any additional metastases remain undetected due to respiratory blurring it is likely the patient would have a less favourable outcome.

Another potentially important indication for gated scanning is to assess the tethering of a tumour to the chest wall. A tumour that is moving freely within the chest cavity is unlikely to have invaded the chest wall. However, a tumour that is tethered to the chest wall due to invasion in unlikely to show any motion on a gated scan. The extent of resection required for a lung tumour is highly dependent on whether tumour has invaded the chest wall (Stoelben and Ludwig, 2009). It is feasible that prior to surgery a gated PET/CT scan could be performed in order to give an indication of chest wall invasion. This would enable surgeons to better prepare for surgery, particularly in patients with borderline lung function in whom compromise of chest wall integrity may lead to significant morbidity.

Therapeutic monitoring

There is increasing interest in the use of PET to measure the effect of treatment in standard clinical practice and clinical trials (Mileshkin et al., 2011, Zhang et al., 2011). Early response assessment could lead to better patient management and significantly shorten the time for clinical trials to provide relevant results. This will save money and allow implementation of different therapeutic strategies earlier in the clinic. In FDG PET the SUV is a semi-quantitative measure of a tumours utilisation of glucose. Accurate measurement of SUV using PET is dependent on isolating all variables that have an effect on the uptake of the tracer by malignant cells. These include blood sugar level, tracer dose, uptake time, as well as the technical performance of the scanner. Only when all these variables are controlled can the SUV be accurately measured. In clinical trials using PET to assess response to treatment, strict protocols are adhered to in order to ensure any change in SUV can be attributed to the efficacy of a treatment and not any technical factor. However, to date, no response criteria have explicitly taken into account the effect that respiratory motion can have on SUV in particular as motion patterns can change due to the therapeutic intervention.

STRATEGIES TO COMPENSATE FOR RESPIRATORY MOTION IN PET/CT SCANNING

There are a number of methods that can be used to compensate for lesion motion due to respiration on a PET/CT scan. The most recent advance is the ability to perform respiratory gated PET and CT scanning using various respiratory monitoring systems. The various approaches described in the literature to account for respiratory motion include:

1. Non-attenuation corrected PET (NAC-PET)
2. Deep Inspiration Breath hold PET (DIBH-PET)
3. Respiratory gated PET and free breathing CT (4DPET/FBCT)
4. Respiratory gated PET and breath hold CT (4DPET/BHCT)
5. Respiratory gated PET and Respiratory gated CT (4DPET/CT)

1. Non-attenuation corrected (NAC) PET

As outlined above, one of the factors that increase the impact of respiratory motion is misregistration leading to inappropriate application of attenuation correction. A simple way to reduce this impact is to look at the PET image without application of attenuation correction. This is a common option used in clinical practice as it does not require any addition camera time or the complex hardware and software options needed to perform respiratory gating (see example in Figure 2.8 – Page 46). A study by Reinhardt (Reinhardt et al., 2006) found that out of 174 pulmonary metastases detected on FDG PET, six (4%) were seen on NAC PET and not on attenuation

corrected (AC) PET. They found that while 41.4% of the 174 lesions were better visualized on the NAC PET there was no significant difference in the overall lesion detection between AC and NAC PET. The six lesions detected on only NAC PET were all relatively small lesions (5-11mm) and would be expected to be more affected by respiratory motion. A limitation of NAC PET scan is that it cannot provide any SUV information and therefore is not a suitable option when attempting to quantify metabolic activity. This technique does not correct any blurring or misregistration caused by respiration and therefore may not provide a reporting physician with confidence about a lesion's intensity or its exact location. The use of NAC PET reconstruction should only be used if a more sophisticated method for correcting a motion artefact is not available.

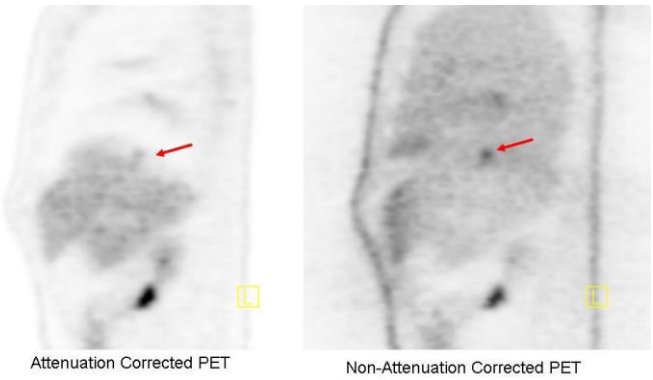

Figure 2.8 – Attenuation corrected versus non-attenuation corrected PET

Lesions on the dome of the liver better visualized on PET without attenuation correction (non-attenuation corrected) compared with attenuation corrected PET.

2. Deep inspiration Breath hold PET (DIBH-PET)

A standard PET scan is acquired in steps of around two to five minutes depending on the camera. As it is not possible for a patient to hold their breath for this long the DIBH protocol was developed to remove the effect that respiration has on a PET image as well as to address the problem of noise on a gated PET scan. The technique of deep inspiration breath hold PET or DIBH-PET is an attempt to match the breathing position on both the CT and the PET scan. This method is adapted from the radiotherapy technique to provide a reproducible tumour position for treatment (Hanley et al., 1999, Rosenzweig et al., 2000) . The protocol first described by Nehmeh (Nehmeh et al., 2007) involves first coaching a patient to inhale to a point that is reproducible and hold their breath at this position for as long as possible. The breathing position is monitored using one of the commercially available respiratory monitoring devices.

A CT scan is first acquired in this breath hold position for attenuation correction and anatomical correlation. A PET scan is then acquired over multiple breath holding phases in the same respiratory position. The patient continues holding their breath until the total acquisition time equals a standard bed step of around three minutes. According to Nehmeh this normally takes nine breath holds. In their study among a cohort of eight patients encompassing 10 lesions they found that the SUV_{max} was on average 32.6% higher (range, 4%-83%) compared to standard whole body PET/CT and reduced the mismatch by an average of 26.6% (range, 3%-50%).

This method has the advantage of eliminating blurring artefacts caused by motion and greatly decreasing the possibility of a mismatch between the CT and PET scan. Also, the image quality is higher than for a single bin from a respiratory gated PET as the acquisition time is three minutes compared to typically one minute for a single bin from a gated PET, providing better count statistics. The drawback is that some patients may find holding their breath multiple times for up to three minutes challenging and therefore patient selection and coaching is important. It also prolongs scan time. However, while this is an effective protocol to provide a snapshot of the lungs, it does not provide any information about the direction or amount of lesion motion.

3. Respiratory gated PET (4D-PET) and free breathing CT

An alternative to DIBH-PET is to perform a respiratory gated or 4D-PET scan corrected with a free breathing CT scan. This method (used in Figures Figure 2.2 and Figure 2.9) involves a list-mode PET acquisition of an area of interest while recording a patient's breathing trace using a respiratory monitoring system. List mode is a technique where all counts are recorded sequentially with time-stamps allowing reformatting within precise time intervals. The list-mode data then can be retrospectively reconstructed into multiple phases of the respiratory cycle, or bins, using the respiratory trace. This additional gated scan can be acquired immediately after the whole body scan and the whole body CT can be used for attenuation

correction of the gated PET scan. As the whole body CT scan is taken while the patient is free breathing the position of the lungs in the respiratory cycle is random. This means that only those frames of the gated scan where the metabolic image is aligned with the CT will be appropriately corrected for attenuation. Often this will be a single bin unless a significant interval of the respiratory cycle is spent in a given position, such as expiration. This method requires the operator to manually evaluate the co-registration between the various PET bins and the CT using normal structures such as the liver dome. This comparison between the PET and CT can be performed on most modern PET display platforms. Finding the best-bin can be challenging and in the case of an abnormal respiratory excursion on the CT there could be no PET bin that matches the CT.

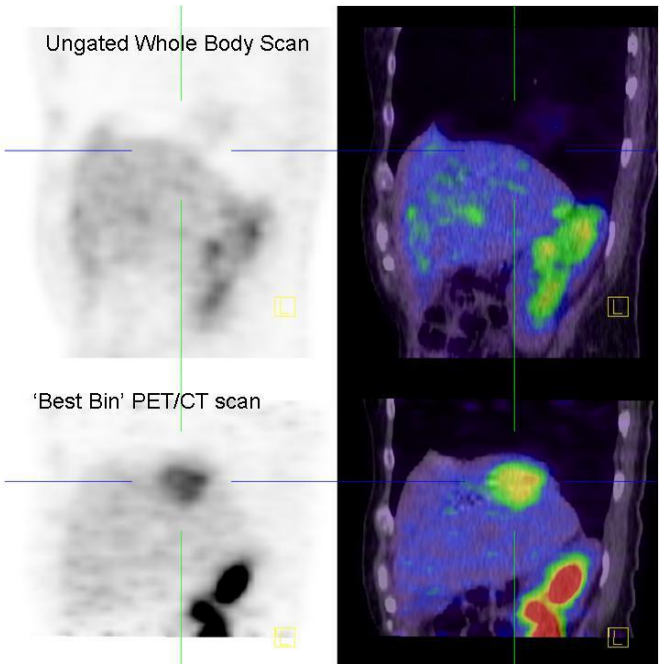

Figure 2.9 – Ungated versus Gated PET in the Liver

Sagittal section of liver showing little evidence of FDG-avid disease on the ungated PET scan and a large liver tumour on the best bin of the gated PET scan.

This was described as the 'best bin' method by Lupi and colleagues in their paper investigating the effect that respiratory gated PET scanning has on the detected metabolic activity in lung lesions (Lupi et al., 2009). They found that the gated scan produced variable but consistently higher SUV's on the gated "best bin" scan compared to the un-gated whole body scan (mean (SD) increase 77.2 % ± 4.6). The variability in the difference in SUV could be explained by the variable amounts of motion lung lesions can display.

This method has the advantage of requiring no additional CT radiation dose and is relatively easy for a patient to comply as no special breathing instruction are required. However, as only the 'best bin' is accurately corrected for attenuation most of the data acquired is not used and the images are inherently noisier than the DIBH method. Also, additional equipment such as a respiratory monitoring system and more advanced display software is required to perform a 4D PET scan. These facilities are not available in all institutions.

4. 4D-PET and breath hold CT

Identifying the 'best bin' can often be difficult as a free breathing CT is taken at a random phase of the respiratory cycle. This is particularly true in areas of high respiratory motion such as around the diaphragm. One strategy to address this problem is to combine a 4D PET scan with a breath hold CT (BH-CT). Fin (Fin et al., 2008) and colleagues described this approach by combining a 4D PET with a shallow

end-expiration BH-CT. One can apply this BH-CT to the end-expiration phase of the 4D PET for attenuation correction and anatomical localisation.

The advantage of this method is that as the CT scan is no longer in a random phase in the respiratory cycle the reporting physician can have confidence that the end expiration phase of the 4D-PET is the 'best bin' and misregistration should be minimised. The disadvantage of this method is the additional radiation exposure from the additional CT and the best bin will exhibit increased noise compared to the DIBH method. It is also difficult to ensure that the breath-hold is actually coinciding with a phase of the breathing cycle as patients tend to take a deeper breath prior to holding their breath.

5. 4D-PET and Respiratory gated CT (4D-CT) or 4D PET/CT

The scanning protocol that provides the most information about respiratory motion in terms of direction and amplitude as well as accurate quantitation is a respiratory-gated PET and CT scan (4D PET/CT). With this approach a gated CT scan is acquired over the area of interest followed by a gated PET. There are two main methods for the acquisition of a gated CT scan. The first involves acquiring a helical CT scan with a very small pitch (0.1) while recording the respiratory trace. The second involves performing an axial cine CT scan in sections with each section scanned for slightly longer than the patient's respiratory period. In both cases the over scanning ensures each part of the patient's anatomy is seen by a sufficient number of projections in each phase of the breathing cycle. The CT data can then be retrospectively

reconstructed into the number of bins equal to the gated PET scan. When the PET scan is processed each PET bin can be corrected for attenuation with the corresponding CT bin. Previously, this required a large amount of processing time and iterative multiple processes. Earlier strategies have therefore also used the 'average' scan as a composite of the 4D CT dataset for attenuation correction (Pan et al., 2005). There are now commercially available products in the newest generation of scanners that have automated this process making it much easier to apply in routine clinical practice.

The greatest advantage of this approach is that every PET bin will be appropriately corrected for attenuation, and thus each bin will accurately represent the distribution of tracer in the patient. If a gated PET scan is corrected for attenuation with a free breathing CT scan there is going to be a large amount of fluctuation in the SUVmax across the reconstructed bins. This observation has also been made by Erdi and colleagues (Erdi et al., 2004). In their study of eight lesions across five patients there was up to a 30% fluctuation in SUV between end inspiration and end expiration. The method of correcting a gated PET with a gated CT also provides information about the amplitude and direction of motion that can be used in a radiotherapy-planning algorithm. The main drawback of this technique is the significant radiation dose conferred to the patient as a result of the gated 4D CT scan. Depending on the exposure factors used the dose can be up to 10 times that received from a standard diagnostic CT scan of the thorax. In the context of an oncology patient planned for therapeutic irradiation of the region in question, this

additional dose can be justified if the additional information is shown to have an impact on the planning of target volumes for radiotherapy and on patient management overall. To date, no study has described the clinical impact or any changes in patient management due to an additional 4D PET/CT scan on either diagnosis or radiotherapy planning.

ADDITIONAL REQUIREMENTS TO IMPLEMENT MOTION MANAGEMENT FOR PET/CT

Key components of a motion management system are appropriate imaging hardware and software. This includes a multislice CT scanner and list mode acquisition for the PET system. Most of these components would be available in modern equipment but may need to be enabled by the manufacturer.

In order to perform respiratory gated scanning on a PET/CT scanner a system for tracking a patient's breathing must be employed. There are at least three commercially available respiratory tracking systems that are employed by the three main PET/CT vendors. These are:

1. Varian Real Time Position Management (RPM) system
2. Anzai Respiratory gating system
3. Phillips Bellows Respiratory gating system

1. Varian RPM

The Varian RPM system employs the use of a box with two or six reflecting dots that is placed above a patient's diaphragm. An infra-red camera attached to the end of the scanning table then feeds a video signal of the reflecting box to a PC that runs the Varian RPM software to track the motion of the box. This system is in common use on both the GE and Phillips PET/CT systems.

2. Anzai Respiratory Gating System

This system uses a belt that is attached to a patient's abdomen with a pressure sensor embedded placed in the belt. As the patient breathes in, pressure is applied to the sensor and a signal is sent to a PC laptop. This system is used on the Siemens PET/CT scanners but is also functional on GE scanners.

3. Phillips Bellows Respiratory tracking system

This system employs a belt that fastens around a patient's abdomen similar to the Anzai system. However, instead of a pressure sensor, a bellows device stretches and relaxes as the patient breathes in and out. This stretching of the bellows can then be plotted as a respiratory trace and fed into a camera for use in gated scanning.

Figure 2.10 – Respiratory monitoring systems

Varian RPM gating system (top left), Phillips Bellows (top right) and Anzai belt and pressure sensor (bottom).

These three tracking systems use uniquely different methods for recording a patient breathing during a PET/CT scan. Otani and co-workers (Otani et al., 2010) compared the differences in the timing tags of the Varian and Anzai systems. They attached both the Varian and Anzai systems to each lung cancer patient, acquired a single 4D-CT scan then reconstructed the scan retrospectively using the two different traces. They found that the position of the timing tags on different systems were not the

same leading to differences in the tumour centroid position and shape in some cases Based on these findings this group recommended that the same monitoring systems be used across all modalities within an institution. This is particularly relevant when 4D PET/CT leads to gating of motion adaptive RT.

Table 2.1 – Motion management protocols

Summary of the various requirements of motion management protocols for PET and PET/CT image acquisition.

	NAC-PET	DIBH-PET	4DPET /FBCT	4DPET /BHCT	4DPET /CT
Additional Time on PET/CT scanner	×	√	√	√	√
Additional Equipment	×	√	√	√	√
Additional Radiation	×	×	×	√	√√
Indication: Improved Quantitation	×	√	√	√	√√
Indication: Lesion detection	√	√	√	√	√
Indication: RT Planning	×	×	×	×	√

CONCLUSION

The clinical significance of respiratory motion of a PET/CT scan depends on a number of factors. The motion management scanning protocol used to address any respiratory motion artefact depends on the question that is asked. For example, if the only requirement is for the detection of a lesion, then simply reviewing the non-attenuation corrected PET may be sufficient. This approach will, however, be insufficient in those cases where there is a large amount of respiratory motion. The alternative is to use a respiratory-gated scanning method. In those scenarios where radiation dose must be minimised, such as the diagnosis of a solitary pulmonary nodule of unknown histology, either a DIBH or 4D-PET scan may be able resolve blurring and misregistration artefacts. This may reduce the chance of a false negative due to respiratory motion. The decision on whether to use DIBH or 4D-PET is a trade-off between increased noise on the 4D-PET or decreased patient compliance for the DIBH scan. In areas of high respiratory motion such as around the diaphragm finding the 'best bin' using the 4D-PET only methods can be challenging. In order to increase the confidence in selecting the 'best bin', a low-dose, mid-expiration breath hold CT is a good alternative. The 'gold standard' protocol for obtaining the most information about respiratory motion is to gate both the PET and the CT. However appropriate dose reduction strategies need to be considered. Due to the relatively high additional CT radiation dose, the use of 4D-CT must be justified in terms of management impact.

An area where 4D-PET/CT is likely to have a high impact is in radiotherapy planning. Until a gold standard for correction of the effects of motion has been determined to be reliable, 4D PET/CT is likely to be the most valuable tool to accurately define target volumes.

In therapeutic monitoring trials using PET to measure response the accurate quantitation of metabolic activity in lesions affected by motion will be difficult to achieve. This is of particular concern in serial PET/CT scans performed for assessing tumour response to treatment. While more accurate measurement of SUV in areas of high motion has been described using various 4D protocols it is not clear which one is best.

In conclusion, there are several approaches to managing the effects of respiration on a PET/CT scan. Each of the protocols described have their advantages and disadvantages. The optimal protocol will need to be tailored to suit each individual patient in order to optimise patient outcome. It is likely that in the future respiratory gated scanning for proven clinical indications will become as routine as cardiac gated scanning is in myocardial perfusion scanning.

2.2 RECENT PROGRESS OF 4D-PET/CT IN THE LITERATURE

This section summarised the recent progress in the literature that occurred in parallel with the presented studies in this thesis and after publication of the above review (Callahan et al., 2011b).

4D-PET/CT IN LUNG CANCER DIAGNOSIS

The diagnosis of lung nodules as either benign or malignant using FDG-PET/CT remains an important clinical tool. However as described above respiratory motion can be a confounder in the correct visualisation of lung lesion metabolic activity. While the technique of 4D-PET to correct for respiratory motion was first described in 2002 (Nehmeh et al., 2002) most of the literature after that date concentrated on differences in the measurement of SUV between 3D and 4D scanning rather than the diagnostic value of 4D-PET/CT over standard PET/CT. The difficulties of using SUV in isolation to determine malignancy was highlighted in a paper by Vicente et. al (Garcia Vicente et al., 2011). In their study of 28 patients with lung nodules an SUV cut-off of 2.5 was used to determine if a nodule was malignant or benign. They compared the SUV of lesion on the 3D scan to the 4D scan and found a higher false positive rate on the 4D scan leading to a decreased specificity (95% vs 70%, $p<0.05$). The problem with concentrating on differences in SUV between 3D and 4D PET/CT scans were again highlighted in a paper by Farid and colleagues (Farid et al., 2015). In their study of 32 patients the SUV in lung nodules on sequentially acquired 3D and 4D PET/CT scans was measured and compared to histological and cytological

findings. Consistent with other authors they showed the SUV on the 4D scan was on average 47% higher than the 3D scan but that a cut off value of 2.5 did not distinguish between benign and malignant lesions on either 3D or 4D studies. This is because the SUV of a lung lesion is only one of the many factors that must be taken into account to correctly classify a lung lesion as benign or malignant.

The largest series to look at the question of the added diagnostic value of 4D-PET/CT, beyond just difference in SUV, was published by Guerra and colleagues (Guerra et al., 2012). In a study of 155 patients from five European centres the author's evaluated if an additional 4D-PET/CT improved the overall accuracy of FDG-PET/CT in correctly classifying lung lesion as either benign or malignant based on a clinician's visual analysis rather than just SUV. In this group the biggest impact of the additional 4D-PET/CT was in lesions initially classified as equivocal on the 3D-PET/CT. On the 3D-PET/CT scan alone 24.3% of lesions were classified as equivocal and only 4.4% were equivocal on the 4D-PET/CT scan. Of the lesions initially classified as equivocal 60% changed to positive and 28% to negative. This increased the overall accuracy of the test by varying amounts depending on how the remaining equivocal lesions were classified. If the equivocal lesion were classified as positive the overall accuracy increase from 82.7% when using the 3D scan to 92.8% when using the 4D scan. If the equivocal lesion were classified as negative the overall accuracy increase from 80.2% when using the 3D scan to 94.2% when using the 4D scan.

While 4D-PET/CT has been described for many years a significant impediment to its routine implementation have been the significant technical challenge in acquiring

and reconstructing a 4D scan. A new method for correcting for respiratory motion known as 'motion freeze' was recently described by Huang et. at. that may make routine application of 4D scanning in characterising lung nodule more feasible (Huang et al., 2014). The motion freeze method uses deformable image registration to deform all the respiratory bins back to a single 3D phase so 100% of the counts are utilised. This method could potentially be acquired during the whole body scan making a separate 4D-PET/CT unnecessary. However one significant limitation of the technology is that the 4D-CT for attenuation correction and deformation must be free of breathing artefacts that may distort the deformation matrix. This is less of an issue with standard 4D-PET/CT as the expiration 4D-CT phase is generally free of artefact even if a patient's breathing is irregular. Further work comparing motion freeze to standard 4D-PET/CT is needed to further validate its use.

4D-PET/CT IN RADIATION ONCOLOGY

The clearest application for 4D-PET/CT to improve clinical practice is in the area of radiation oncology. This is reflected in the significant number of contributions to the literature in this area in recent years. A consensus report released by the IAEA looking at PET/CT for target volume delineation for NSCLC concluded that PET/CT imaging is an essential component of radiotherapy treatment planning for lung cancer (Konert et al., 2015). In their consensus report the authors noted that tumour motion caused by normal respiration is an important factor that can contribute to inaccuracy when using standard free breathing PET/CT imaging. Along

with their conclusion that PET/CT should be used in lung cancer treatment planning they stated that more research is needed into 4D-PET/CT. This conclusion was based on work by Hanna and colleagues that showed that target volumes derived for conventional 3D-PET/CT did not correspond well with those derived form a 4D-CT indicating that respiratory motion is underestimated in 3D-PET/CT (Hanna et al., 2012b).

3D VERSUS 4D-PET/CT DEFINED TARGET VOLUMES

The findings of Hanna and colleagues, that 3D-PET/CT defined volumes underestimate the true extent of respiratory motion, has been further strengthened in recent studies. In a study of ten patients comparing an 4D-CT IGTV to a 3D-PET IGTV, Duan and colleagues found that regardless of the segmentation method used the 3D-PET could not replace the 4D-CT defined IGTV in spatial position or form (Duan et al., 2015). A similar finding was made by Aristophanous who found that 4D-PET is able to better define the full extent of motion caused by respiratory motion when compared to 3D-PET (Aristophanous et al., 2012). In their study comparing 3D and 4D volumes in 22 lesions, Aristophanous found that the 4D volume was significantly larger than the 3D Volume ($p<0.01$) regardless of the contouring method used. In another study comparing 3D and 4D defined volumes Lamb and colleagues found that 3D imaging also underestimated target volumes for mediastinal lymph nodes (Lamb et al., 2013). In their series of 11 mediastinal lymph

nodes they found that a 13mm expansion of the 3D based volume was needed to cover the 4D based volumes.

The current practice for defining target volumes in lung cancer is to add a large margin to a GTV in order to compensate for any uncertainties in tumour motion. However as noted by Jani and colleagues 4D-PET/CT offers the chance to reduce these margins in an effort to minimise dose to normal tissue (Jani et al., 2015). In their phantom study Jani analysed the margins needed to be added to ungated PET and 4D-PET MIP volumes in order to maintain full ITV coverage. The margins required to be added to the 4D-PET MIP volumes to achieve full target coverage was nearly half that of the ungated PET (4.7mm vs 8.5mm, $p<0.05$). The authors hypothesised that a combination of 4D-PET MIP defined volumes and non-uniform margin could be used to reduce normal tissue dose.

4D-PET/CT AND DOSE PAINTING

PET/CT imaging to guide dose painting in radiation therapy is a new strategy to try and improve local control of lung tumours while limiting any increased dose to organs at risk (Shi et al., 2014). It involves delivering purposely inhomogeneous dose to a target with higher doses delivered to areas of higher risk. Initial feasibility studies described the use of standard PET/CT imaging without respiratory gating (Moller et al., 2011). However a recent paper by Yip and colleagues comparing textural features of 3D and 4D PET images highlight the need to take respiratory motion into account if dose painting is attempted (Yip et al., 2014). In their study of

34 lung lesions that completed a 3D and 4D PET/CT, the textural features of the tumours were better resolved on the 4D-PET compared to the 3D PET. If sub-volumes within a tumour are to be accurately contoured a 4D-PET is clearly required to properly contour the areas to receive a boost.

In parallel with advancements in the literature investigating the clinical utility of 4D-PET/CT an number of groups have looked into improving and refining the 4D-PET/CT technique through new hardware and quality assurance protocols.

RESPIRATORY TRACKING HARDWARE ADVANCEMENTS

The most common device for the tracking of respiratory motion is the Varian RPM system. A number of new breathing apparatus have been presented as a way to improve the tracking of patient respiratory motion. Koivumaki and colleagues presented a comparison of a bioimpedance-based respiratory tracking system to one of the current standard apparatus, the Varian RPM system (Koivumaki et al., 2015). Bioimpedance-based tracking uses changes in a weak electric current fed through the thorax to track the internal motion of organs. This method has been shown to be a highly accurate and was able to measure both respiratory phase and depth (Houtveen et al., 2006). Koivumako was able to show that the bioimpedance-based system could be used to gate PET images and was similar to the Varian RPM but with the added benefit of a more accurate measurement of organ motion.

Didierlaurent and colleges presented their new respiratory gating device, the pneumotachograph or SPI, based on air flow measured by bidirectional sensors (Didierlaurent et al., 2013). In their paper they also compared the new device to the Varian RPM system in the acquisition of a 4D-PET/CT scan. In a phantom experiment they were able to show the SPI device improved binning reproducibility when compared to the RPM system for irregular breathing patterns. The trigger time lag was found to be 0.0 +/- 37.1ms for the SPI system compared to -153.6 +/- 320.1 ms for the RPM system ($p<0.05$).

IRREGULAR BREATHING AND BREATHING TRAINING

The standard method for 4D-PET/CT acquisition does not involve any breathing training or coaching of patients. However Teo and colleagues recently showed that breathing irregularities can decrease the quantitative accuracy of 4D-PET/CT (Teo et al., 2012). Using a phantom study they showed that a gated PET under ideal conditions will produce SUVs that are within -5.4 +/- 5.3% of a static PET image. However, the accuracy of 4D PET decreased to -17.1 +/- 10.8% for a highly irregular breather. This was still better than PET imaging without any gating where the accuracy for a regular and highly irregular breathers was -28.5 +/- 18.2% and -27.9 +/- 18.2% respectively.

In an effort to address the issue of irregular breathing Yang and colleagues presented their work investigating an audio-visual (AV) feedback system designed to improve breathing regularity during a 4D-PET scan (Yang et al., 2012). In their phantom study

with and without AV biofeedback they showed a significantly smaller target diameter which indicated less image blurring ($p<0.001$). An AV feedback system could be an important tool to ensure reproducibility in breathing pattern between planning scans and radiotherapy treatment. However patients with significant airways disease may find compliance with this method difficult limiting its widespread use.

QUALITY ASSURANCE OF 4D-PET/CT

One area that until recently received little attention is the quality assurance of 4D-PET/CT scans. Dunn and colleagues presented a modified commercially available motion phantom (QUASAR, Modus Medical) that was able to replicate individual patients' respiratory motion (Dunn et al., 2012). This phantom could be used to verify a patient's specific respiratory profile so that a patient breathing pattern during a planning 4D-PET/CT scan could be replicated on a daily basis for their treatment.

In another effort to address quality concerns an end to end workflow with a respiratory motion phantom was developed by Bowen and colleagues (Bowen et al., 2015). In their phantom study they showed that without motion compensation imaging errors on a PET/CT scan due to respiratory motion can lead to treatment delivery errors of between 5-30%. The RT treatment errors were reduced to less than 2% when motion compensation methods were applied. The authors stated that the end to end phantom workflow they presented is a method of quality assurance

of 4D-PET/CT guided radiotherapy from the planning 4D-PET/CT scan to treatment delivery.

NEW 4D-PET/CT INDICATIONS

Much of the initial work looking into the use of 4D-PET/CT was concentrated on the motion of lung tumours. However recent studies have described the application of 4D-PET/CT outside the lungs. A new area of interest is the treatment of liver metastases using stereotactic radiotherapy. This is a highly conformal radiotherapy treatment technique that uses very small margins. As a result managing the effects of respiratory motion is important to ensure accurate tumour coverage. The use of 4D-CT scanning alone in this clinical scenario is problematic due to that lack of radiographic contrast. Without contrast liver lesions can be difficult to visualise on a CT scan. In one study of 18 patients being planned for SABR of liver lesions, Bundschuh and colleagues compared CT, MR and PET/CT target volumes (Bundschuh et al., 2012). They found that target volumes defined on 4D-PET/CT imaging had significantly lower interobserver variability compared to CT and MRI and was better at distinguishing tumour from scar tissue in previously treated patients ($p<0.01$). In this study 4D-PET/CT imaging also detected previously undocumented lesions in two patients that lead to management changes in those patients. The authors noted that 4D-PET is needed to optimised co-registration of the functional PET data to morphologic information. Riou and colleagues also reported that 4D-PET/CT better defined respiratory movements compared to 3D-PET/CT in a cohort of 14 patients

being planned for SABR of liver lesions (Riou et al., 2014). Again in Riou's study they reported one case where an additional undocumented liver metastasis was detected on the 4D-PET/CT that was not seen on the 3D-PET/CT.

Another organ affected by respiratory motion is the oesophagus. In a pilot study of 18 patients with oesophageal cancer Wang and colleagues showed that 4D-PET/CT was an appropriate method for contouring a GTV (Wang et al., 2012). However substantial work in this indication is needed to establish a role for 4D-PET/CT in oesophageal cancer. Other organs significantly influenced by respiratory motion are the kidneys and adrenals which are also potential targets for SABR

NORMAL LUNG FUNCTION ASSESSMENT USING 4D-PET/CT

The normal lung is a major dose limiting organ in the treatment of malignancies of the thorax with radiotherapy (Kong et al., 2011). In the treatment of lung cancer the lungs are contoured and dose limits are set as if the lungs are a single homogenous equally functioning mass. However from functional imaging exams like SPECT ventilation and perfusion (VQ) scanning it can be observed that there are often areas of the lung that are functioning better than others. An example of a patient with heterogeneous lung perfusion is shown in Figure 2.11(Page 69).

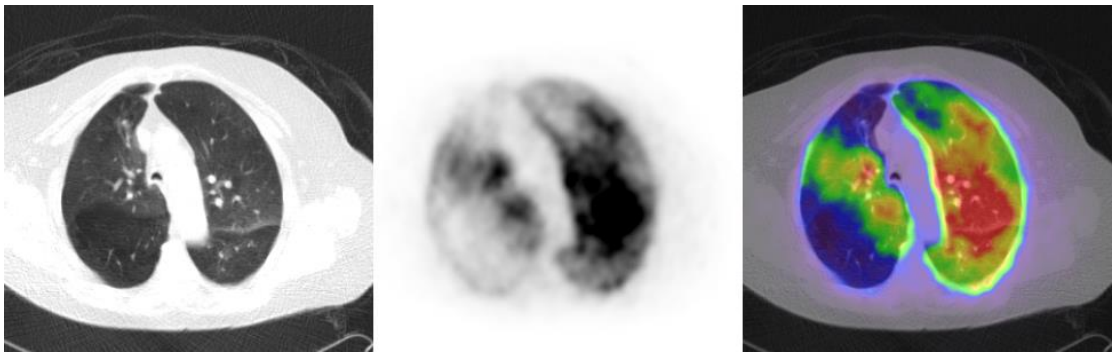

Figure 2.11 – Perfusion PET/CT scan

This is a trans-axial image of a CT scan fused with a perfusion PET scan that shows blood flow to aerated lungs. In the right most cell the red shows areas of well perfused lung and purple/blue areas are poorly perfused with blood. Images: J Callahan (2015)

Using the functional information obtained by SPECT perfusion imaging it has been shown that avoidance of functional lung is possible (Christian et al., 2005). In a publication by Hofman and colleagues it has now been shown that it is possible to perform a lung ventilation and perfusion scan on a PET scanner by substituting the standard radioisotope technetium-99m for the positron emitting gallium-68 (Hofman et al., 2011). This opens up the possibility of using respiratory gating in VQ scanning which is not available on a nuclear medicine gamma camera. By performing a VQ scan on a PET/CT scanner the higher resolution and sensitivity of the scanner can be utilised to more accurately measure the effects of radiation on the lung as shown by Siva and colleagues (Siva et al., 2015b). Recently progress has been made in the generation of a ventilation image from a 4D-CT scan alone (Kipritidis et al., 2014).

This would enable the omission of a separate ventilation scan to lower the radiation dose for patient having a VQ scan for any indication.

The next chapter of this thesis, published in *Cancer Imaging (Callahan et al., 2014b)*, addresses the first aim of this thesis, namely 4D-PET/CT in lung cancer diagnosis. When a patient initially presents with a suspicious lung nodule this lesion must be diagnosed. The data presented in chapter three looks at the added value of 4D-PET/CT in correctly characterising a suspicious lung lesion.

CHAPTER 3 - A PROSPECTIVE INVESTIGATION INTO THE CLINICAL IMPACT OF 4D-PET/CT IN THE CHARATERISATION OF SOLITARY PULMONARY NODULES.

Jason Callahan[1,3], Tomas Kron[2], Michal Schneider[3], Rodney J Hicks[1]

1. Peter MacCallum Cancer Centre, Division of Radiation Oncology and Cancer Imaging
2. Peter MacCallum Cancer Centre, Department of Physical Sciences
3. Monash University, Department of Medical Imaging and Radiation Science

Cancer Imaging, 2014, 14:24

The use of low-dose CT for screening of lung cancer has been shown to be an effective early detection method leading to a decrease is lung cancer related mortality (Church et al., 2013). However the increase in CT screening has led to a higher number of indeterminate solitary pulmonary nodules to be detected which is where FDG-PET plays a critical role (Alpert et al., 2015). Due to its aggressive nature the timely diagnosis of lung cancer can greatly affects a patient's outcome. If the effects of respiratory motion compromise the diagnostic accuracy of an FDG-PET/CT scans a patients overall prognosis can be affected. The addition of a 4D-PET/CT scan can remove the effects of respiratory motion and may an impact on management of patients with a suspicious lung nodule. The correct diagnosis of lung nodules is the first challenge for patients with lung cancer and this chapter presents a prospective evaluation of 4D-PET/CT to investigate its impact of the correct diagnosis of lung nodules.

3.1 INTRODUCTION

Solitary pulmonary nodules found incidentally by anatomical imaging modalities such as computerised tomography (CT) can present a challenging diagnostic problem. The use of fluorodeoxyglucose (FDG) positron emission tomography/ computerised tomography (PET/CT) to characterise a pulmonary nodule with a low to moderate pre-test probability of malignancy is now a well-established diagnostic paradigm (Gould et al., 2013). A meta-analysis of the use of PET/CT to correctly classifying solitary pulmonary nodules found that PET had a sensitivity of 88-96% and specificity of 70-90% for malignant nodules (Cronin et al., 2008). However, despite its high reported sensitivity and specificity one factor that can confound the interpretation of a PET/CT scan is the effects of respiratory motion, particularly when the lesion is small or close to the diaphragm (Osman et al., 2003).

The aim of using FDG-PET/CT is to measure the metabolic signal in a lung nodule to differentiate benign from malignant disease and this technique has been in clinical use for over two decades (Gupta et al., 1992). However, a lesion that is moving due to respiration can have significant mis-registration between PET and CT scan and an underestimation of the true lesion metabolic signal because of blurring and inappropriate correction for the effects of soft tissue attenuation (Nehmeh and Erdi, 2008, Callahan et al., 2011a, Garcia Vicente et al., 2010). If a malignant lesion in not correctly classified it may lead to a delay in the appropriate management of this lesion. A method to correct the effects of respiratory motion in PET/CT is respiratory

gated or 4D-PET/CT (Nehmeh et al., 2004). This technique entails the recording of the patients breathing pattern during the acquisition of the scan, followed by retrospectively creating a cine image of the patient breathing which removes the blurring effects of respiration.

While the effects of respiratory motion on measuring metabolic signal in PET/CT scanning are well known, it is still standard practice in most centres to scan patients while breathing freely with no correction for the effects of respiratory motion. This is mostly due to the increased complexity of acquiring a 4D PET/CT scan as well as additional equipment cost and scan time. There have been a number of studies describing improved co-registration and quantitation in lung lesions with 4D-PET/CT (Garcia Vicente et al., 2010, Lupi et al., 2009, Park et al., 2008). However, there has been much less information about the impact of 4D-PET/CT in the characterisation of pulmonary nodules as either benign or malignant. The most comprehensive paper looking at this question was a retrospective multi- centre study of 155 patients demonstrating that 4D-PET improved the overall accuracy in correctly classifying lesions from 85.7% to 92.8% (Guerra et al., 2012). One weakness of this study was the relative heterogeneity of the data in terms of technical specification of the various cameras, uptake times and acquisition parameters at the six centres involved in the study. Another study published in 2010 by Vicente *et al.* investigated the impact of 4D-PET/CT in 42 lung lesions with a very low FDG signal initially thought to be benign. They found a change in classification from benign to malignant in 17/42 (40%) cases (Vicente et al., 2010). To date there is a lack of prospective data in the

literature investigating the impact of using 4D-PET/CT in all patients with a radiologically-indeterminate SPN.

Hence, the aim of this study was to investigate the impact of 4D-PET/CT in the characterisation of solitary pulmonary nodules in a routine clinical environment, using a homogenous acquisition and automated processing technique with a current-generation, time-of-flight PET/CT device.

3.2 METHODS

PATIENT POPULATION

Twenty consecutive patients were prospectively recruited between November 2011 and July 2012. The study was approved by the Peter MacCallum Clinical Governance and Ethics Committee, and all patients provided written informed consent. All patients recruited had been referred to the Peter MacCallum Centre for molecular imaging to have a FDG-PET/CT to investigate a newly detected solitary pulmonary nodule on CT. Patients were included if they had a lesion of at least 10mm in size that was either deemed of indeterminate nature based on CT appearances or deemed not to be amenable to biopsy despite being considered suspicious of malignancy. A patient's pre-test risk of malignancy was not an inclusion criterion. Patients were included regardless of their smoking status or any prior malignancy.

PATIENT PREPARATION

After a fasting time of at least six hours, patients were administered with an FDG dose of 3.2 MBq/kg. Patients were instructed to lie quietly in an uptake room for at least 60 minutes. All patients were scanned on a GE-Discovery690 (GE Medical Systems Milwaukee, WI) with a mean uptake time of 66 min (range 60-75mins). Patients were positioned supine with their arms up and the infrared reflective marker block for the Varian RPM respiratory tracking system (Varian Medical Systems, Palo Alto, CA) placed on their abdomen. A standard whole body PET/CT (WB-PET) scan was completed and then immediately followed by a 4D-PET/CT centred over the pulmonary nodule of interest.

WHOLE BODY PET/CT ACQUISITION AND PROCESSING

Patients were instructed to breathe freely throughout the whole body PET/CT scan. A CT scan extending from the base of brain to the proximal thighs was acquired with the following exposure parameters; 140kv, Smart mA range 40-150, rotation time 0.5sec, pitch 0.984. This was immediately followed by a whole body-PET scan with the following acquisition parameters; 3D frame mode, 192matrix, 2.5mins/step, 11slice overlap. The WB-PET was then reconstructed using OSEM iterative reconstruction with 2 iteration, 18 subsets, 5mm Gaussian filter, time of flight and SharpIR .

4D-PET/CT ACQUISITION AND PROCESSING

Immediately following the completion of the WB-PET the patient moved into position to begin the 4D-CT scan. After moving the patient into position the breathing was allowed to stabilise and recorded using the Varian Real-Time Patient Monitoring (RPM) system. The Varian RPM system uses an infrared camera to track the motion of a box placed on the patient's abdomen. Once the breathing had stabilised, a step and shoot 4D-CT scan was performed using the following parameters: Cine CT, 10mA, 140kV, Cine duration = breathing period + 1.5secs, and the cine time between images = breathing period / 10. After completion of the 4D-CT scan, the respiratory trace was saved and a new trace was established to use for the 4D-PET.

Immediately after the 4D-CT was completed the patient was moved into the PET position and the breathing was allowed to stabilise again before beginning the PET acquisition. This was acquired as a 3D list mode acquisition while recoding the patient's breathing trace. The 4D-PET was acquired for 10 minutes.

The GE automatic phase matching software was used to process the 4D-PET/CT scan. The 4D-CT was retrospectively binned into five frames using the saved respiratory trace. The acquired 3D-List mode PET scan was retrospectively binned into five frames and each phase of the 4D-PET was automatically corrected for attenuation with the respective phase of the 4D-CT. The 4D-PET was reconstructed using the same reconstruction parameters as the WB-PET.

CHARACTERISATION OF LESIONS

A five point scale as outlined by Fletcher et. al. (Fletcher et al., 2008) was used to classify the nodules. Fletcher's five point criteria are outlined in Table 3.1 (Page 80). The scans were reported as a single read where the physician was first shown the WB-PET/CT scan and asked to characterize the pulmonary nodule using the five categories. The same reporting physician was then shown the 4D-PET/CT scan and asked if the additional information changed the classification of the pulmonary nodule. In order to replicate our usual reporting process, the reporting clinician was able to review all relevant clinical information and any prior imaging results. The reporting physician also incorporated the morphologic appearances of the nodules into account when classifying nodules into the five categories as per standard clinical practice. For example a solid nodule with smooth well-defined margins and no uptake was likely to be benign whereas a lesion with high uptake and a densely spiculated margin is likely to be malignant. If based on all the available information the nodule could not be confidently categorised as either benign or malignant they were categorised as indeterminate. For indeterminate nodules on CT, the PET scan was given a stronger weighting than the CT appearances but for lesions unsuitable for biopsy, both modalities were considered in arriving at a final diagnosis. Accordingly, the initial diagnosis was risk-adapted and only the incremental diagnostic information of the gated study was assessed. The 20 scans were reported by four imaging specialists who each had a minimum of 10 years clinical reporting experience.

PATIENT FOLLOW-UP

Patients were followed up until a definitive diagnosis was obtained. Follow up was obtained for all 20 patients and compared to the WB-PET and 4D-PET diagnosis. If the nodule was resected, histopathology was used to confirm the diagnosis. Any lesions that resolved on subsequent imaging without oncological intervention were considered of a benign origin.

STATISTICAL ANALYSIS

Frequencies were calculated for the five classification types to compare the frequencies of classification in WB-PET/CT and 4D-PET/CT scanning. The sensitivity, specificity and accuracy with confidence intervals were also calculated to compare the findings of the two scanning techniques. As an indeterminate lesion is neither benign nor malignant we have calculated the accuracy with indeterminate lesions classified as either being all malignant or all benign. This is the same method employed by Guerra et. al. to look at the added diagnostic value of 4D-PET/CT (Guerra et al., 2012). A McNemars test was used to detect any difference in the proportion of lesions classified as indeterminate on WB-PET/CT compared to 4D-PET/CT.

Table 3.1 - Fletcher's PET and CT criteria for rating SPN

Category	Relationship between SPN18F-FDG uptake and likelihood of malignancy	Relationship between CT SPN characteristics and likelihood of malignancy
Definitely benign	No increased uptake—uptake essentially the same as in reference lung tissue (generally corresponds to an SUV of 0.6–0.8)	Central laminated or diffuse calcification Popcorn pattern of calcification Lesion with cavitation and wall thickness <1mm
Probably Benign	Uptake substantially less than in blood pool (general mediastinal activity) but greater than in reference lung tissue (SUV greater than 0.6–0.8 but less than 1.5–2.0)	Large (>2 cm) dominant nodule with satellite lesions Solid nodule with polygonal shape or smooth and well-defined margin Diameter <10 mm; lobulated margin contours
Indeterminate	Uptake 2–3 times that in reference lung tissue but less than in blood pool (generally corresponds to SUV of 1.5–2.0 but less than 2.5)	All other characteristics not defined in other likelihood categories
Probably Malignant	Uptake greater than in blood pool (blood pool generally corresponds to an SUV of 2.5)	Diameter>2 cm (nodules .3 were excluded from study) Ground-glass opacity with round shape Mixed ground-glass opacity with central zone of high attenuation
Definitely Malignant	Uptake much greater than in blood pool—anything substantially greater than SUV of 2.5	Densely spiculated margin, ragged margin Lesion with cavitation and wall thickness >16 mm

3.3 RESULTS

LESION DIAGNOSIS

As outlined in Figure 3.1 (page 81), 13 patients had a diagnosis confirmed by histopathology, 4 resolved on imaging (mean 6 months, 3.7-11.6 months) and 3 were stable more than 12 months after the PET scan (mean 14 months, 12-18 months)._ Of note are three patients that were classified as probably benign on imaging but showed an interval increase in size at an early imaging follow-up. These were subsequently confirmed as malignant on histopathology without and interval change in stage. Thus, only 2 patients underwent biopsy for a non-malignant process and no patients were inappropriately observed.

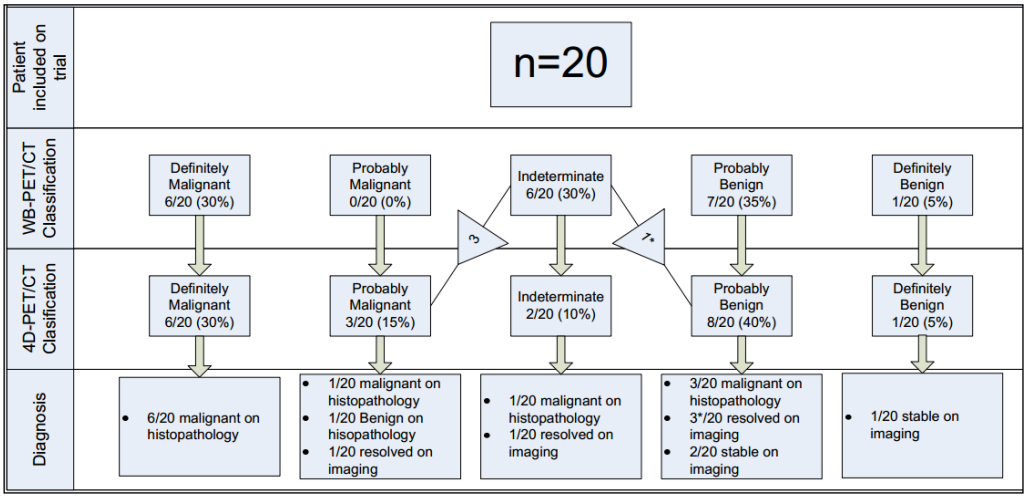

Figure 3.1 – 3D and 4D SPN classification

Classification of solitary pulmonary nodules observed on WB-PET/CT and 4D-PET/CT scans and subsequent diagnosis (Total N lesions = 20)

IMPACT OF 4D-PET/CT IN LESION CLASSIFICATION

The proportion of patients in each category and their subsequent diagnosis are outlined in Figure 3.1 (page 81). In this cohort, there were no changes in the PET classification of nodules initially classed as either benign or malignant on standard WB PET/CT. The only changes in classification between WB and 4D-PET/CT scans were in lesions initially classified as indeterminate.

LESIONS INITIALLY CLASSIFIED AS BENIGN OR MALIGNANT ON WB-PET/CT

Fourteen out of the 20 patients were classified as either benign (8/20 (40%)) or malignant (6/20, (30%)) based on the WB-PET/CT result. Of these fourteen cases there was no change in lesion classification with the addition of the 4D-PET/CT. All six cases classed as malignant, were subsequently confirmed true positive. Three out of the eight lesions classified as benign on FDG-PET were subsequently found to be malignant on follow up indicating they were incorrectly classified on both WB and 4D-PET/CT scans. One of the three incorrectly classified lesions was a carcinoid, while the other two were small adenocarcinomas.

LESIONS INITIALLY CLASSIFIED AS INDETERMINATE ON WB-PET/CT

Six of the 20 lesions (30%) were initially classified as indeterminate on the WB-PET/CT scan. The results for these six lesions are outlined in Table 3.2 (Page 83). In four out of these six lesions, the 4D-PET/CT influenced the reporting physician to change their classification. However the reduction in the proportion of indeterminate lesions from 6/20 to 2/20 was not statistically different (p=0.1336).

Table 3.2 – Indeterminate Solitary pulmonary nodules

This table shows the progression of lesions initially categorised as indeterminate on Whole Body PET/CT, any change in classification with the additional 4D-PET/CT and in lesions final diagnosis.

WB-PET/CT finding	4D-PET/CT finding	Final Diagnosis	Method of diagnosis
Indeterminate	Indeterminate	BENIGN	Resolution on imaging
Indeterminate	Indeterminate	MALIGNANT	Lesion Resected - Adenocarcinoma
Indeterminate	Probably Benign	BENIGN	Resolution on imaging
Indeterminate	Probably Malignant	BENIGN	Lesion Resected - Granulomatous
Indeterminate	Probably Malignant	BENIGN	Resolution on imaging
Indeterminate	Probably Malignant	MALIGNANT	Lesion Resected - Carcinoid

In one out of these four cases, the continued absence of metabolic signal on the 4D-PET/CT in a lower lobe lesion influenced the physician to classify the lesion as probably benign, which was found to be correct. In three out of the four cases higher FDG signal was detected (SUVmax increase: 1.8-4.8 [167% increase], 1.4-2.0 [43%] and 1.8-2.5 [34%], respectively) on the 4D-PET/CT scan leading the reporting physician to classify the lesion as more likely to be malignant. Two of three of these lesions were subsequently found to be benign. Figure 3.2 (page 85) shows an

example of a 2.6cm lesion that was initially indeterminate but changed to probably malignant based on the additional signal detected on the 4D-PET/CT. This lesion was subsequently resected and found to be a granulomatous lesion. Figure 3.3 (page 86) shows a case where the higher SUVmax on the 4D-PET/CT influenced the reporting physician to reclassify the lesion from indeterminate to probably malignant. This was subsequently resected and found to be malignant. Table 3.3 (page 84) shows the relative sensitivity, specificity and overall accuracy for in initial classification on the WB-PET/CT alone and then with the addition of the 4D-PET/CT. If all indeterminate lesions were defined as malignant irrespective of acquisition method, the 4D-PET/CT scan had a sensitivity, specificity and accuracy the WB PET/CT but these results did not reach statistical significance. However, when the indeterminate lesions were defined as benign, the accuracy and specificity of 4D-PET/CT was lower than WB PET/CT with the addition of the due to two additional false positive findings that had been classified as benign on the WB-PET/CT scan but again the results did not reach statistical significance.

Table 3.3 - Sensitivity, specificity

The relative sensitivity, specificity and overall accuracy with 95% confidence intervals of WB-PET/CT compered to 4D-PET/CT in (total N=20) when indeterminate lesions were classified as either being Malignant (left column) or Benign (right column)

	Indeterminate as malignant		Indeterminate as Benign	
	WB-PET/CT	4D-PET CT	WB-PET/CT	4D-PET CT
SENSITIVITY	73% (39-93%)	69% (39-91%)	55% (23-83%)	67% (35-90%)
SPECIFICITY	56% (21-86%)	71% (29-96%)	100% (66-100%)	75% (35-97%)
Accuracy	65% (35-87%)	70% (39-90%)	75% (51-91%)	70% (39-90%)

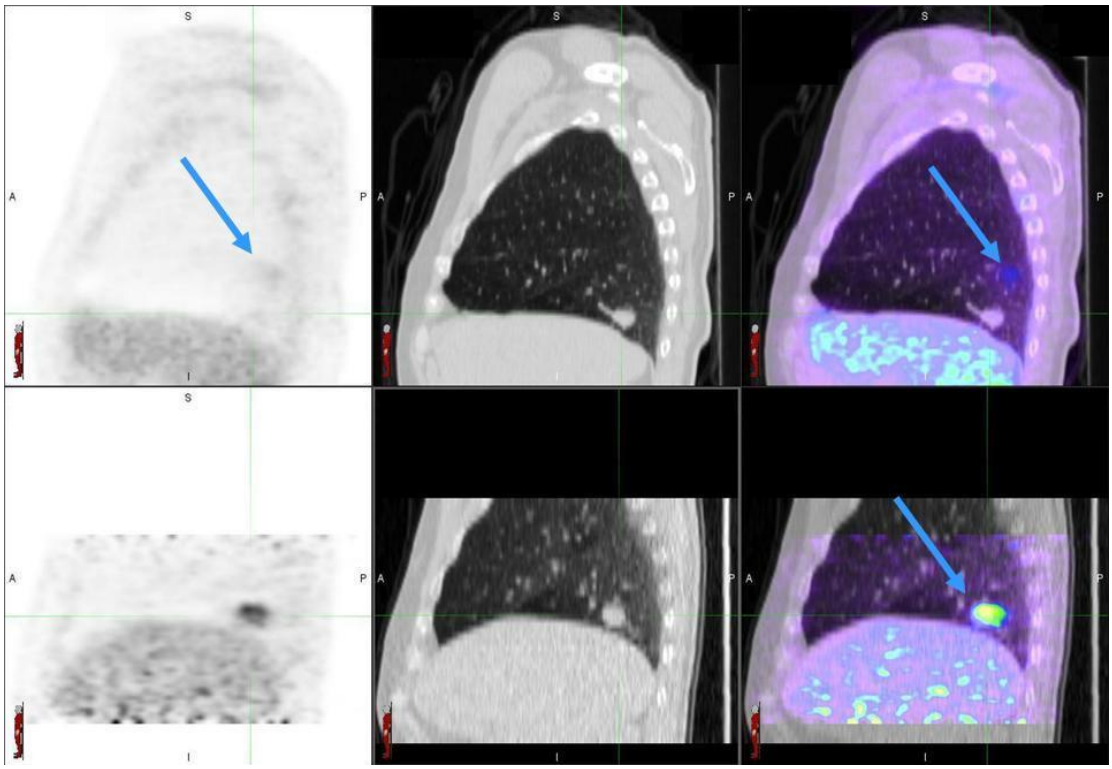

Figure 3.2 – 3D versus 4D PET/CT

Lesion in the Right Lower Lobe was initially indeterminate based on the WB-PET/CT scan (top row - SUVmax=1.8). The 4D-PET/CT scan (bottom row –SUVmax=4.8) revealed FDG uptake in the lesion influencing the reporting physician to re-classify the lesion as probably malignant. The blue arrow in the top left hand cell shows how the significant mis-registration between the PET and CT scans is then well corrected on the 4D-PET/CT in the bottom right hand panel.

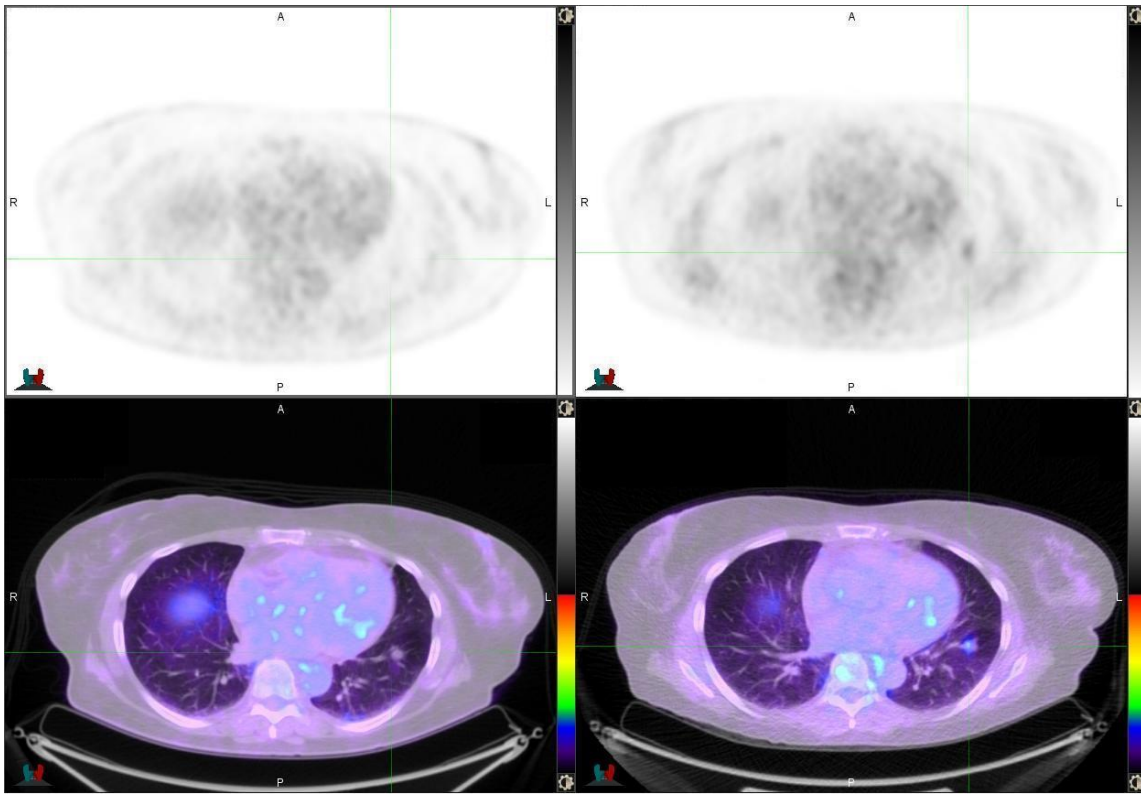

Figure 3.3 – 3D versus 4D PET/CT

Lesion in the left lower lobe that was original classified on the WB-PET/CT (left column) as indeterminate and was subsequently changed to probably malignant on the 4D-PET/CT (right column). The SUVmax increased from 1.4 to 2.0. This lesion was subsequently confirmed as an adenocarcinoma.

3.4 DISCUSSION

At our facility, the use of PET/CT to classify solitary pulmonary nodules is restricted to lesions that are either indeterminate on CT criteria or, if suspected to be malignant, considered to be unsuitable for percutaneous biopsy. In the latter situation, FDG PET/CT is used both for planning the best technique and site for biopsy (Kalade et al., 2008) and for staging in the event that malignancy is confirmed. Accordingly, there is a significant pre-test selection bias in this prospective series. However, we believe this to be an appropriate clinical setting in which to evaluate the incremental value of respiratory-gated (4D) PET/CT.

We have found that when the reporting physician is able to classify a lesion as either benign or malignant on conventional WB PET/CT, an additional 4D-PET/CT did not change their diagnosis. The only clinical situation where the 4D-PET/CT was found to impact the reporting physician's classification was when the initial finding on the WB-PET/CT was considered to be indeterminate. In this study, the rate of indeterminate findings reduced from 30% to 10% with the addition of 4D-PET/CT. This is consistent with the work by Guerra and colleagues who noted that the main discrepancy between WB-PET/CT and 4D-PET/CT was in indeterminate findings which were reduced from 24.3% to 4.4% with the addition of a 4D-PET/CT (Guerra et al., 2012).

In the four indeterminate lesions that had a change in classification from indeterminate to probably malignant, two were found to be benign. It is clear that mitigating the effects of the respiratory motion artefact to provide a more representative estimation of true FDG-avidity does not change the inherent weakness of FDG in differentiating between a malignant lesion and an inflammatory process (Figure 3.2 and Figure 3.3). Additionally, respiratory gating can't overcome the issues posed by partial volume effects or improve the sensitivity of PET in the presence of low FDG-avidity, as seen in some low-grade malignant nodules including carcinoid tumours.

The results of this prospective cohort is also similar to that presented by Vicente et al (Vicente et al., 2010) who showed that in lesions with low FDG avidity (N = 42) the addition of 4D-PET/CT decreased specificity (100% to 72%) due to additional false positive findings. However, there was an increase in the overall accuracy (from 45% to 62%), due improved sensitivity. As has been shown in a number of studies, the 4D-PET/CT scanning technique removes the respiratory motion artefact and reveals the true metabolic signal (Lupi et al., 2009, Nehmeh et al., 2004, Garcia Vicente et al., 2010). While an improvement in the sensitivity of detection of malignancy may be desirable, even at the risk of additional false positives, most tumours with low FDG-avidity tend to have a less aggressive natural history and it may be reasonable to observe these for growth on CT rather than subjecting patients to the morbidity that can be associated with pathological characterisation.

It has been proposed that dual time point imaging may be useful in differentiating benign from malignant lung nodules (Lin et al., 2012). However, a meta-analysis did not find that this technique improved the overall accuracy of FDG-PET for this indication (Lin et al., 2012). This may be because the lung nodules at both time points are still affected by respiratory blurring. The dual time point method assumes an increase in SUV uptake is indicative of malignancy but one needs to consider that the measurement of SUV in moving lesions is less accurate (Guerra et al., 2012, Lupi et al., 2009, Nehmeh and Erdi, 2008, Vicente et al., 2010)**.** An additional confounding factor for lesions subject to the respiratory motion in standard WB-PET/CT is inaccurate attenuation correction due to mis-registration. The dual time point method does not address any of these confounding factors. In this study, the 4D PET/CT was performed after the WB PET/CT and it is therefore possible that some of the increased sensitivity observed related to delayed imaging.

The routine addition of a 4D-PET/CT using this acquisition protocol is unlikely to be feasible for all patients in a busy clinical PET centre. The described 4D-PET/CT scanning technique requires additional scan time, infrastructure and patient co-operation. There is also an increase in radiation dose due to the 4D-CT scan. This is a particularly important consideration in the patient cohort who may not have any malignancy. Therefore, it is important to determine when to apply this scanning technique to improve the overall accuracy of FDG-PET. The results of this and other studies study suggest that the most efficient use of 4D-PET/CT is in those pulmonary nodules that are of an indeterminate nature based on the standard WB-PET/CT

technique. This process requires the reporting physician to review the WB-PET/CT prior to the patient leaving the imaging centre. While this can be disruptive for those patients completing a 4D-PET/CT it will avoid a lot on unnecessary 4D scanning for lesions that are unlikely to have their classification impacted by a 4D scan.

A limitation of the data presented is the relatively small number of patients. However, given that the results are similar to the larger retrospective cohort of Guerra *et al., (Guerra et al., 2012)* we believe that these prospective findings strengthen the overall body of evidence demonstrating that 4D-PET/CT is best applied in indeterminate pulmonary lesions.

In this paper we have also not used a SUVmax cut off for the classification of malignancy because any cut off value is arbitrary and certainly an optimal diagnostic threshold has not been defined for modern time-of-flight scanners or using respiratory gating to date. The lesion shown in Figure 2 had a SUVmax of 4.8 but was subsequently found to be granulomatous. While this lesion was incorrectly classified as malignant, in reality the clinical implication of this result is that malignancy should be excluded by early pathological characterisation if possible. Also, as shown in a recent paper by Lee et. al. (2012), the degree of FDG uptake is dependent on the tumour type meaning that an arbitrary cut off value may incorrectly classify lower grade tumours (Lee et al., 2012). It is for these reasons that an arbitrary SUVmax cut-off value without taking into account the patient's likelihood for malignancy is likely to be less accurate.

With the widespread use of CT to detect solitary pulmonary nodules there will be an increasing need to use PET to characterise indeterminate lesions found by this imaging modality (Zhan et al., 2013). Adenocarcinoma is now the most common lung malignancy, which will challenge the ability of FDG-PET to correctly classify lesions due to the variability in glucose uptake across the different type of adenocarcinomas (Lee et al., 2012). An additional 4D-PET cannot overcome false positive or negatives due to tracer kinetics, but there may be an impact on management if glucose uptake sufficiently predicts mitotic behaviour allowing allocation to a CT observational strategy without concern of interval stage migration. A 4D acquisition may be a tool to improve the overall accuracy of FDG-PET in this setting.

3.5 CONCLUSION

The addition of 4D-PET/CT is most likely to have an impact on those nodules initially classified as indeterminate on standard WB-PET/CT. In lesions classified as benign or malignant on standard WB-PET/CT the addition of a 4D-PET/CT is less likely to impact lesion classification. While 4D-PET/CT does improve the measurement of the metabolic signal, it does not overcome inherent limitations of FDG in differentiating a malignant lesion from inflammatory processes, correct for partial volume effects or compensate for the low intrinsic FDG-avidity of some malignancies.

The next chapter addresses the second aim of this thesis which is to validate the use of 4D-PET/CT in radiation therapy planning. After a lung cancer has been diagnosed the next step is to treat the cancer. A lung cancer that cannot be removed surgically is typically treated with radiation therapy. The next chapter presents a novel post-processing method to make 4D-PET/CT feasible to be used in the planning of radiation therapy.

CHAPTER 4 - VALIDATION OF A 4D-PET MAXIMUM INTENSITY PROJECTION FOR DELINEATION OF AN INTERNAL TARGET VOLUME.

Jason Callahan[1,4], Tomas Kron[2,6], Michal Schneider-Kolsky[4], Leon Dunn[3], Mick Thompson[1], Shankar Siva[5,6], Yolanda Aarons[5], David Binns[1] and Rodney J Hicks[1,6]

1. Peter MacCallum Cancer Centre, Department of Cancer Imaging
2. Peter MacCallum Cancer Centre, Department of Physical Sciences
3. RMIT university, Department of Applied Physics
4. Monash University, Department of Medical Imaging and Radiation Science
5. Peter MacCallum Cancer Centre, Department of Radiation Oncology
6. The University of Melbourne, Peter MacCallum Department of Oncology

Int J Radiation Oncol Biol Phys, Vol. 86, No. 4, pp.749-754, 2013

The first and most important step in the treatment of a lung tumour with radiation therapy is defining the target. For a lung lesion that is moving due to normal respiration often both a PET/CT and 4D-CT are acquired to help define the target. A post processing technique to create a maximum intensity projection from the 4D-CT is a commonly used and validated clinical tool. However the 4D-CT technique does have its limitations, particularly when a tumour abuts other soft tissue structures. At the commencement of this thesis there was no validated 4D-PET equivalent of the 4D-CT method. In this chapter I present our work validating a 4D-PET maximum intensity projection as a clinical tool that can be used to define the target to be treated with radiotherapy.

4.1 INTRODUCTION

Technological advances in the field of radiation oncology have made it possible to deliver a highly conformal and accurate radiation dose to a target tissue (Martel, 2004). Techniques such has intensity modulated radiotherapy and stereotactic ablative body radiotherapy (SABR) allow the precise shaping of the radiation dose around a 3D target (Bezjak et al., 2012, Goldsmith and Gaya, 2012). Accompanying the rapid implementation of these novel techniques is often a reduction in radiation therapy margins, which reinforces the importance of accurate target delineation.

The internal target volume (ITV) used in radiotherapy planning accounts for motion or variation in size, shape or position of the clinical target volume due to physiological variations (Chavaudra and Bridier, 2001). For radiation therapy planning of lung tumours the major consideration for the ITV is respiratory motion. Two commonly used strategies for defining the ITV of lung tumours is either FB-PET/CT scan or a 4D-CT scan. A FB-PET scan is performed in multiple beds steps of between 2-5mins. The blurred target outline on the FB PET scan can be help to define the ITV (MacManus et al., 2009). The more common method is to use a 4D-CT derived maximum intensity project (MIP) to define the ITV.

A staging PET/CT scan is currently considered standard of care for lung cancer patients prior to commencement of therapy due to its high impact on management (Hicks et al., 2001, Gregory et al., 2012). In recent years the PET/CT scan had also been incorporated into the radiotherapy planning process due to its high tumour to

background ratio when compared to CT (MacManus et al., 2009). This is especially the case in areas affected by atelectasis, lung collapse and nodal disease (Greco et al., 2007). As FB-PET is an equilibrium acquisition scan, some researchers have proposed that an ITV can be delineated directly from the visualised target on FB-PET (Caldwell et al., 2003). However, the assumption that lesion blurring on a FDG PET scan takes into account all the lesion motion ignores a number of important confounding factors. Firstly, this assumption does not account for the incorrect application of attenuation correction due to mis-registration between the PET and CT scans (Killoran et al., 2011). Secondly, it ignores the fact that the dwell time of a lesion due to different breathing patterns is likely to have an impact on the apparent distribution of activity (Callahan et al., 2011b). Additionally, if a lesion is adjacent an area of higher background activity, such as the liver, than the blurred area caused by respiration can blend into the background. These confounding factors mean that it is likely that the blurring effect caused by respiration will result in an underestimation of the true ITV.

It has been possible for a number of years to perform a 4D-PET scan (Nehmeh et al., 2004). There have also been technological advances on the newest generation of PET/CT scanners that allow automatic phase matching between a 4D-CT and 4D-PET to improve attenuation correction and anatomical correlation. There has been some work investigating the accuracy of 4D-PET to define target volumes (Aristophanous et al., 2012), by dividing the 4D-PET into multiple bins which are contoured individually and then summed to create an overall ITV.

In this study we validate the concordance between a new post-processing reconstruction technique, the 4D-PET-MIP and the standard 4D-CT-MIP in both a phantom and patient data across multiple breathing patterns and lesion sizes. We also compare 4D-PET-MIP volumes to summed 4D-PET volumes. The paper builds on work by Lamb *et al.* who recently described the use of a 4D-PET-MIP to define an internal target volume (Lamb et al., 2011). Presented in this study is a validation of 4D-PET-MIP in both phantom and patient data. It is our hypothesis that a 4D-PET-MIP will generate volumes more concordant with 4D-CT-MIP than FB-PET in both a phantom and in patients with lung lesions. We also investigate whether the ITV is underestimated on FB-PET/CT when compared to 4D-PET/CT-MIP.

4.2 METHODS AND MATERIALS

PHANTOM STUDIES

In order to test our hypothesis a phantom was designed that could be imaged on both CT and PET cameras. We mixed FDG with radiographic contrast so that there was spatial and density consistency for both CT and PET scans. The phantom was prepared with a high target to background ratio to reduce uncertainty in contour the edge of lesions.

PHANTOM 1 – AIR BACKGROUND

A water tight container with three hollow spheres (Data Spectrum, Hillsborough NC) suspended in air was prepared. The volumes of the three spheres were: 0.5, 1.0 and 2.0 mL with outer diameters of 11.9, 14.4 and 17.8 mm. The spheres were filled with a solution of F-18 and radiographic contrast. A solution of radiographic contrast and saline was mixed to a concentration of 0.004ml of contrast to every 1mL of saline. To this solution F-18 was added producing an activity concentration of 114kBq/mL. These spheres had average HU units of 350.

PHANTOM 2 – SOFT TISSUE BACKGROUND

In order to simulate lesions in a soft tissue background a second solution of radiographic contrast and saline was prepared and added to the container. The concentration of radiographic contrast and saline was 0.001ml of contrast to every 1mL of saline. This produced a background with average HU units of 100. To this solution F-18 was added producing an activity concentration of 5 kBq/mL

Motion patterns

A Perspex body phantom (Modus Medical Quasar) was modified for programmable motion control and used to reproduce realistic patient breathing patterns (Dunn et al., 2012). After observation of 100 patient breathing traces from patients undergoing a 4D-PET/CT scan, we identified four general categories of breathing patterns that would be tested in this phantom study outlined below

PHANTOM – ACQUISITION OF FREE BREATHING AND 4D-PET/CT SCANS

The phantom was scanned on a GE-Discovery690 (GE Medical Systems Milwaukee, WI) PET/CT scanner with the Varian RPM respiratory tracking system (Palo Alto, CA). Using the programmable respiratory motion device, a four second breathing period and two cm of superior-inferior motion was used for each breathing pattern. Four PET/CT scans were performed sequentially.

Type 1 – Inspiration (2 seconds) = Expiration (2 seconds)

Type 2 – Inspiration (1 second) < Expiration (3 seconds)

Type 3 – Inspiration (3 seconds) > Expiration (1 second)

Type 4 – Expiration pause (2 Seconds)

For each scan, first a 4D-CT scan was performed using the following parameters: 10mA, 140kV, 0.4 sec cine time between images and cine duration of 5 seconds. Immediately thereafter, a PET scan was acquired as a list mode acquisition with the respiratory trace recorded by the Varian RPM system for 10 minutes. The phantom experiment was then repeated with a background of radiographic contrast mixed with F-18 to an average HU value equivalent to soft tissue.

PATIENT SELECTION

A total of 32 patients with either a primary or secondary lung lesions were available from ongoing institutional review board approved prospective trial protocols that included a 4D-PET/CT scan. All patients were scanned on the GE Discovery690 PET/CT scanner. Patients were included if they met the following criteria:

- Free breathing whole body PET/CT and 4D-PET/CT acquired sequentially in the same session without the patient mobilising from the scanning table
- Homogenous FDG avid lung lesion surrounded by air to allow clear delineation without interference by normal structures
- At least 5mm of lesion motion caused by respiration as measured by 4D-CT

A total of nine patients met all eligibility criteria and were included for the analysis.

IMAGE RECONSTRUCTION

The moving phantom acquisitions were reconstructed as un-gated (free breathing), gated (4D) PET and 4D CT scans. The phantom scans, whole body PET/CT and 4D PET/CT scans were reconstructed using the following parameters: OSEM iterative reconstruction with 4 iterations and 9 subsets, 192x192 matrixes, 55mm FOV and a slice thickness of 3.27mm. Both the 4D-CT and PET images were reconstructed into 10 bins based on a percentage of the respiratory cycle (i.e. 0%, 10%,…). The GE automatic phase matching was used for attenuation correction of the 4D PET images. The phase matching process automatically matches each CT phase to the

corresponding PET phase for attenuation correction. A 4D-CT maximum intensity projection (4D-CT MIP) was generated from the 4D-CT data using the GE-Advantage4D software package.

An in house image analysis program (MARVn-3.31) was used to generate a 4D-PET maximum intensity projection (4D-PET-MIP). The generation of a 4D-MIP was performed in the same manner as the generation of a 4D-CT MIP. The maximum voxel value for each voxel across the 10 bins was used as the new voxel value in the 4D-MIP reconstruction.

LESION CONTOURING

In both the phantom and patients the lesions were contoured on the following image data sets:

1. FB-CT
2. 4D-CT-MIP
3. FB-PET
4. 4D-PET-Sum (volumes from 10 bins are summed)
5. 4D-PET-MIP

PHANTOM

The three spheres of the phantom were contoured using the MIM image contouring tools (MIM-5.4.4, MIM Software Inc. Cleveland, OH). The spheres on the PET scans were contoured using a 40% of Max threshold technique and the PET edge contouring tool. The spheres on the CT scan were automatically contoured using a HU cut-off of 200.

PATIENTS

The lesions on the PET scans were also contoured using MIM with a 40% of max threshold and the PET edge contouring tool. The CT lesions on the patient scan were contoured by a single experienced technologist using the 3D brush tool in one sitting. All contours were reviewed by a board certified radiation oncologist.

DICE CO-EFFICIENT (DC)

The concordance between the volumes contoured on the 4D-CT-MIP and the FB-PET as well as those contoured on the 4D-CT MIP and the 4D-PET-MIP was measured using a DICE co-efficient (DC) (Hanna et al., 2010). A DC of 1 indicates perfect concordance between the PET and CT volumes. A DC of 0 indicates no concordance between the two volumes.

The DC was calculated using the following formula:

$$\frac{2 \text{ x } \text{CTvol} \cap \text{PETvol}}{\text{CTvol} + \text{PETvol}}$$

CT_{vol} = CT internal target volume

PET_{vol} = PET internal target volume

STATISTICAL ANALYSES

All statistical tests were carried out using GraphPad Prism 5 (GraphPad Software, LaJolla, Ca) and a p-value of < 0.05 was deemed significant. The average, range and standard deviation (SD) of the DC between the groups were also compared.

4.3 RESULTS

A selection of the images acquired of the phantom are shown in Figure 4.1 (Page 104). A visual inspection of the images revealed that the 4D-PET MIP images were more concordant with 4D-CT MIP than FB-PET. The size, shape and distribution of activity on the FB-PET image appear to be influenced by the breathing pattern. A breathing period that does not a have equal inspiration and expiration period appears to create an area of high activity when compared to the rest of the lesion. The effect is not apparent on the 4D-PET MIP images with homogenous distribution

of activity across all lesion sizes except for the smallest lesion in the type 4 breathing pattern. The most marked influence of breathing pattern affecting the apparent distribution of activity was observed in the type 4 breathing pattern. This breathing pattern has the longest dwell time in a single position creating a 'hot spot' with a faint tail.

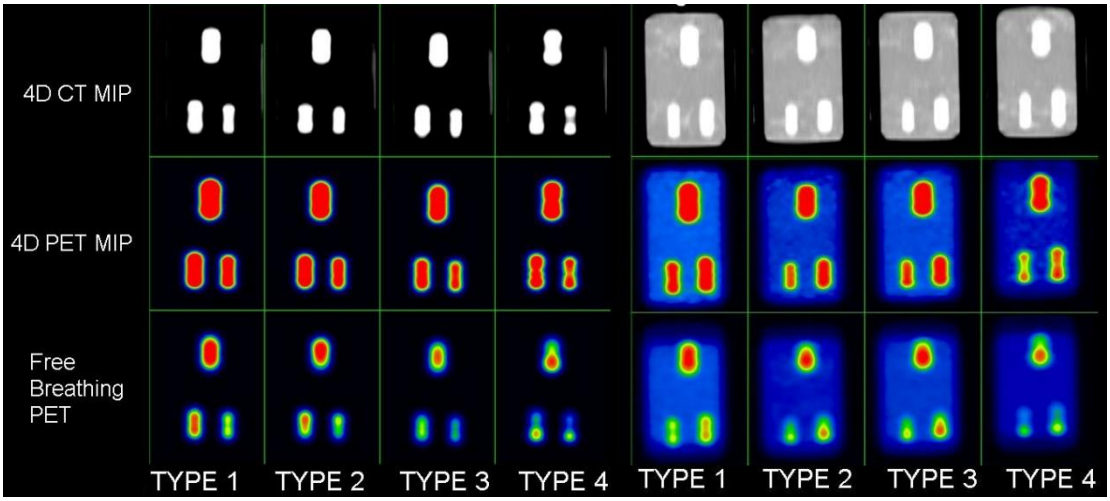

Figure 4.1 – 4D-PET MIP in a phantom

Imaging results from the phantom across all breathing patterns with and without background. Top row: 4-dimensional computed tomography maximum intensity projection images. Middle row: 4-dimensional positron emission tomography maximum intensity projection images. Bottom row: free-breathing positron emission tomography images.

VOLUME CONCORDANCE IN A PHANTOM

Table 4.1 (page 105) shows the average DC in air and background using the two segmentation techniques. The FB-PET/CT showed the lowest volume concordance across all lesions sizes, breathing patterns, in air and with background using two segmentation techniques. A paired t-test showed no significant difference in volume concordance between summed 4D-PET and 4D-PET-MIP with either segmentation technique in either air (p=0.1285, p=0.0621) or background (p=0.0059, 0.0569). There was a significant difference in volume concordance between 4D-MIP and FB-PET with both segmentation techniques in air (p=0.0017, p=0.0461) and background (p=0.0085, p=0.0045).

Table 4.1 – Dice coefficient in a phantom

	Mean DC 40% of Max	Range	SD	Mean DC PET Edge	Range	SD
4D-PET/CT MIP - AIR	0.84	0.72-0.99	0.07	0.73	0.6-0.79	0.07
4D-PET Sum/CTMIP - AIR	0.82	0.61-0.96	0.07	0.75	0.55-0.84	0.07
FB PET/CT - AIR	0.73	0.53-0.90	0.09	0.67	0.52-0.76	0.09
4D-PET/CT MIP - Background	0.78	0.57-0.89	0.10	0.73	0.62-0.86	0.07
4D-PET Sum/CTMIP - Background	0.75	0.54-0.92	0.11	0.76	0.67-0.87	0.08
FB PET/CT - Background	0.63	0.15-0.83	0.09	0.62	0.44-0.81	0.08

Abbreviations: 4D = 4-dimensional; CT = computed tomography; DC = Dice coefficient; FB = free-breathing; max = maximum; MIP = maximum intensity projection; PET = positron emission tomography; SD standard deviation; sum = summed

VOLUME CONCORDANCE IN PATIENTS

Nine consecutive patients met the inclusion criteria and were included for analysis. Table 4.2 (page 106) is a summary of the volume concordance between the different groups. As in the phantom experiment the poorest volume concordance was in the FB-PET/CT group. A paired t-test showed no significant difference in volume concordance between the 4D-PET-MIP and 4D-PET summed groups using both segmentation techniques (p=0.3353, p=0.7377). A paired t-test showed a significant difference between the 4D-PET/CT ground and the FB-PET/CT group using both segmentation techniques (p=0.0004, p=0.0006).

Table 4.2 – Dice coefficient in patient cohort

	Mean DC 40% of Max	Range	SD	Mean DC PET Edge	Range	SD
4D-PET/CT MIP	0.72	0.66-0.78	0.04	0.73	0.63-0.79	0.05
4D-PET Sum/CT MIP	0.70	0.57-0.81	0.07	0.73	0.55-0.82	0.09
FB PET/CT MIP	0.62	0.45-0.80	0.10	0.57	0.41-0.74	0.10
FB PET/CT	0.45	0.22-0.58	0.13	0.44	0.25-0.66	0.15

Abbreviations: 4D = 4-dimensional; CT = computed tomography; DC = Dice coefficient; FB = free-breathing; max = maximum; MIP = maximum intensity projection; PET = positron emission tomography; SD standard deviation; sum = summed

TARGET VOLUMES IN PATIENTS

Figure 4.2 the difference between FB-PET volumes and 4D-PET-MIP. The FB-PET volumes were on average 40% (SD: 20%, range: 13%-68%) smaller than 4D-PET

volumes using a 40% of max threshold and 45% (SD: 23%, 3%-73%) using PET edge. A paired t-test showed the difference between the volumes in the two groups was significantly different using both segmentation techniques (p=0.0006, p=0.0005). The patient example in Figure 4.3 (page 108 shows how the blurring effect on the FB-PET can underestimate the ITV when compared to the 4D-PET-MIP volume.

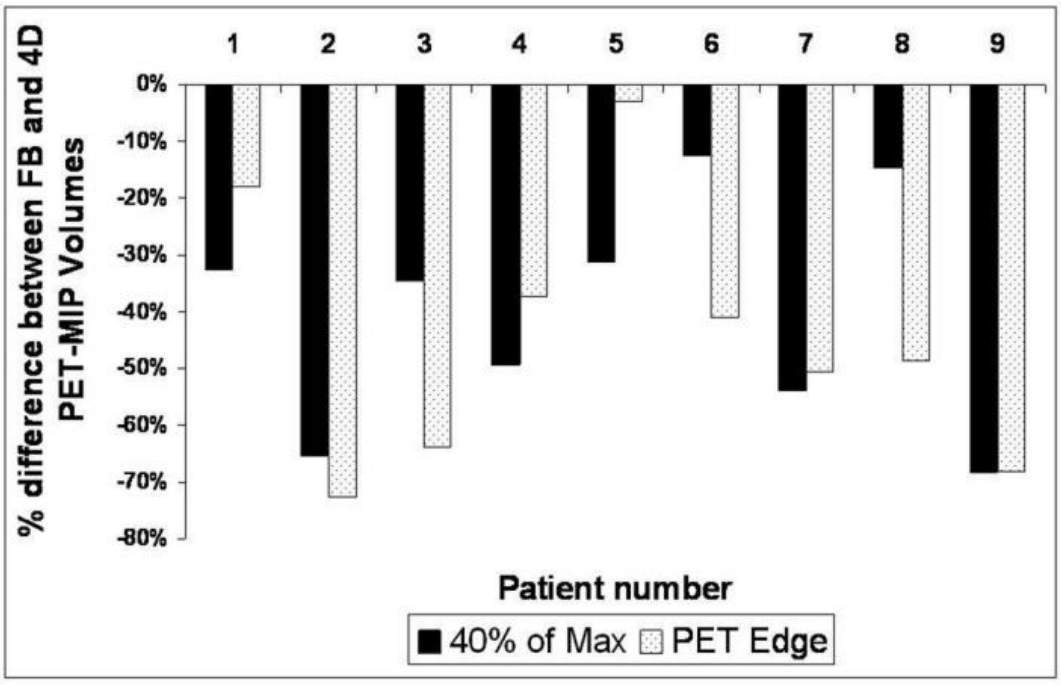

Figure 4.2 – 3D versus 4D tumour volumes

Difference between free-breathing positron emission tomography and 4-dimensional positron emission tomography volumes in nine patients according to both 40% and positron emission tomography edge contouring.

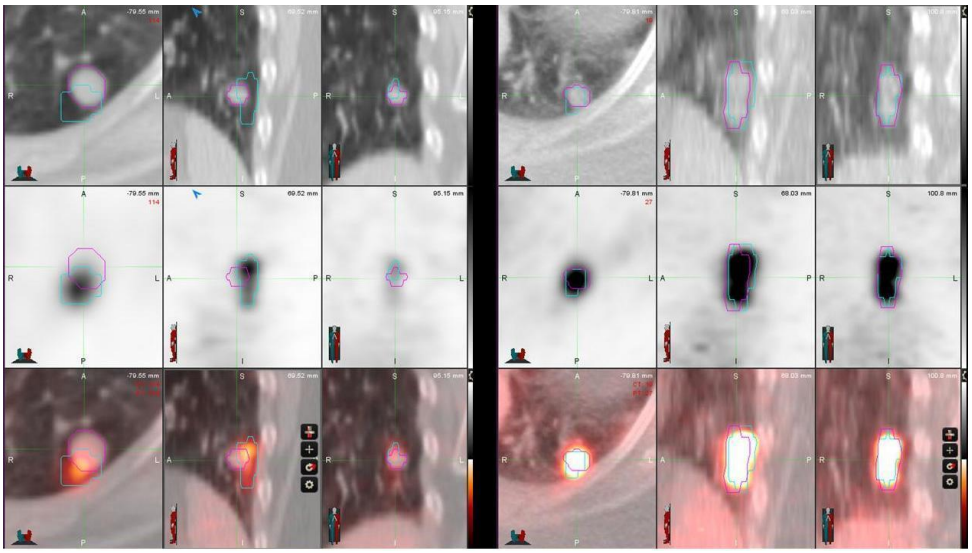

Figure 4.3 – 3D versus 4D patient volume comparaison

Left lower lobe lung lesion in a 65-year-old woman who was a candidate for stereotactic ablative body radiation therapy, showing the poor concordance between the free-breathing positron emission tomography and free-breathing computed tomography volumes (left) compared with the high concordance between 4-dimensional positron emission tomography/computed tomography and computed tomography maximum intensity projection (right).

4.4 DISCUSSION

Oncologists are familiar with the 4D-MIP concept from 4D-CT and clearer delineation may afford more conformal treatment with less side effects. The uncertainties caused by the blurred edge of a FB-PET/CT or the lack of soft-tissue contrast on the 4D-CT-MIP are less present on a 4D-PET-MIP. A 4D-PET-MIP is likely to be more practically useful than a summed 4D-PET in the busy clinical environment as only one volume needs to be contoured rather than individual bins.

In this work we have shown that a 4D-PET MIP reconstruction analogous to 4D-CT-MIP produces volumes more concordant with 4D-CT MIP than FB-PET. We have also shown that there is no significant difference between summed of 4D-PET volumes and a single 4D-PET-MIP volume and that FB-PET consistently underestimates the ITV when compared to 4D-CT MIP.. This is consistent with the recent publication by Hanna and colleagues (Hanna et al., 2012b). In their work comparing ITV derived from FB-PET/CT to 4D-CT MIP in 16 patients receiving stereotactic ablative radiotherapy (SABR) the target volumes derived from FB-PET did not correspond well to those derived from 4D-CT-MIP.

In conventional lung radiation therapy without respiration correlation, large margins are built into the PTV in order to account for uncertainties associated with respiratory motion. These large margins are likely to compensate for the underestimation when using FB-PET for ITV delineation. However in recent years techniques such as SABR have been introduced for patients with lung cancer and lung metastases (Creach et al., 2012). In SABR the margins are much smaller and fewer fractions are given so an underestimated ITV is likely to have more of a clinical impact. A method to manage the effects of respiratory motion is paramount in high precision techniques such as SABR and a 4D-PET/CT-MIP provides a clinically practical solution. It will be particularly useful for lung lesions that are close or connected to other soft tissue structures.

The apparent heterogeneous distribution of activity on a FB-PET observed in this study would have implications for dose painting based on heterogeneous PET

uptake. The process of dose painting involves escalating radiation dose to areas of high FDG uptake within a tumour as described by van Elmpt at al (van Elmpt et al., 2012). The concept of dose painting assumes that areas of higher SUV are as a result of a biological difference in the tumour. We have shown in our phantom study that areas of apparently high FDG avidity can be created by non-sinusoidal patient breathing patterns. The blurred edges in FB-PET can also confound any automatic segmentation methods as there is no certainty where the edge of the tumour lies. Therefore biological dose painting and dose intensification based primarily on differential FDG-PET avidity within lung tumours should be approached with caution when using FB-PET alone. Care should be taken to manage the effects of respiratory motion if dose painting based on PET uptake is being considered among tumours affected by respiratory motion.

Limitations of this work include the limited number of patients studied as well the effect that tumour heterogeneity has on a 4D-PET-MIP. It is likely that a large heterogeneous tumour may present some challenges in defining a contour on a 4D-PET MIP using any automated method. A larger cohort of patients with many different tumour sizes, shapes and morphology should be conducted to further investigate the strengths and limitation of the PET-MIP technique. This work also does not look at lesions that are adjacent to soft tissue structures such as the liver, mediastinum or chest wall. Due to the high contrast on a 4D-PET-MIP it is likely that definition of ITVs in these areas could be more reproducible than a 4D-CT-MIP which

has poor soft tissue contrast. This work also only employs a single observer and more work into inter-observer variability in ITV delineation with a PET-MIP would be warranted. The mixing of radiographic contrast with FDG may have caused a minor overestimation of SUV in the phantom. In a study by Aide et. al. the overestimation of SUV cause by contrast mixed with tracer to a concentration of 100 HU was 2.6% (Aide et al., 2011). This is a similar concentration to that used is our phantom and this was not considered clinically relevant. We have also not looked at how well lesions are visualised on a 4D-PET-MIP compared to a 4D-CT-MIP when a lesion has very low FDG avidity.

4.5 CONCLUSION

A 4D-PET-MIP produces volumes with the highest concordance with 4D-CT-MIP across multiple breathing patterns and lesion sizes in both a phantom and among patients with solitary lung nodules. There is no significant different between summed 4D-PET volumes and 4D-PET-MIP volumes. Free Breathing PET/CT consistently underestimates ITV when compared to 4D PET/CT for a lesion affected by respiratory motion.

The next chapter addresses the third aim of this thesis and was published in the journal *Radiation Oncology (Callahan et al., 2014c)*. The data in the next chapter goes on to investigate the differences between the current standard of 3D-PET/CT for target volume delineation compared to the validated 4D-PET/CT method described in chapter four.

CHAPTER 5 - GEOGRAPHIC MISS DUE TO RESPIRATORY MOTION: A COMPARISON OF 3D VS 4D PET/CT DEFINED TARGET VOLUMES

Jason Callahan[1,4], Tomas Kron[2,6], Shankar Siva[5,6], Nathalie Simoens[7], Amanda Edger[5], Sarah Everitt[5], Michal E Schneider[4] and Rodney J Hicks[1,6]

1. Peter MacCallum Cancer Centre, Department of Cancer Imaging
2. Peter MacCallum Cancer Centre, Department of Physical Sciences
3. RMIT university, Department of Applied Physics
4. Monash University, Department of Medical Imaging and Radiation Science
5. Peter MacCallum Cancer Centre, Department of Radiation Oncology
6. The University of Melbourne, Peter MacCallum Department of Oncology
7. University of Nijmegen, Netherlands

Radiation Oncology, 12/2014; 9(1): 291

The work presented in chapter four shows that a 4D-PET-MIP is equivalent to a standard 4D-CT-MIP. This means that using 4D-PET/CT for target volume delineation is now a viable clinical tool which will bring all the established advantages of PET for target delineation. In this chapter we look at the implications of respiratory motion in terms of the risk of missing a tumour if the standard 3D scanning methods are used. This chapter will present a substantial rationale for moving from 3D to a 4D planning environment.

5.1 BACKGROUND

The use of integrated PET/CT in establishing radiotherapy target volumes is becoming increasingly accepted as the optimal approach for many malignancies, in particular lung cancer (MacManus et al., 2009, Greco et al., 2007). When defining target volumes for lung cancer the information obtained from the two imaging modalities provides complementary information about both tumour morphology (CT) and physiology (PET) (Grills et al., 2007). This allows optimal definition of the tumour with good reproducibility while sparing delivery of dose to normal organs (Bayne et al., 2010, Mac Manus et al., 2006). However a lung tumour can exhibit significant respiratory motion due to normal breathing, thus increasing the risk of geographic miss (Seppenwoolde et al., 2002, Ross et al., 1990). Therefore, target volumes need to be defined in order to minimize the potential of geographic miss during respiratory motion.

In many centres, PET/CT scans acquired in the radiotherapy treatment position is typically performed without compensating for the effects of respiratory motion. Areas most affected by respiratory motion are the lungs, liver and upper abdomen, particularly for structures close to the diaphragm. The standard method to account for motion is to apply a large margin to the gross tumour volume (GTV) to ensure adequate tumour coverage in a one-size fits all approach. However, a number of studies have found that target volumes are underestimated on a standard 3D-PET/CT scan when compared to target volumes defined on respiratory gated or 4D

imaging (Callahan et al., 2013, Hanna et al., 2012a, Lamb et al., 2011). This is primarily due to the effect of respiratory motion leading to count averaging across voxels through which the lesion moves or in which it resides for a relatively short period of the respiratory cycle.

When respiratory motion is taken into account the most common approach is to acquire a 4D-CT scan and this has become a routine clinical tool in some centres (Keall et al., 2006, Wang et al., 2013, Li et al., 2008). A recent study has found that adding a 4D-PET to a 4D-CT scan alters target volumes for lung tumours in approximately 23% of cases (Guerra et al., 2014). This would indicate that it may be important to incorporate both 4D-PET and 4D-CT information into the planning process.

The purpose of this study was therefore to investigate geographic miss of lung tumours due to respiratory motion for target volumes defined on a standard 3D-PET/CT scan when compared to target volumes defined on a 4D-PET/CT scan, assuming that the tumour should reside within the target volume for 100% of radiation delivery. In addition, we assessed the potential of applying individualised margins by exploring the degree of geographic miss when different margins are applied to the target volume to investigate the potential of individualised margins.

5.2 METHODS

PATIENTS

A total of 29 consecutive patients with staged for pulmonary malignancy that had completed both a 3D-PET/CT and 4D-PET/CT contemporaneously between August 2011 and May 2012. All patients gave their informed consent to participate in a study. Patients were included if they had an ^{18}F-fluoro-2′-deoxy-d-glucose (FDG) avid lung nodule with an SUV greater than 2.0 and larger than 15mm in smallest diameter. These levels were chosen to minimise the effects of partial voluming and to ensure that the lesion could be resolved on the PET scan. This study was approved by the Clinical Research and Ethics Committee of the Peter MacCallum Cancer Centre.

SCANNING PROTOCOL

All patients were scanned on a GE Discovery 690 (GE Medical Systems Milwaukee, WI). The patients were scanned using the same acquisition protocol outlined in our previous work validating a 4D-PET maximum intensity projection (MIP) for target volume delineation (Callahan et al., 2013). The protocol involves first acquiring a standard whole-body PET/CT with the patient breathing freely. Then a single bed step 4D-PET/CT scan centred over the lesion of interest is immediately acquired after the standard PET/CT without the patient moving in between scans.

GROSS TUMOUR VOLUME (GTV) DEFINITION

The lesion contouring protocol used was based on our published work that uses information from both the PET and CT scans to define the GTV (Bayne et al., 2010). All lung lesions were contoured by a single radiation oncologist experienced with this protocol. First, a 3D-GTV was defined on the standard whole-body PET/CT scan. Then a 4D-GTV was defined by the same observer on a 4D-PET/CT MIP. The 4D-PET/CT MIP consisted of a fused 4D-CT MIP and 4D-PET MIP as outlined in our previous work (Callahan et al., 2013). All contouring was performed on MIM Maestro imaging software (MIM 5.4.4, MIM Software Inc. Cleveland, OH, USA).

PLANNING TARGET VOLUME (PTV) DEFINITION

Using the MIM contour expansion tool eight PTV's were created, four 3D-PTV contours and four 4D-PTV contours. Firstly, three symmetrical PTV contours were created by expanding the 3D-GTV isotropically by 5mm, 10mm, and 15mm. Subsequently, an asymmetrical contour was created by expanding the GTV anisotropically by 15mm in the superior/inferior (SI) direction and 10mm in the axial directions. Finally, these same four PTV's (5mm, 10mm, 15mm and anisotropic) were then created based on the 4D-GTV. This process is illustrated in Figure 5.1.

.

TREATMENT PLANNING

All plans were generated on the XiO planning system (Computerized Medical Systems CMS, St Louis, MO, USA) using 6MV photons with 120 leaf millennium multileaf collimator (MLC) on a Varian machine. A 2.5mm grid size was used and a fast superposition algorithm to account for tissue inhomogeneity. Each plan contained three or four fields arranged according to the tumour and critical organ location, prescribing 60Gy in 30Fractions consistent with institutional protocols and ICRU guidelines. All plans were calculated for 95% of the prescribed dose covered the PTV.

Each case had four plans developed, beginning with the 15mm FB-PTV. The same beam arrangement was maintained for subsequent volumes, FB-10mm, FB- 5mm and Asymmetrical FB-PTV. The MLC arrangement was adjusted for the variation in volume size. The plans were transferred to the corresponding 4D - PTV and dosimetry was analysed using the dose volume histogram tool.

MEASUREMENT OF TUMOUR MOTION

The tumour was first contoured on the 4D-CT scan in peak expiration phase when the tumour has the least amount of motion. Then the contour was automatically propagated across all the 4D-CT phases with deformable contour propagation (Yakoumakis et al., 2012). The contours were manually checked for any gross errors introduced by the automatic process. This process copied a contour from one image

to the next and applied a deformation to the contour to account for movement of an object. The motion of the tumour was measured by recording the distance the centroid position of the contour moved in the SI plane.

After contouring the patients were placed into 4 motion groups based on the amount of motion in the superior/inferior (SI) plane. The motion groups used were; < 5mm, ≤ 10mm, 10 ≤ 20mm and greater than 20mm. The tumour size was automatically measured in the superior/inferior plane by MIM. The ratio of the lesion motion to tumour size was then investigated for correlation between motion and miss. For example a 20mm lesion that moved 20mm would have a motion to size ratio of 1.0. If a 40mm lesion motion moved 20mm the ratio would be 0.5. This parameter takes into account both tumour size and motion.

ANALYSIS OF GEOGRAPHIC MISS

Our previously published criteria were adapted to investigate geographic miss in 3D vs 4D defined target volumes (Everitt et al., 2009). 4D-PET/CT has been shown to account well for tumour motion it was considered the reference for which the 3D-PET/CT was compared against (Park et al., 2008, Callahan et al., 2011a, Geets, 2013). The types of geographic miss were defined as follows:

- Type 1 miss – Any part of the 4D-GTV outside the 3D-PTV
- Type 2 miss – Any part of the 4D-PTV outside the 3D-PTV
- Type 3 miss – Any part of the 4D-PTV receiving less than 95% of the prescribed dose (where planning was based on the 3D-PTV.

The Type 3 miss was further divided into four groups:

- No Type 3 miss – 100% 4D-PTV receiving 95% of the prescribed dose
- Minor Type 3 miss – >95% of 4D-PTV receiving 95% prescribed dose
- Moderate Type 3 miss – 90-95% OF 4D-PTV receiving 95% prescribed dose
- Significant Type 3 miss – <90% of the 4D-PTV receiving 95% prescribed dose

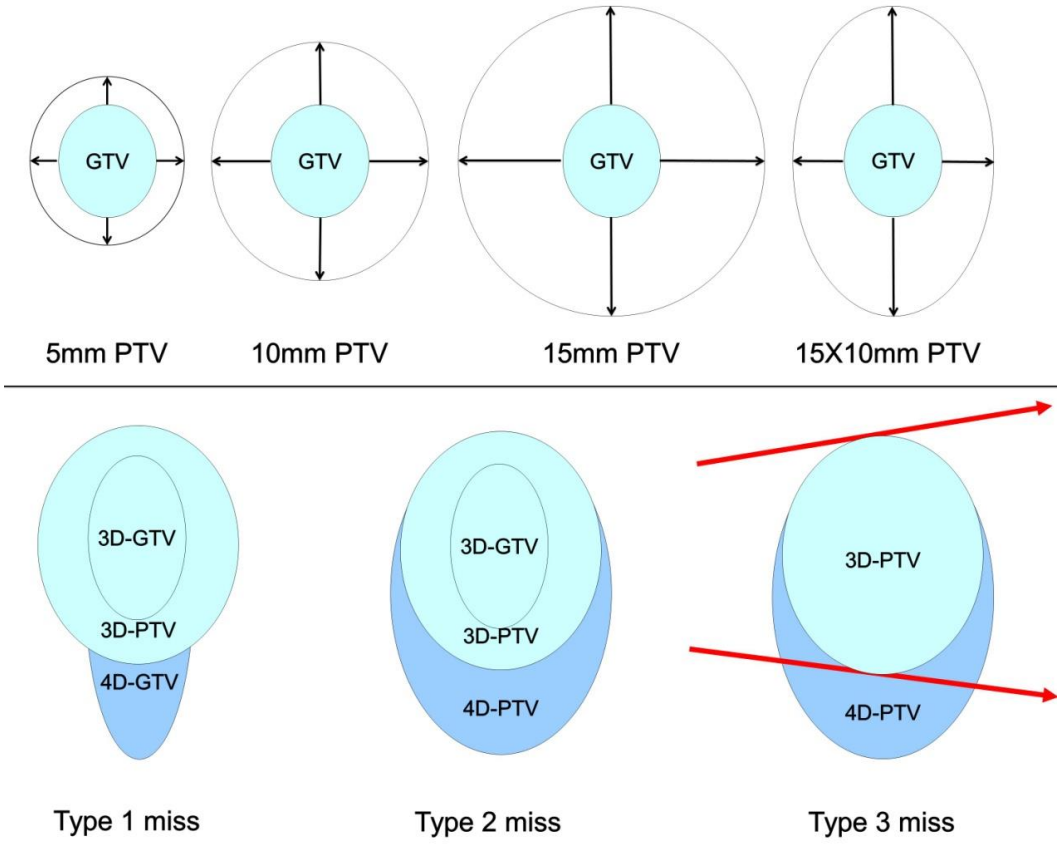

Figure 5.1 – Margin expansions and geographic miss.

The top row shows the four different margin expansions applied to the GTV to create four PTV contours. The bottom row shows the types of geographic miss as a result of tumour motion due to respiration investigated.

DATA ANALYSIS

All statistical tests were carried out using GraphPad Prism 5 (GraphPad Software, LaJolla, Ca). The mean (±SD) 3D and 4D volumes were compared and tested for difference using a paired students' t-test. For each type of miss the mean (±SD) volume that was missed was calculated. A chi-squared test was used to determine if there was a difference in the proportion of patients with a miss between the different PTV margin groups. Pearson's correlation coefficients were used to examine the association between lesion motion and the volume of geographic miss as well as the ratio of size to motion and geographic miss. A p-value of < 0.05 was deemed a significant difference.

5.3 RESULTS

VOLUME COMPARISON

29 patients were included in the study with a mean age of 68 (range 45-87), 18 (62%) patients were male and 11 (38%) were female. A comparison of the 3D and 4D volumes is shown in Table 5.1 (page 122). The 4D-GTV was on average 50% (range 2%-446%) larger than the 3D-GTV ($p<0.01$). In turn the 4D-PTV's were larger than the 3D-PTV's across all margins applied ($p<0.01$). The 10mm 4D-PTV was on average 19% smaller than the 15mm 3D-PTV ($p<0.01$).

Table 5.1 – 3D versus 4D Volumes
A comparison of mean 3D-PET/CT defined volumes to 4D-PET/CT defined volumes (total n = 29)

	3D Volume (ml)	4D Volume (ml)	Diff	p value
GTV	15.7	23.5	50%	0.0013
PTV 5 mm	38.5	53.9	40%	0.0001
PTV 10 mm	72.8	96.1	32%	<0.0001
PTV 15 mm	119.2	155.9	31%	<0.0001
Asym	85.5	112.0	31%	<0.0001
15 mm vs 10 mm	119.2	96.1	19%	<0.0001

TYPE 1 MISS - ANY PART OF THE 4D-GTV OUTSIDE THE 3D-PTV

The proportions of patients with a Type 1 miss are shown in Figure 5.2a (Page 123). When a standard 15mm or asymmetrical PTV margin was used there was only one case of Type 1 miss in the group with the highest range of lesion motion. There was a significant difference in the proportion of patients with a Type 1 miss between the symmetrical PTV groups (15mm vs 10mm; p=0.02, 10mm vs 5mm; chi-squared test, p<0.01). There was no difference between the standard 15mm PTV group and the asymmetrical PTV group.

As the lesion motion in the superior/inferior plane increased the proportion of patients with a Type 1 miss increased across all PTV margins (Figure 5.2a – Page 123). Additionally, as the motion increased the percentage volume of the 4D-GTV that was missed by the 3D-PTV increased across all margins (Figure 5.2b – Page 123). An example of a patient with a type 1 miss using all four PTV margins is shown in Figure 5.3 (page 124).

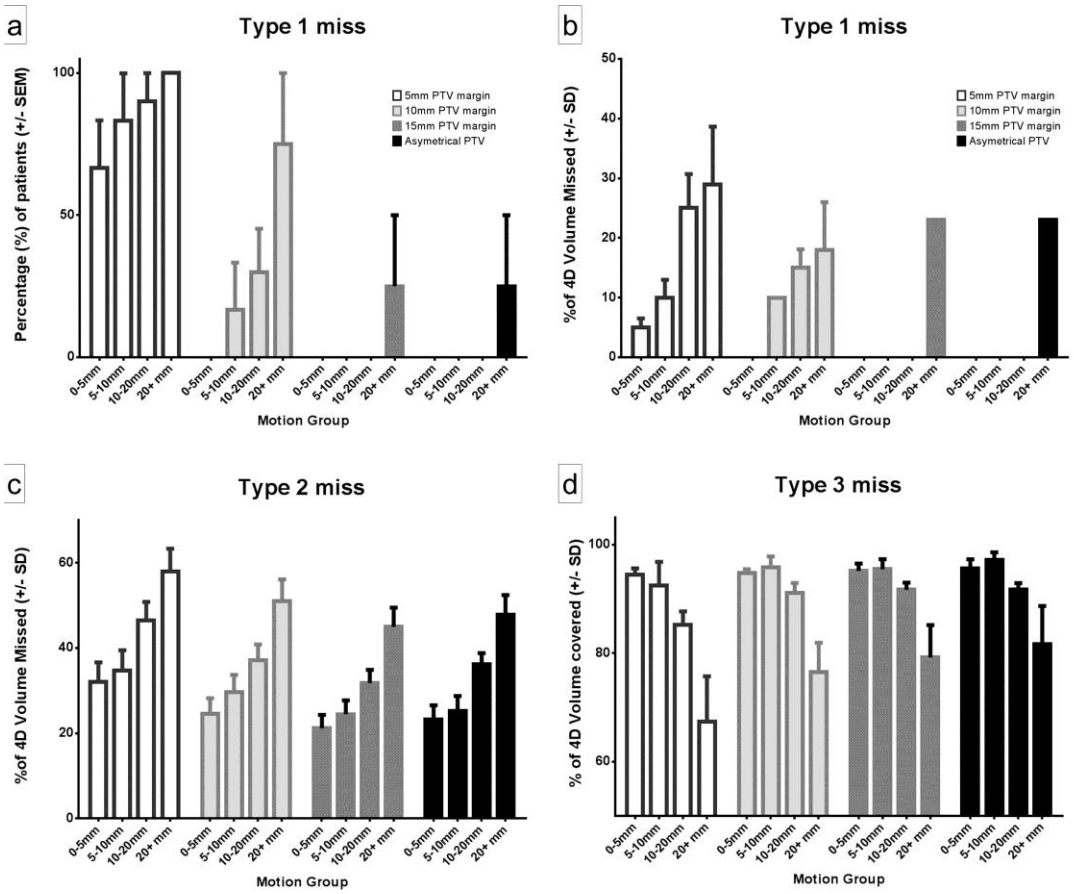

Figure 5.2 – Summary of results for the three types of geographic miss.

a) The proportions of patients with a type 1 miss in the four motion groups using the different PTV margins.
b) The mean % of the 4D-GTV that was missed by the 3D-PTV when there was a type 1 miss.
c) The mean % of the 4D-PTV that was missed by the 3D-PTV.
d) The mean coverage of the 4D-PTV with 95% of the prescribed dose.

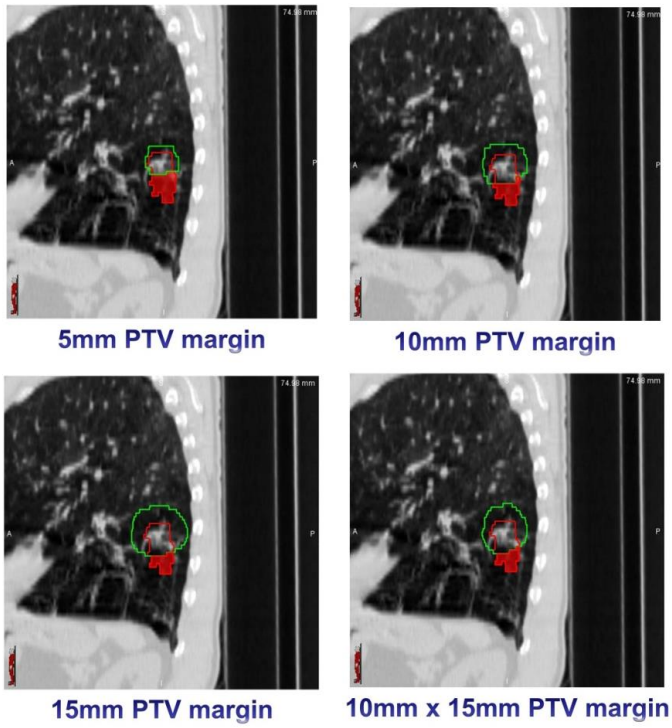

Figure 5.3 – Type 1 Miss

CT scan of a patient with a small lower lobe tumour. The 4D-GTV is shown in red and the 3D-PTV is shown in green. The highlighted red area is the part of the 4D-GTV that was not covered by the 3D-PTV for the margin applied.

TYPE 2 MISS - ANY PART OF THE 4D-PTV OUTSIDE THE 3D-PTV

All patients for all PTV margins had a Type 2 geographic miss. The mean percentage of the 4D-PTV that was missed by the 3D-PTV is outlined in Figure 5.2c (Page 123). A Pearson correlation showed a significant correlation ($p<0.01$) between lesion motion and the amount of the 4D-PTV that was missed by the 3D-PTV across all PTV margins (15mm r = 0.61, 10mm r = 0.60, 5mm r = 0.53, asym r = 0.60). A stronger correlation was found when the motion to lesion size ratio was used (15mm r = 0.67, 10mm r = 0.66, 5mm r = 0.65, asym r = 0.68).

TYPE 3 MISS - ANY PART OF THE 4D-PTV RECEIVING LESS THAN 95% OF THE PRESCRIBED DOSE (WHERE PLANNING WAS BASED ON THE 3D-PTV)

There was a Type 3 miss in 25 out of 29 cases in the 5, 10, and 15mm PTV margin groups. The asymmetrical margin had one additional Type 3 miss. The mean coverage of the 4D-PTV by the 3D-PTV plan is outlined in Figure 5.2d (Page 123). A Pearson correlation showed an association ($p<0.01$) between lesion motion and the percentage of the 4D-PTV that was missed by the 3D-PTV with all PTV margins (15mm r = 0.57, 10mm r = 0.54, 5mm r = 0.57, asym r = 0.47). A stronger correlation was found when the motion to lesion size ratio was used (15mm r = 0.61, 10mm r = 0.60, 5mm r = 0.64, asym r = 0.57). An example of a patient with a significant Type 3 miss is shown in Figure 5.4 (Page 125).

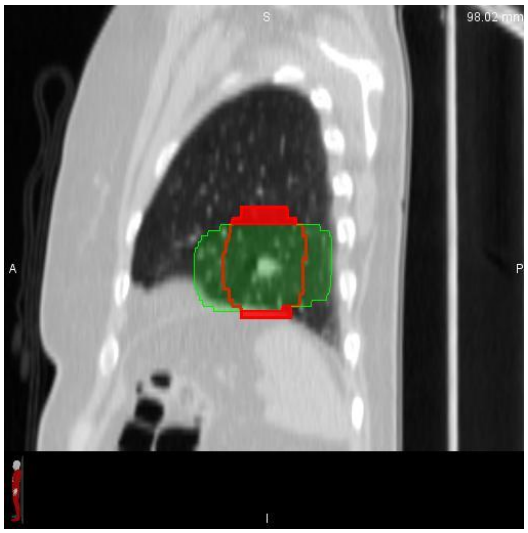

Figure 5.4 – Type 3 miss

A CT scan of a patient with a small lower lobe tumour. The 4D-PTV is shown in red and the green area show the 95% isodose line. The solid red area is the part of the 4D-PTV that would not receive the prescribed dose and constitutes a Type 3 geographic miss.

Table 5.2 below outlines the data for the severity of the Type 3 miss based on the average 4D-PTV coverage. On average if there was less than 5mm of motion any miss was minor (< 5%) and not likely to be clinically significant. When there was a high range of lesion motion (> 20mm) the average target volume coverage resulted in a significant Type 3 miss. The mean coverage with 95% of the prescribed dose in the >20mm group was; 5mm=67%, 10mm=76%, 15mm=79% and asym=81%).

Table 5.2 – Severity of Miss

The severity of the Type 3 geographic miss in each of the motion groups based on the mean [±SD] coverage of the 4D-PTV with 95% of the prescribed dose (total n = 29)

	5 mm PTV Severity	Mean 4D PTV coverage % [±SD]	10 mm PTV margin	Mean 4D PTV coverage % [±SD]	15 mm PTV margin	Mean 4D PTV coverage % [±SD]	Asymmetrical PTV	Mean 4D PTV coverage % [±SD]
0- < 5 mm (n = 8)	Minor	97 [2.9]	Minor	97 [1.7]	Minor	98 [3.3]	Minor	98 [4.2]
5- < 10 mm (n = 6)	Moderate	93 [5.9]	Moderate	95 [7.9]	Moderate	95 [4.8]	Minor	95 [5.4]
10- <20mm(n= 11)	Significant	86 [8.8]	Moderate	92 [5.3]	Moderate	92 [4.4]	Moderate	92 [3.9]
20+ mm (n = 4)	Significant	67 [16.7]	Significant	76 [10.9]	Significant	79 [12.0]	Significant	81 [14.0]

5.4 DISCUSSION

In this study we compared a standard technique of delineating the GTV on a 3D-PET/CT to an improved technique of 4D-PET/CT. Our work has found that 3D-PET/CT defined target volumes underestimate the true extent of respiratory motion despite being considered a 'slow' imaging modality that combines imaging information from all phases of the breathing cycle. This underestimation of the tumour motion led to increasingly severe geographic miss as the tumour motion increased. This is consistent with other studies comparing 3D and 4D-PET/CT volumes (Hanna et al., 2012a, Callahan et al., 2013, Callahan et al., 2011a).

Results of this study also revealed that the ratio of lesion size to the amount of motion also appears to impact the severity of geographic miss. For example a small lesion that moves a large distance would likely have a worse geographic miss than a large lesion that moves across the same distance.

It has been possible for some time to perform both a 4D CT and a 4D PET scan in the same session on a PET/CT scanner (Nehmeh et al., 2002). While the technology has advanced and become more widely available it is still not commonly applied. One reason for this may be due to the limited number of studies showing clinical benefit that would compensate for the additional resources required to complete a 4D-PET/CT scan. The main reason to acquire a 4D scan to define target volumes is to minimise the risk of a geographic miss, thereby increasing the probability of attaining tumour control and enhanced patient outcomes. Sura and colleagues (2008) studied

patterns of local failure in 34 lung lesions in 26 patients. They found that for a lung tumour receiving more than 60Gy the site of failure was mostly at the margins of the GTV (Sura et al., 2008). As 3D-PET/CT scan underestimate target volumes a possible explanation for the observed local failures is tumour motion due to normal respiration. A lung tumour that moves out of a defined target area may receive insufficient dose to areas that are missed, thereby increasing the risk of local failure.

Not surprisingly, these data show that the severity of the geographic miss rises significantly when a PTV margin is reduced from the standard 15mm. This further confirms our institutional practice of using at least a 15mm margin if there is no motion management in place. When employing highly conformal techniques such as stereotactic body radiotherapy (SABR) it is common to add only 5mm margins to the GTV. If only a 3D-PET/CT scan or 3D-CT alone is used to delineate a GTV for stereotactic treatment these data suggests that there is a high likelihood of a significant geographic miss. The planning techniques are different in SABR with sharper dose gradients at the edge of the PTV and this may lead to an even more significant miss than described in this work.

In the delivery of radiation therapy to lung tumours there is always a need to reduce the dose to normal lung in order to minimise pulmonary toxicity. 4D-PET/CT imaging is not widely available so many centres may not be able to use this technique. Therefore in this study we compared geographic miss of a standard 15mm margin to a 15x10mm asymmetrical margin. In this study, rates of geographic miss were similar for symmetrical and asymmetrical margins. This was because most of the

tumour motion occurs in the SI plane and reducing the margins in the other planes does not greatly increase the risk of a geographic miss. Using an asymmetric PTV margin is a method that could be employed on a 3D-PET/CT scan to reduce lung dose however further work in a larger cohort is warranted.

In most patients, if a 15mm margin is applied to a 4D-GTV the resultant 4D-PTV will be significantly larger than a 3D-PTV, thereby potentially increasing normal lung dose. Conventional GTV to PTV margins allow for motion and set-up uncertainties. Assuming that the magnitude of both these uncertainties is similar and independent of each other our original margin of 15mm on the 3D-GTV could be reduced. The use of 4D imaging provides not only the magnitude of motion but also defines the centre location more accurately than 3D scanning. We feel a margin reduction to 10mm is justified in cases where motion has been accounted for in the GTV. As Table 1 shows this has the potential to reduce the actual irradiated volume significantly. The mean 4D-GTV with a 10mm margin was 96.1ml, which was significantly smaller than a 3D-GTV with a 15mm margin (119.2ml). However, individual radiotherapy departments would need to adjust safety margins individualised to department specific equipment and processes.

4D target volumes provide potential to customise a patients target volume and resultant radiotherapy plan based on their individual tumour motion (Everitt et al., 2009). What we and other authors have established that tumour motion is highly variable between patients and can be visualised using 4D scanning (Li et al., 2011, Hof et al., 2009). As it is becoming common practice to use a PET/CT in the planning

process it would be an efficient use of resources to add a 4D-PET/CT at this time point. Depending on the amount of tumour motion observed a target volume could be tailored to suit their individual lesion trajectory. This will either ensure correct tumour coverage for a highly mobile tumour or allow normal tissue dose reduction in fixed tumours. Conversely these data show that if a radiotherapy department does not have any motion management equipment with their PET/CT scanner then they should not attempt to reduce safety margins from the larger 15mm expansion. Further work investigating personalising target volumes is warranted and may improve local tumour control or reduce risks of side effects.

Based on our retrospective study there is no way to know if the types of geographic miss measured translated to decreases in tumour control. However it is known that the radiation dose to a tumour is a good predictor for local control (Geets, 2013). Also a geographic miss such as described in this study would constitute a protocol violation and as was shown by Peters et. al. adherence to protocol is a good predictor of overall survival (Peters et al., 2010). It is therefore reasonable to infer that any form of geographic miss would lead to a reduction in tumour dose and subsequently increase the risk of treatment failure. A 4D-PET/CT scan incorporated into a planning PET/CT is an achievable method of accurately establishing and accounting for the adverse effects of respiratory motion on treatment success.

5.5 CONCLUSION

Without any form of motion suppression the current standard of a 3D- PET/CT and 15mm PTV margin employed for lung lesions has an increasing risk of significant geographic miss in particular when tumour motion increases. Use of smaller asymmetric margins in the cranio-caudal direction does not comprise tumour coverage. Reducing PTV margins for volumes defined on 3D-PET/CT will greatly increase the chance and severity of a geometric miss due to respiratory motion. 4D-imaging reduces the risk of geographic miss across the population of tumour sizes and magnitude of motion investigated in the study.

The next chapter goes on to address the fourth aim of this thesis and was published in the *European Journal of Nuclear Medicine and Molecular Imaging (Callahan et al., 2014a)*. A major factor influencing the quality of life for patient post radiation therapy is the effect on the normal lung. The next chapter describes the application of 4D-PET/CT in ^{68}Ga-VQ PET/CT as a way to develop novel strategies to reduce lung toxicity caused by radiation therapy.

CHAPTER 6 - HIGH RESOLUTION IMAGING OF PULMONARY VENTILATION AND PERFUSION WITH GA-VQ RESPIRATORY GATED (4D) PET/CT

Jason Callahan[1,4], Michael S. Hofman[1,6], Shankar Siva[5,6], Tomas Kron[2,6], Michal Schneider[4], David Binns[1], Peter Eu[1] and Rodney J Hicks[1,6]

1. Peter MacCallum Cancer Centre, Department of Cancer Imaging
2. Peter MacCallum Cancer Centre, Department of Physical Sciences
3. RMIT university, Department of Applied Physics
4. Monash University, Department of Medical Imaging and Radiation Science
5. Peter MacCallum Cancer Centre, Department of Radiation Oncology
6. The University of Melbourne, Peter MacCallum Department of Oncology

Eur J Nucl Med Mol Imaging, Vol. 41, No 2, pp.343-349, 2014

The biggest limiting factor that determines the amount of radiation that can be delivered to a lung tumour is the surrounding normal lung tissue. Also the amount of dose received by the normal lung is an important factor that dictates a patient quality of life and risk of complications post therapy. The mechanisms of radiation induced side effects are still not well understood. A new generator produced isotope, Ga-68, has meant that a VQ lung scan can now be performed on a PET/CT scanner to take advantage of its higher resolution and sensitivity. With this improvement in resolution we can use this new test to examine the effect of radiation on the lung and come up with new and novel strategies to improve dose delivery while limiting side effects. Along with the improved resolution, a VQ scan performed on a PET/CT scanner can also be acquired as a 4D scan. This chapter present our study investigating the feasibility of adding a 4D scan to a PET-VQ scan. The addition of a 4D scan should improve the co-registration between the PET and CT components of the scan as well as enable more accurate co-registration to associated planning scans.

6.1 INTRODUCTION

It has been fifty years since Henry N. Wagner's first description of pulmonary lung perfusion imaging using macro-aggregated albumin (MAA) (Wagner et al., 1964). The technique remains in widespread use around the world, primarily for assessment of suspected pulmonary embolism. However, it also has applications in many other clinical settings including quantitative assessment of lung function. Advances over the last five decades have included single photon emission tomography (SPECT), hybrid imaging with SPECT/CT and use of newer radiotracers for inhalation, particularly micro particulate aerosols like Technegas (Cyclomedica, Lucas Heights, Australia) (Leblanc et al., 2007, Jogi et al., 2010, Roach et al., 2010).

The availability of the Germanium-68/Gallium-68 (^{68}Ge/^{68}Ga) generator in recent years has opened up a whole new era of exploration in molecular imaging. This is a radionuclide generator, similar to the ^{99}Mo/^{99m}Tc generator, which produces the positron emitting isotope ^{68}Ga. ^{68}Ga is a versatile isotope that can be used to label a wide range of tracers previously the domain of gamma emitting isotopes such as ^{99m}Tc and ^{111}In. The most successful and well documented of these are the somatostatin analogues of DOTA-TOC and DOTA-TATE (Hofman et al., 2012, Buchmann et al., 2007). This ability to label established tracers with a ready source of positron emitting isotope has provided the opportunity to exploit the superior imaging characteristics of the positron emission tomography (PET) camera over the gamma camera (Hicks and Hofman, 2012). One new area of investigation is the use

of ^{68}Ga-labelled carbon nanoparticles (Galligas) and macro-aggregated albumin (^{68}Ga-MAA) to perform a ventilation / perfusion (VQ) scan on a PET scanner (Kotzerke et al., 2010a, Mathias and Green, 2008, Kotzerke et al., 2010b).

Our group has previously reported the potential advantages of VQ PET/CT in a pilot series of patients being investigated for pulmonary embolism (Hofman et al., 2011). In this series it was found that the image quality was either equivalent or superior to VQ SPECT/CT. In addition, it was found that in both free breathing SPECT and PET there was mis-registration between SPECT/CT and PET/CT scans due to the effects of respiratory motion. Respiratory motion reduces quality due to blurring of activity in addition to inaccurate attenuation correction due to CT mis-registration. The newest generation of PET/CT scanners allow the acquisition of multiple bed-step respiratory gated (4D) PET and CT scans. This acquisition technique potentially provides imaging in both inspiration and expiration cycles.

In this work we investigate the effects of respiratory motion on VQ scanning. We aim to describe acquisition parameters, and assess which phases of respiratory gating produces images with highest spatial overlap between PET and CT. It is our hypothesis that 4D imaging will improve co-registration between PET and CT modalities enabling more accurate ability to quantify regional lung function, which is of particular relevance to predicting outcomes of lung surgery or radiotherapy.

6.2 MATERIAL AND METHODS

PATIENTS

Fifteen patients were prospectively recruited as part of a study assessing serial change in lung function during radiotherapy (Australian New Zealand Clinical Trial Registry Trial ID 12613000061730). All patients had locally advanced or inoperable non-small cell lung cancer and were planned for radiation therapy with curative intent. Mean age of patients was 67 (range 46-88) (10 patients were male, five were female). This patient cohort consisted largely of ex-smokers with pre-existing airways disease, with a mean forced expiratory volume in one second (FEV1) of 1.87L (0.83L-2.82L) and carbon monoxide diffusing capacity (DLCO) of 54% (27%-87%). Exclusion criteria included major airways reversibility demonstrated on pulmonary function testing, defined as a change in forced expiratory volume over one second (FEV1) of greater than 200mls and 15% predicted after introduction of a bronchodilator. All patients were to complete a ^{68}Ga-VQ 4D-PET/CT prior to commencement of radiation therapy. The study was approved by the Peter MacCallum Clinical Governance and Ethics Committee, and all patients provided written informed consent.

PET/CT PROTOCOL

A ^{68}Ga-VQ 4D-PET/CT scan was performed on all 15 patients. The scan consisted of three parts:

- 4D – CT
- 4D-ventilation PET
- 4D-perfusion PET

The patient was positioned supine on a GE-Discovery 690 PET/CT scanner (GE Medical Systems Milwaukee, WI) in a default planning position using the radiotherapy palette and head rest with their arms raised. The extension tubing attached to the intravenous cannula was placed in an easily accessibly position to allow administration of the ^{68}Ga-MAA without requiring the patient to move between ventilation and perfusion scans. The patients breathing was tracked using the Varian RPM respiratory tracking system (Varian Medical Systems, Palo Alto, Ca). The patients were instructed to breathe freely for the duration of the scans. No breathing training or coaching was used.

GALLIGAS INHALATION

Galligas was prepared using the Technegas generator (Cyclopharm) as described previously (Hofman et al., 2011). Approximately 200 MBq of ^{68}Ga was added to the carbon crucible. The patients were placed in a supine position and Galligas inhaled using the standard ventilation technique. A Gammasonics 450P (Gammasonics Pty

Ltd, Five Dock, NSW) Geiger counter was used to measure the amount of inhaled gas. The monitor was placed over each lung and the highest detected dose rate was recorded in μSv/hr. The dose rate over the lungs was recorded to determine the association between the Geiger counter and PET camera count rate.

4D-CT ACQUISITION

A scout scan was performed to plan the scanned area. The axial extent of the 4D-CT was determined by the length of two PET bed positions. The top of the field of view was aligned with the apex of the lungs. The position for the CT, ventilation and perfusion scans were matched. After moving the patient into position the breathing was allowed to stabilise and recorded using the Varian Real-Time Patient Monitoring (RPM) system (Varian Medical Systems, Palo Alto, Ca). The Varian RPM system uses an infrared camera to track the motion of a box placed on the patient's abdomen. Once the breathing had stabilised a 4D-CT scan was performed using the following parameters: Cine CT, 10mA, 140kV, Cine duration = breathing period + 1.5secs, and the cine time between images = breathing period / 10. These exposure parameters produced and average computed tomography dose index (CTDI) of 5.9 mGy and dose length product (DLP) of 169 mGy-cm. After completion of the 4D-CT scan the respiratory trace was saved and a new trace was established to use for the ventilation PET.

4D-VENTILATION PET

The patient was moved into PET position and the breathing was allowed to stabilise again before beginning the ventilation PET acquisition. This was acquired over two bed position as a list mode acquisition while recording the patient's breathing trace. Each bed position was acquired for five minutes, but this could be increased at the operator's discretion if the count rate was low due to poor inhalation or due to a low administered dose of Galligas.

4D-PERFUSION PET

The preparation of ^{68}Ga-MAA was performed using the process described in our previous paper (Hofman et al., 2011). A mean dose of 50 MBq (range 21-62 MBq) ^{68}Ga-MAA was dispensed into a Braun Injekt® 2ml syringe to minimise residual activity. Without the patient moving, the ^{68}Ga-MAA was injected through the extension tube with repeated flushing of the syringe with 20 ml of normal saline. A new respiratory trace was then established and allowed to stabilise. Once the new trace had been started the perfusion PET was the acquired for five minutes per bed step. The perfusion PET was also acquired as a two-bed, list-mode acquisition in the same position as the ventilation scan. The count rate for the perfusion scan was recorded for comparison with the ventilation count rate.

IMAGE RECONSTRUCTION

The 4D CT data were reconstructed using the GE Advantage4D processing package (V 1.01-1p, GE Medical Systems Milwaukee, WI). Using the Varian respiratory trace the data was retrospectively binned equally in the five bins based on a percentage of the respiratory cycle with the first phase representing the end inspiration position and the third phase the end-expiration. A 4D-CT average (AveCT) reconstruction was also produced for each scan. A 4D-CT average reconstruction is created by using the average HU across the five respiratory bins.

The ventilation and perfusion PET data were reconstructed as a free breathing (FB) static scan using the end inspiration CT for attenuation correction. The data was also retrospectively binned into five bins based on a percentage of the respiratory cycle using the GE automatic phase matching. This automatically matches each PET bin to the respective CT bin for attenuation correction. The FB-PET and 4D-PET images were reconstructed using ordered subset expectation maximization (OSEM) iterative reconstruction using the following parameters: 4 iterations, 9 subsets, 192 matrix, 5mm Gaussian smooth.

4D IMAGE REGISTRATION DATA ANALYSIS

The lungs were contoured using MIMimage analysis software (MIM 5.4.4, MIM Software Inc. Cleveland, OH) on the following data sets:

- CT – AveCT, InspCT, ExpCT
- Ventilation – FB-Vent, InspVent, ExpVent
- Perfusion – FB-Perf, InspPerf, ExpPerf

The lungs on all three CT data sets were contoured using an upper Hounsfield unit of -150. Due to the significant heterogeneity caused by the prevalence of airways disease in this patient population there were no PET automatic contouring methods that could be applied to all patients. Therefore a visually adapted threshold was applied to the PET data to contour the ventilation and perfusion scans using the region grow tool. An SUV threshold was determined on the FB-Vent and Perf images by a single experienced observer. The contours were then confirmed by a nuclear medicine physician. The threshold selected was optimised to include all areas of tracer accumulation in the lung and any accumulation of tracer in the main bronchi was manually excluded. The same threshold was then applied to inspiration and expiration data sets. Any normal structures such as trachea and stomach were manually excluded from the contoured volume.

The amount of diaphragmatic motion at the most cranial convexity of the diaphragm was also measured in the cranio-caudal direction from the 4D-CT. In the coronal plane the distance from end inspiration to end expiration was measured at the level of the carina.

The spatial overlap between PET and CT contoured lung volumes was compared using a Dice co-efficient (Hanna et al., 2010). The Dice co-efficient (DC) was calculated using the MIM image analysis software. A DC of 1 indicates perfect concordance between volumes whereas a value of 0 indicates no concordance between volumes. The DC can be represented using the following formula:

$$DC = \frac{2(CTvol \bigcap PETvol)}{(CTvol + PETvol)}$$

The DC between PET and CT volumes were compared in the following groups: 1: FB-PET/CT (end Insp CT), 2: InspPET/InspCT, 3: ExpPET/ExpCT, and 4: FB-PET / AveCT for both the ventilation and perfusion PET studies.

STATISTICAL ANALYSIS

All statistical tests were carried out using GraphPad Prism 5 (LaJolla, Ca, USA). A repeated measures one-way ANOVA with multiple comparison post hoc Tukey tests was performed to determine any statistical difference between the groups. A p-value of < 0.05 was deemed significant. A linear regression analysis was performed to determine the correlation between ventilation dose rate on the Geiger counter and count rate on the PET camera.

6.3 RESULTS

VENTILATION SCAN COUNT RATE - GEIGER COUNTER VS PET SCANNER

A linear regression analysis of the count rate measured on the Geiger counter in uSv/hr versus the count rate measured on the PET camera in kilocounts per second (KCPS) revealed an r^2 value of 0.67 (Figure 6.1 – Page 143). The average dose rate achieved on the Geiger counter was 37 µSv/hr, which equated to an average count rate on the camera of 31 KCPS. Due to shortage of gallium from an aging generator and poor patient compliance the ventilation count rate in 2/15 patients was only 10 KCPS. While the FB-PET was diagnostic for these patients the count rate for the 4D-Ventiation scan was too low for analysis and these studies were excluded from the analysis.

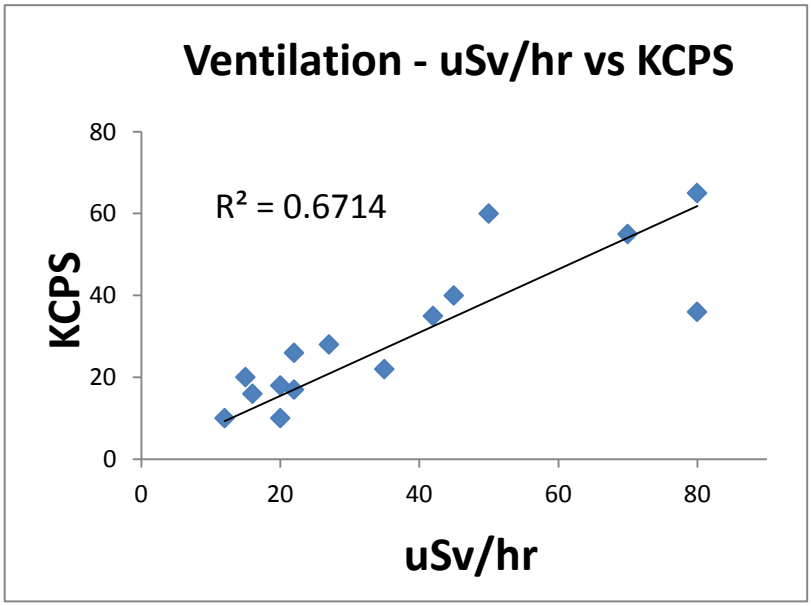

Figure 6.1 – Ventilation count rate

Relationship between ventilation count rate on the Geiger counter and the count rate on the PET camera

VENTILATION VS. PERFUSION COUNT RATE

The mean count rate for the perfusion scan was 203 KCPS. The count rate was on average 7.8 times the greater on the perfusion scan than the ventilation. However, in one patient there was significant trapping of the Galligas in the central airways and insufficient ^{68}Ga-MAA injected due to production problems. This led to a suboptimal VQ ratio (3.2 times) producing shine through of the Galligas into the perfusion scan. However despite residual counts from the preceding ventilation study contributing to apparent activity on the perfusion scan, the study was still considered of sufficient quality to be included in the analysis.

LUNG MOTION

The diaphragmatic motion during the 4D-CT scan was highly variable with a range of 0.4-3.4cm (SD: 0.81) in the right lung and 0-2.8 (SD: 0.83) in the left lung. In this cohort of 15 patients three patients showed no diaphragmatic motion in the right hemi diaphragm secondary to a phrenic nerve palsy (see supplementary Movie 1). There was a corresponding compensation by the other lung with over 3cm of diaphragmatic motion measured in each patient.

IMAGE CO-REGISTRATION

As shown in Table 6.1 (Page 145) the DC for both ventilation and perfusion scans were highest in groups 3 (ExpPET/CT) and 4 (FB-PET/AveCT) indicating the best volume overlap and therefore best image co-registration between the modalities.

The multiple comparison Tukey test's showed no significant difference in DC for either ventilation or perfusion scans between groups 3 and 4 ($p>0.05$). There was a significant difference in DC for both ventilation and perfusion scans between groups 1:3, 1:4, 2:3 and 2:4 ($p<0.05$). This indicates that groups 1 (FB-PET/CT) and 2 (InspPET/CT) have significantly poorer image co-registration than groups 3 and 4 as any differences between the groups can be attributed to misregistration between the PET and CT scans. Qualitative assessment of the image co-registration suggested that the poorer co-registration in groups 1 and 2 was primarily related to mis-registration around the lung bases as shown in Figure 6.2 (page 146). This area is small in proportion to the overall lung volume but the differences in image co-registration were consistent and significantly different. The PET and CT scans are best registered on Exp-PET/CT, which shows an absence of blurring around the lung bases. There is a substantial area of mis-registration between PET and CT scan around the lung based on both FB-PET/CT and Insp-PET/CT in most patients with preserved diaphragmatic motion.

Table 6.1 - Mean (±SD) DC in the four groups

	Mean (±SD) Vent – DC	Mean (±SD) Perf – DC
Group1: FB-PET/CT	0.78 (0.09)	0.78 (0.08)
Group2: Insp-PET/CT	0.79 (0.07)	0.78 (0.08)
Group3: Exp-PET/CT	0.82 (0.07)	0.80 (0.08)
Group4: FB-PET/AveCT	0.82 (0.07)	0.80 (0.08)

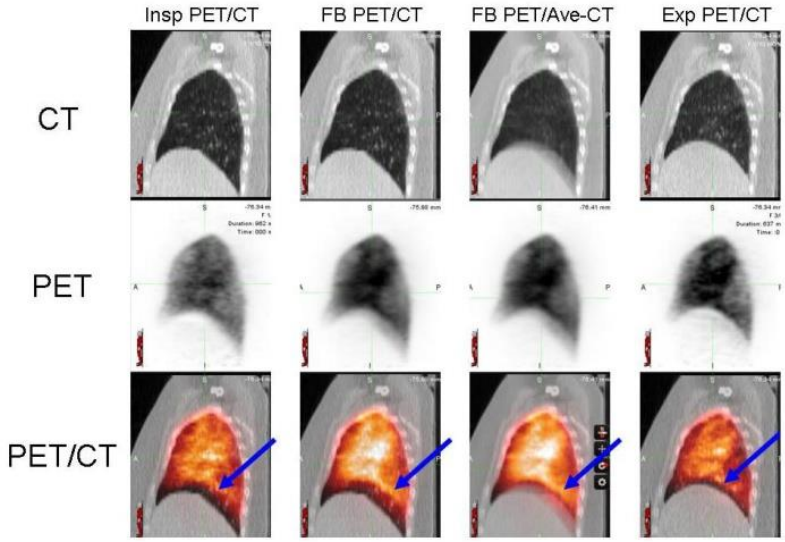

Figure 6.2 – 3D versus 4D VQ PET/CT

Perfusion PET/CT showing effects of respiratory motion on image co-registration around the lung bases in the four groups analysed.

6.4 DISCUSSION

We have found that ^{68}Ga-VQ 4D-PET/CT is feasible without additional scan time required compared to our previously described non-gated technique (Hofman et al., 2011). In standard free breathing acquisition, the effects of respiratory motion on the images are unpredictable with resultant significant mis-registration between PET and CT. In this paper we have shown that adding respiratory gated scanning to a VQ-PET/CT scan enables any mis-registration due to respiratory motion to be corrected. Our results show that the benefit of adding 4D scanning in terms of image co-registration is predominantly around the lung bases.

We have also reported evolving technical and practical considerations in performing VQ-PET/CT scanning. We have shown that a simple hand held Geiger counter is suitable to monitor the amount of inhaled Galligas in order to obtain appropriate count rates on subsequent PET acquisition. As in conventional VQ scanning, it is also possible to acquire sequential ventilation and perfusion by maintaining a suitable count rate ratio between the scans. As with Technegas, clumping of Galligas in the central airways can still result in shine through of activity if sub-optimal VQ ratio is not achieved.

The long acquisition time of SPECT and PET introduces additional complexity in image interpretation as patients are breathing freely during scanning. As a result activity in the lungs can be blurred due to continuous motion during the acquisition, particularly at the lung bases. This respiratory motion artefact can be corrected by using respiratory gating technology. This has been applied with conventional SPECT VQ scintigraphy but is limited owing to inferior count statistics and lack of commercially available gating systems. A method to perform respiratory gating during a SPECT scan was described by Suga *et al.* who found improved lesion-to-normal lung contrast (Suga et al., 2004). However, this technique only involved imaging the lungs in the end-inspiration position. An advantage of PET/CT is the availability of respiratory gating systems that permit 4D acquisition of both PET and CT datasets (Nehmeh et al., 2004, Callahan et al., 2013), allowing for anatomical correlation of functional deficits. Additionally, respiratory gating of both PET and CT

enables accurate attenuation correction of the PET date to be performed for each bin.

There are multiple advantages of VQ-PET/CT compared to conventional VQ scintigraphy. The addition of 4D respiratory gating further enhances the PET technique with superior sensitivity, spatial and temporal resolution compared to conventional scintigraphy (Hofman et al., 2011). In this study the blurring caused by respiratory motion on the FB-PET scan was well corrected on the 4D-PET scan. In particular, the expiration phase of the 4D-PET fused with the expiration 4D-CT showed excellent co-registration with no evident blurring. This could enable accurate monitoring of lung ventilation and perfusion over multiple time periods by having a relatively reproducible breathing position in the expiration phase as compared to the unpredictability of free breathing and deep inspiration lung positions. In institutions where a $^{68}Ge/^{68}Ga$ generator and a PET scanner are available the technique may be readily adopted as an alternative to conventional scintigraphy. The ability to more precisely quantify pulmonary blood flow and ventilation offers an opportunity to explore existing and new clinical applications in a variety of settings, particularly those where there is a clinical need to try to predict the consequences of radiation therapy or surgical lung interventions.

It is standard practice to use a 4D-CT-Ave scan for planning of radiotherapy (Li et al., 2008). In this cohort we found that the 4D-CT-Ave reconstruction fused with a FB-PET provided much better co-registration than FB-PET/CT alone. In FB-CT the position of the diaphragm is random and therefore the amount of mis-registration is

unpredictable. Our results indicate that a FB-PET fused with a 4D-CT-Ave is best combination for use in radiotherapy planning. The average imaging takes into account respiratory motion and removes the uncertainty caused by the random position of the diaphragm.

The 4D CT data provides valuable additional information that may be clinically useful. In this series, we identified several patients with a phrenic nerve palsy and resultant compensatory increase in motion by the opposite lung. This has implications for planning of any target volumes in the compensating lung. A recent study by Dinkel *et al.* used 4D-MRI to analyse lung tumour motion in patients with a hemi-diaphragmatic paralysis (Dinkel et al., 2009). In their study they found the average displacement of the tumour was 6.6mm as well a lateral shift of the mediastinum due to the compensatory effect of the unaffected lung. In these patients the increase in motion in the opposite lung has potential implications for dose deposition from radiation therapy in both the affected and compensating lungs. The addition of a 4D-CT however does potentially increase the radiation exposure for patients. However to address this issue we lowered the 4D-CT exposure factors to a level that produces CTDI values similar to a non-contrast CT scan of the chest while still producing adequate image quality for this purpose.

Recently, studies have investigated using the information obtained from a 4D-CT scan to infer information about lung ventilation (Nyeng et al., 2011, Yamamoto et al., 2011). However, as demonstrated in Figure 6.3 (page 150), aerated lung on CT is not necessarily contributing to ventilation. Further, the 4D-CT ventilation techniques do

not provide any information about lung perfusion, which is particularly relevant to radiation lung damage as the vascular endothelium is one of the most radiation sensitive tissues in the lungs (Hill, 2005) .

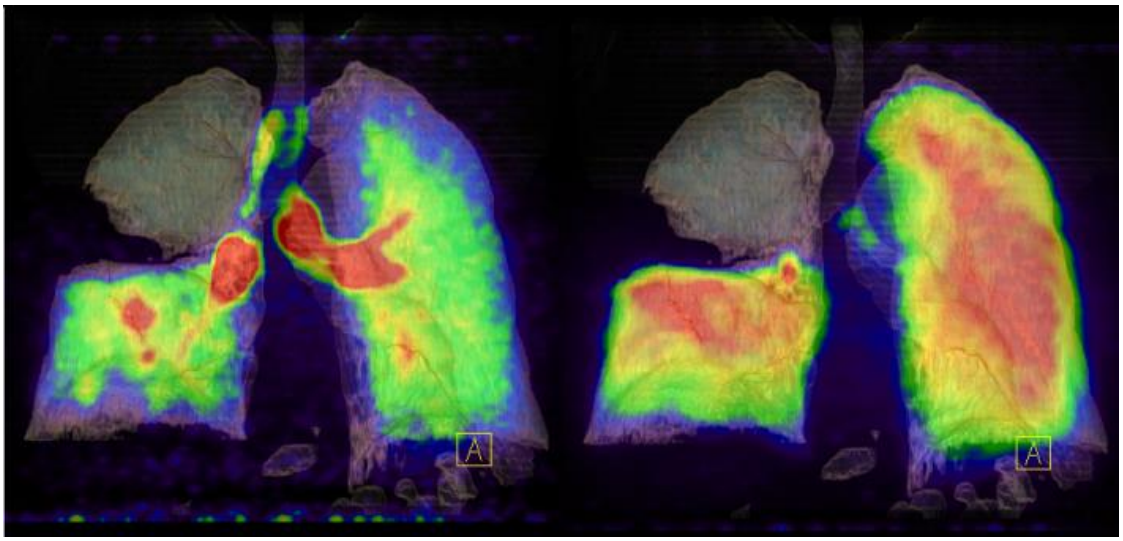

Figure 6.3 – Volume Rendered VQ PET/CT

Volume rendered PET/CT images showing large areas of aerated lung in the right upper lobe with no evident ventilation (left) or perfusion (right). Precise co-registration of PET and CT datasets is provided with respiratory gated acquisition.

The limitations of this study include the lack of breathing training by the patients, leading to potentially poor co-registration between the inspiration phases of the CT and PET scans. A system such as the audio-visual biofeedback method use for 4D-CT acquisition as described by Cui et al. may improve co-registration between modalities in the inspiration phases (Cui et al., 2010). However, this increases the

complexity of acquisition as well as the time required on the scanner potentially limiting its widespread use.

6.5 CONCLUSIONS

^{68}Ga-VQ 4D-PET/CT is feasible and the blurring caused by respiratory motion is well corrected with 4D acquisition, which principally reduces artefact at the lung bases. The FB-PET/Ave-CT and Exp PET/CT produces images with highest spatial overlap. The 4D-CT also provides valuable information. With its higher resolution compared to standard SPECT/CT the ^{68}Ga-VQ 4D-PET/CT technique has broad range of potential clinical applications including improving diagnostic algorithms for patients with suspected PE, pre-operative evaluation of regional lung function and improving assessment or understanding of pulmonary physiology in the vast range of pulmonary diseases.

CHAPTER 7 - DISCUSSION

Despite significant improvements in the outcomes for many cancers, the survival for patients with lung cancer is still amongst the worst of all malignancies. The mean five year survival for patients receiving radical Chemotherapy and radiotherapy (ChemoRT) at our institution 15 years ago was estimated at 15% (Mac Manus et al., 2000). In 2013 MacManus and colleagues reported a 4-year survival rate of greater than 30% (Mac Manus et al., 2013). The authors noted that these survival figures were superior to virtually all other randomised trials of radical RT or chemo RT for NSCLC published to date. The higher survival rate was attributed to the addition of a staging PET/CT scan which allowed better patient selection and target volume delineation. FDG-PET/CT is now considered the primary imaging modality for staging patients with lung cancer (Akhurst et al., 2015)

The work in this thesis presents the application of a new technology, 4D-PET/CT, for patients with lung cancer, from their initial diagnosis, treatment with radiation and to improvements in their quality of life post therapy. This chapter will outline what we have learnt from the published studies presented in this thesis and how they compare with the results of other work in the literature. Further, the discussion will elaborate on the implication of these studies on current practice and ongoing research.

7.1 THE CLINICAL APPLICATION OF 4D-PET/CT IN LUNG CANCER DIAGNOSIS

The use of FDG PET to aid in the diagnosis of solitary pulmonary nodules is a well-established clinical indication with many authors reporting high sensitivity and specificity (Gould et al., 2013). However, in our experience the rates of nodules classified as indeterminate is likely to be much higher than those reported in the literature. The data presented in chapter three of this thesis has highlighted that 30% of the cases were of an indeterminate aetiology based on the 3D-PET/CT scan alone. This was consistent with the study by Guerra and colleagues who used a similar methodology in a retrospective cohort and found an indeterminate rate of 24% on the 3D-PET/CT (Guerra et al., 2012). The aim of using PET/CT in this clinical application is to provide the managing clinician with clear information as to how the patient should best be managed. In the case of an indeterminate finding the PET/CT scan has not aided in the clinical management of these patients. An indeterminate finding then requires the clinician to decide to either subject the patient to a more invasive investigation or wait and watch the lesion.

In our study we found that the addition of a 4D-PET/CT scan provided additional information for the classification of these lesions. As the metabolic activity of the lung nodules were more accurately measured, the reporting clinician was able to make a more informed decision about the lesions aetiology based on correct information free from motion artefact. The information could then be more appropriately acted upon within the know limitations of FDG to differentiate

between benign and malignant lung lesions. The fact that in two cases the lung lesion was incorrectly classed as malignant did not mean they were inappropriately managed. A lung nodule that is FDG avid has a high likelihood of malignancy and cannot be safely observed. Furthermore, many FDG-avid inflammatory processes require specific aetiological diagnosis and treatment. Tuberculosis and histoplasmosis are examples of FDG-avid nodular disease that benefit from diagnosis and active treatment (Salhab et al., 2006, Stelzmueller et al., 2015).

In the presented work we have shown that in a sub-set of patients with lung nodules an additional 4D-PET/CT can aid in improving the diagnosis and therefore management of patients with solitary pulmonary nodules. In our centre 4D-PET/CT is now used only on those lung lesions that cannot be confidently classified on standard PET/CT imaging. This has proven to be an efficient and effective way to use this technology in a busy clinical environment.

7.2 THE CLINICAL APPLICATION OF 4D-PET/CT IN RADIATION ONCOLOGY USING A PET/CT MIP

The clinical application of 4D-CT in radiotherapy treatment planning for patients with lung cancer has become routine in many centres. Modern CT scanners are now equipped with the necessary hardware and software to acquire and process 4D-CT scans using relatively uncomplicated methods (Moorees and Bezak, 2012). A 4D-CT maximum intensity projection (MIP) can be easily reconstructed using automated software and uploaded to planning systems for target volume delineation.

In contrast, 4D-PET/CT is much less commonly used in clinical practice. A likely reason is the complexity of acquiring, processing and interpreting two complex scans on two imaging modalities at the same time. In the past a 4D-PET/CT scan required many in house and customised solutions which limited its routine widespread use. The difficulties in using 4D-CT to accurately provide attenuation correction for a 4D-PET is also a potential reason for the late introduction of 4D-PET/CT in the clinic. However the newest generation of PET/CT scanners now have many advanced automated acquisition and processing tools. These tools make the clinical use of 4D-PET/CT much more feasible and allow a wider utilisation of this technology outside of institutions that have specialist imaging or physics support.

In clinical practice a MIP derived from a 4D-CT scan is generally used to define an internal target volume (ITV) that takes into account lesion motion due to respiration. An example of a 3D-CT and 4D-CT MIP is shown in Figure 7.1 (page 155). This is a practical method for ITV delineation that is easily incorporated into standard contouring workflows. While a 4D-CT derived MIP has been validated and used for some time there has been no work on a 4D-PET equivalent.

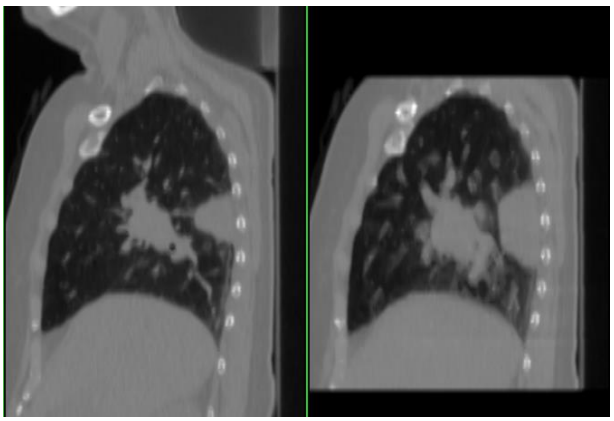

Figure 7.1 – 3D-CT versus 4D-CT MIP

The panel on the left is an example of a 3D-CT with a large posterior lobe tumour. The panel on the right is the same patient but reconstructed as a 4D-CT MIP. The large size of the tumour on the 4D-CT MIP represents the tumour motion captured in a single frame.

In chapter four of this thesis we presented our work validating a 4D-PET/CT MIP as a viable alternative to 4D-CT alone. Most importantly we found that the concordance between 4D-PET and 4D-CT MIP was very high in both a phantom and in patient studies. The concordance between the modalities was much higher than standard 3D-PET/CT, which is currently employed in many centres as an alternative to 4D-CT for ITV delineation. We also showed that contouring all the 4D-PET and CT bins then summing the contours together showed equivalent volume concordance to just contouring the single 4D-PET/CT MIP volume. This trend was the same regardless of the contouring method used.

A 4D-CT may be sufficient to account for tumour motion when a lesion is not close to any other soft tissue structure. However, if a lung lesion is sitting directly on top of the liver, the tumour and liver merge on a 4D-CT MIP making it impossible to see the tumour boundaries. An example of this is shown in Figure 7.2 (page 157). As can be seen by the pink contours in Figure 7.2 the tumour on the 4D-PET/CT MIP has a high target to background ratio. The same would apply in cases of peripheral lung collapse where again the lack of soft tissue contrast on a 4D-CT would make accurate delineation impossible. The high lesion to background contrast on a 4D-PET scan makes the boundaries of a tumour clearly visible which enables easy delineation. This improved target delineation on PET imaging is the reason that it has become such an invaluable part of the radiation therapy planning in the treatment for patients with lung cancer. 4D-PET/CT is a natural extension of this established

clinical paradigm and as a single data set the 4D-PET/CT MIP is a viable tool to improve clinical practice.

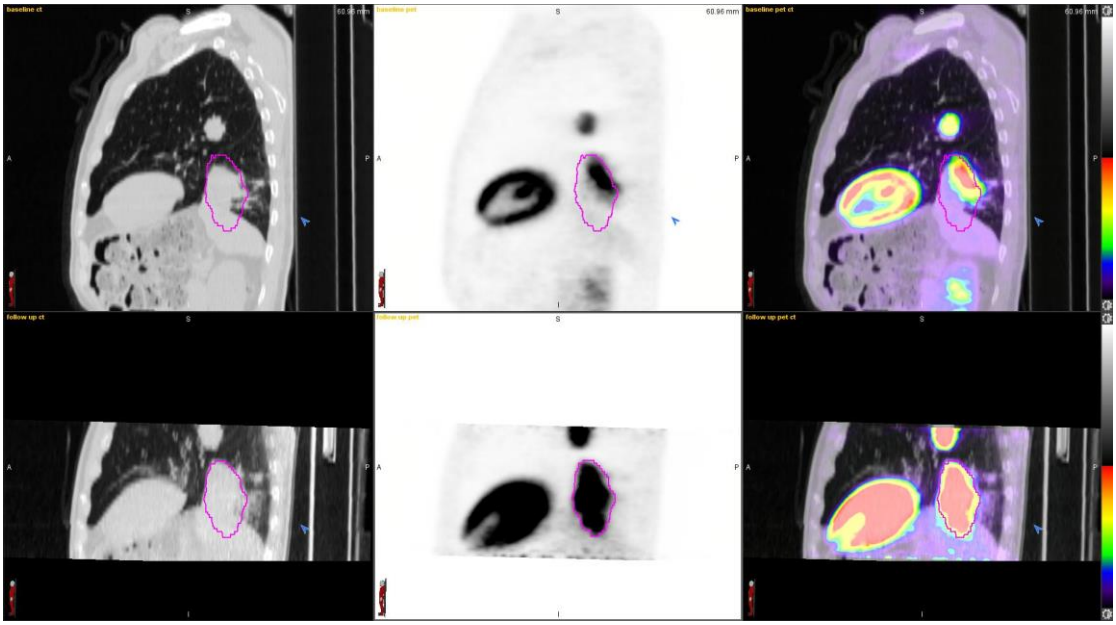

Figure 7.2 – 3D-PET/CT vs 4D-PET/CT MIP

The top row shows a patient with a lower lobe tumour as seen on a 3D-PET/CT. The bottom row shows the same tumour on the 4D-PET/CT MIP with the tumour contoured in pink. The between Tumour and liver can only be clearly seem on the PET-MIP dataset. Images J Callahan (2015)

7.3 GEOGRAPHIC MISS AND RESPIRATORY MOTION

There is significant interest in the clinical application of 4D PET/CT scanning in radiation oncology (Konert et al., 2015). This stems from the desire to minimise the chance of missing a moving lung tumour due normal respiratory motion. In recent years PET/CT scanning has become an integral part of the planning process. It is now commonplace in our institution to acquire a 3D-PET/CT in treatment position and

use that scan for target volume delineation. In chapter five we compared this current clinical standard to the new scanning technique of 4D-PET/CT in terms of geographic miss. While there is no standard definition of a clinically relevant geographic miss, the definitions used in chapter five are based on work by Everitt and colleagues who proposed these categories in the absence of a consensus definition in the literature (Everitt et al., 2009).

What was found is that while our current practice of a 15mm PTV margin mitigates the most severe Type 1 miss, the other types of geographic miss are still an issue when using our standard practice (Callahan et al., 2014c). This information provides further evidence for the need to move beyond 3D-PET/CT imaging into a fully 4D-PET/CT planning environment. The combination of the data presented in chapters four and five shows that incorporating a 4D-PET/CT into our standard planning workflow is both clinically feasible and would result in an improvement in our clinical practice by minimising the risk of geographic miss. The 4D-PET/CT MIP reconstruction will not increase the workload on the radiation oncologists, as it is an image type with which they are already familiar through 4D-CT MIPs. A 4D-PET/CT could be routinely added to any planning PET/CT for lung cancer patients minimising the need for multiple examinations on different imaging modalities. A recent study has also found that a 4D-PET/CT defined ITV has significantly higher inter-observer agreement than 3D-PET defined volumes (Chirindel et al., 2015). The introduction of 4D-PET/CT into the planning workflow would be a clear improvement in clinical practice over using 3D-PET/CT alone. There are some factors that may limit the

routine use of 4D-PET/CT in radiotherapy planning PET. These include increased cost due to additional hardware for a PET/CT scanner and an increase in scanning time. While there is an increase in radiation dose when a 4D-CT scan acquired this should be put in it correct clinical context. If these scans are being used for patients about to receive 60 Gray of radiation for treatment then relative to this large dose of radiation the additional dose from a 4D-CT is insignificant. However issues of radiation dose does preclude the routine use of 4D-PET/CT scanning when it has no added clinical benefit.

The results of the studies presented in chapters four and five were both based on retrospective cohorts. While these results do suggest that 4D-PET/CT would improve clinical practice these finding should be confirmed in a larger prospective cohort. In order to measure the clinical impact of 4D-PET/CT in radiotherapy planning a scoring system to measure impact should in the future be devised similar to our previously published methodology for assessing the clinical impact of PET in lung cancer (Hicks et al., 2001). In this study impact of the PET on patient management was measure as high, medium, low or no impact. The definitions for a prospective trial to measure the impact of a 4D-PET/CT could be as follows:

- High impact: inclusion of additional target volume not defined on 3D-PET/CT (e.g. additional lymph node included)
- Medium impact: Method of treatment delivery was changed (e.g. change in radiation treatment volume)

- Low impact: 4D-PET/CT did not indicate the need for change.
- No impact: Treatment plan was not changed despite being inconsistent with 4D-PET/CT findings.

By applying these criteria in a large prospective cohort the clinical impact can be accurately established.

The clinical application of 4D-PET/CT MIP for planning RT target volumes is not only limited to lung tumours. There is now an increasing push to use SABR for both inoperable liver cancer and liver metastases (Huertas et al., 2015, Andratschke et al., 2015) and potentially other organs close to the diaphragm that are subject to respiratory motion. The high target to background ratio for 4D-PET in the liver is a clear advantage of this technique. This can be observed in the case present in Figure 7.3 (page 161). The liver tumour is unable to be visualised on the non-contrast 4D-CT MIP but can be confidently contoured on the 4D-PET MIP as show in the pink contours. In chapter five we showed that a 3D-PET/CT with only 5mm margin would result in severe geographic misses in most cases. With the steep drop off in dose gradient when using SABR any geographic miss could result in a significant under dosing of a target. The true extent of respiratory motion may not be well visualised on any of the current imaging modalities employed for liver tumours. A 4D-PET/CT MIP is ideally suited to increase the confidence in target volume delineation (Callahan et al., 2013).

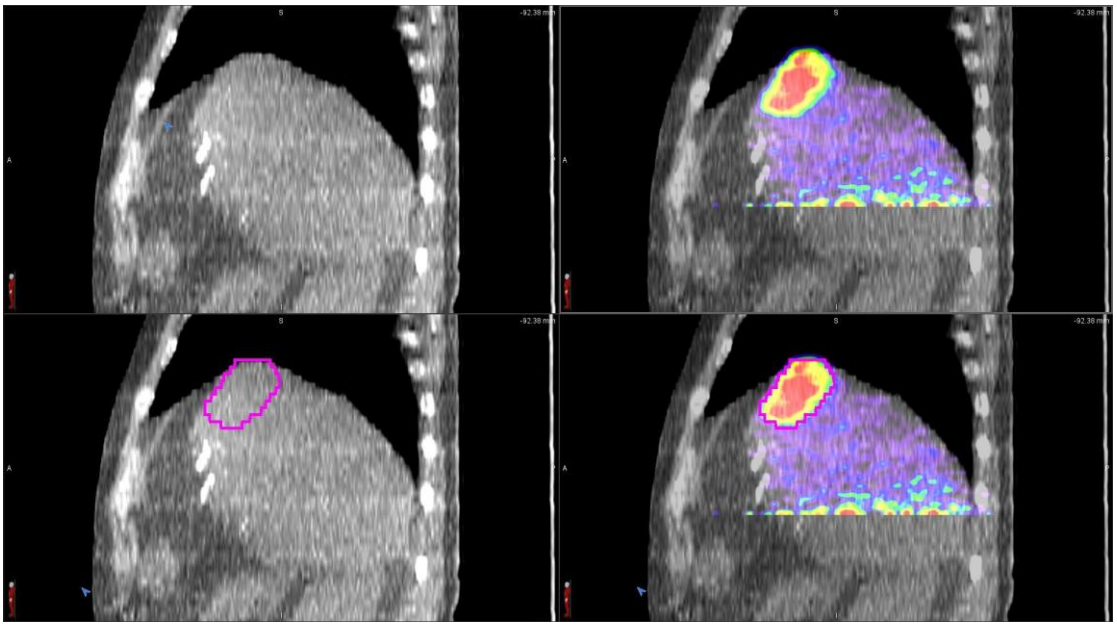

Figure 7.3 – 4D PET/CT MIP in a Liver Tumour

The left hand column shows a 4D-CT MIP and the right hand column is the fused 4D-PET/CT MIP. The liver tumour has been contoured in pink and the maximum displacement of the tumour was measured at 19mm. Images J Callahan (2015)

7.4 CUSTOMISED TARGET VOLUME DELINEATION FOR LUNG TUMOURS

In chapter five we compared 3D and 4D defined target volumes using the standard one size fits all approach to treatment. If the same simple approach for PTV margin expansion was carried over to a 4D scan then there would likely be significantly larger doses to normal tissue when compared to the 3D irradiated volume which could lead to higher rates of tissue toxicity (Yorke et al., 2002). However, as respiratory motion is already taken into account in the 4D volume, the same margin expansion should be no longer necessary. With the validation of 4D-PET/CT as a viable clinical tool we can now consider moving beyond this simple approach to a more customised and patient specific algorithm for defining target volumes.

The first clear step in a 4D-PET/CT planning environment is to remove the compensation for respiratory motion from the PTV expansion. In a study of 20 patients comparing 3D-CT and 4D-CT defined target volumes, Cole and colleagues showed that 4D-CT defined target volumes were significantly smaller than 3D-CT volumes (Cole et al., 2014). This is because in their study the compensation for respiratory motion was removed from the 4D-PTV expansion that they used. With the smaller 4D defined target volumes the authors predicted that the rates of lung toxicity were 22% less for the 4D-CT defined volumes. This is consistent with the finding in chapter five where it was found that a 10mm 4D-PTV expansion was significantly less than a 15mm 3D-PTV expansion. In less mobile tumours, such as those in the upper lobes of the lung, a standard PTV expansion which includes

compensation for motion is often insignificant and therefore the expansion overcompensates for motion (Cole et al., 2014). If there is little or no respiratory motion, the 4D defined volumes reflect this accurately. The reverse is also true in that a tumour that exhibits significant respiratory motion (>30mm) may be missed when using standard PTV margin expansions. The clinical application of 4D scanning allows customisation of a patients target volume to their specific tumour motion rather than assuming that all tumours exhibit the same amplitude of motion. This would be a significant clinical improvement over current practice and potentially lead to lower tissue toxicity and better tumour coverage.

7.5 4D-PET/CT GUIDED OPTIMISATION OF RADIATION THERAPY TO REDUCE LUNG DOSE

In Chapter six we present the first description of 4D imaging in Ga-VQ PET/CT scanning. In a previous published study from our institution, significant artefact from respiratory motion was observed in a number of cases when using this technique (Hofman et al., 2011). An example from this initial pilot study is shown in Figure 7.4 (Page 164). In Figure 7.4 there is mis-registration between the PET and CT scans around the lung bases. In the context of this trial looking for pulmonary embolus, this artefact, while not ideal, did not significantly impair the correct interpretation of the scan. However, in the context of a GaVQ trial that investigated the biological effects of high dose radiation, as well as functional adaptation of treatment based on GaVQ scanning this type of artefact would be a significant

source of error. It is for this reason that the addition of 4D scanning into a GaVQ scan was investigated.

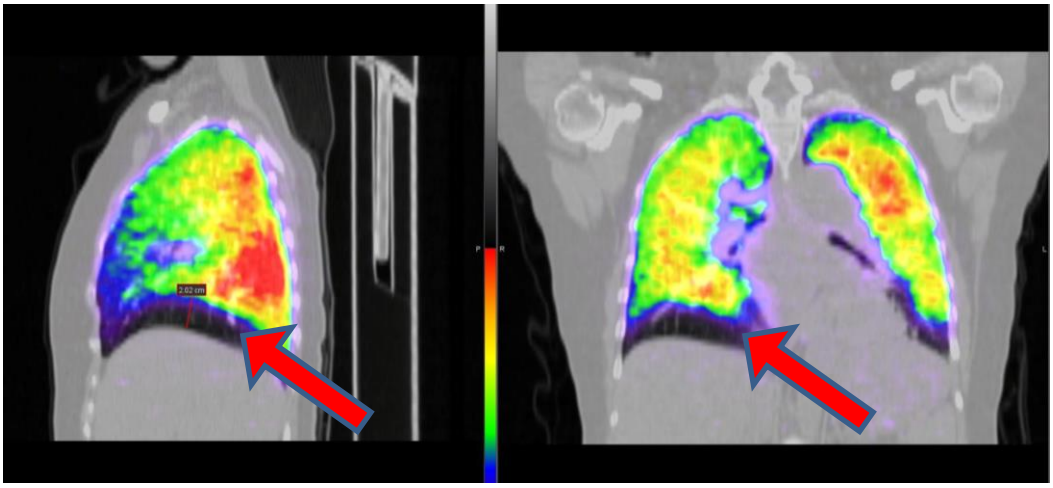

Figure 7.4 – 3D-PET/CT ventilation scan

This scan shows significant mis-registration (red arrow) around the lung bases on a ventilation PET/CT scan without correction for respiratory motion. Images J Callahan (2015)

In the study presented in chapter six, we showed that 4D imaging is feasible and corrects respiratory motion artefact well for every case. The protocol described in chapter six has been now used by other researchers who have gone on to investigate whether the functional information provided by the 4D-PET/CT VQ scan can be exploited to reduce radiation dose to functioning lung (Siva et al., 2015b, Siva et al., 2015d). The ultimate aim would be to reduce loss of lung function caused by radiation treatment for patient with many lung co-morbidities. The researchers were able to show, in a simulated environment, that radiotherapy plans could be adapted

to reduce radiation dose to areas of well perfused lung defined on the GaVQ PET. A larger prospective trial is currently underway to confirm these findings. Without effective correction for respiratory motion these types of analyses would be unlikely to produce accurate results due to inconsistencies between the PET/CT VQ scan and the planning scans. Using the technique described in chapter six presents an effective clinical application for 4D PET/CT to improve clinical practice in an effort to reduce radiation induced lung toxicity.

7.6 MONITORING OF BIOLOGICAL RESPONSE OF NORMAL LUNG TO RADIATION THERAPY USING 4D-PET/CT

The relationship between radiation dose and biological effect of radiation therapy to the lungs is not well understood. A recent meta-analysis found that despite adherence to recommended lung dosing constraints, radiation induced pneumonitis is still experienced in nearly 30% of cases and fatal pneumonitis in 1.9% (Palma et al., 2013). This could be due to the fact that these dosing constraints are not based on a patient's own biology. Improving our understanding of the biological effects of radiation on the lungs will aid in developing strategies for reducing these potentially fatal complication. The functional information obtained from a Ga-VQ scan using the methodology described in chapter six is ideal for these investigations.

Researchers have previously investigated standard VQ-SPECT in an effort to measure a dose effect relationship between radiation and loss of lung function. An analysis of VQ-SPECT noted that a limitation of using SPECT was the inaccuracies introduced by

patient breathing and that there was no way to eliminate these errors using SPECT (Zhang et al., 2010). A local dose-effect relationship on lung perfusion post SBRT as measured by SPECT was also analysed by Scheenstra and colleagues (Scheenstra et al., 2013). In order to minimise the effect of breathing on their results all patients with lower lobe tumours were excluded. The protocol described in chapter six eliminates this as a source of error and all patients can be included.

A recent publication be Siva and colleagues, using the protocol defined in chapter six, investigated dose dependant functional loss after definitive radiation therapy (Siva et al., 2015c). The combination of the improved resolution of PET and correction for respiratory motion meant that a near perfect dose response relationship was observed between loss in perfusion and delivered radiation dose ($r^2 = 0.99$, $p < 0.01$). This data indicated that a 4D-PET/CT GaVQ scan prior to treatment can be used to predict the proportion of functional lung that will be lost due to the radiation. It has now been shown that a 4D-PET/CT GaVQ scan enables both the accurate measurement of radiation injury to the lung and the development of strategies to avoid areas of functioning lung in order to minimise loss of function post therapy (Siva et al., 2015d, Siva et al., 2015c, Siva et al., 2015b).

CHAPTER 8 - CONCLUSIONS AND FUTURE DEVELOPMENTS

The results presented in this thesis have shown that 4D-PET/CT has a clinical impact on the management of patients with lung cancer, from the point of diagnosis, to their treatment and the monitoring of the effects of radiation therapy. The use of 4D-PET/CT is now establishing itself as routine clinical tool that will improve outcomes for patients with highly mobile lung tumours as well as other malignancies in areas affected by respiratory motion. As 4D technology improves and becomes easier to use, the clinical application of this scanning technique will become more ubiquitous and establish itself as just another tool in the arsenal of oncology clinicians.

ONGOING WORK AND CONSIDERATIONS FOR FUTURE TRIALS

The work presented in this thesis adds to the increasing body of work that is establishing a role for 4D-PET/CT in clinical practice. While some questions have been addressed in the presented studies, there are still many questions to be addressed in ongoing and future clinical trials. The majority of the work to date has been centred on using 4D-PET/CT for lung lesions and much less work has been done investigating the use of 4D-PET/CT for liver tumours and other upper abdominal malignancies. In many ways 4D-PET/CT is likely to have an even greater impact on patient management for such tumours, particularly in the liver due to the added confounding factor of higher background activity. Also 4D-CT for radiotherapy

planning is problematic due to the generally poor soft tissue contrast in the liver to define the tumours. Going forward this is the next likely area of active research into the clinical use of 4D-PET/CT.

The use of respiratory gating in PET-VQ scanning continues to be an area of active research with many published studies using the methodology outlined in this thesis. As well as the ongoing work by Siva and colleagues another group led by Kipritidis are attempting to create a ventilation image using a 4D-CT scan and to compare this to the 4D Ventilation scan to refine their technique (Kipritidis et al., 2014). In another study Hardcastle and colleagues used the 4D-PET/CT VQ technique to assess the use of deformable registration algorithms (Hardcastle et al., 2015). In a case study, Hofman was able to visualise a case of segmental lobar pneumonia on a 4D-PET/CT VQ scan that was not visulised on the standard SPECT-VQ scan (Hofman et al., 2014).

The methodology outlined in chapters four and five was reproduced in a cohort of lung SABR patients with similar results (Siva et al., 2015a). The extra precision and ability to better correlate finding across modalities means that 4D scanning will be an integral part of any radiotherapy study that includes PET.

The results presented in this thesis form a firm basis for including 4D scanning as a validated clinical tool. As the technology improves and more studies are published, 4D-PET/CT scanning will become a routine scanning procedure for all PET centres that assist in the management of patients with lung cancer.

CHAPTER 9 - REFERENCES

References

AFSHAR-OROMIEH, A., MALCHER, A., EDER, M., EISENHUT, M., LINHART, H. G., HADASCHIK, B. A., HOLLAND-LETZ, T., GIESEL, F. L., KRATOCHWIL, C., HAUFE, S., HABERKORN, U. & ZECHMANN, C. M. 2013. PET imaging with a [68Ga]gallium-labelled PSMA ligand for the diagnosis of prostate cancer: biodistribution in humans and first evaluation of tumour lesions. *Eur J Nucl Med Mol Imaging,* 40**,** 486-95.

AIDE, N., KINROSS, K., BEAUREGARD, J. M., NEELS, O., POTDEVIN, T., ROSELT, P., DOROW, D., CULLINANE, C. & HICKS, R. J. 2011. A dual radiologic contrast agent protocol for 18F-FDG and 18F-FLT PET/CT imaging of mice bearing abdominal tumors. *Mol Imaging Biol,* 13**,** 518-25.

AKHURST, T., MACMANUS, M. & HICKS, R. J. 2015. Lung Cancer. *PET Clin,* 10**,** 147-158.

ALPERT, J. B., LOWRY, C. M. & KO, J. P. 2015. Imaging the solitary pulmonary nodule. *Clin Chest Med,* 36**,** 161-78, vii.

ANDRATSCHKE, N. H., NIEDER, C., HEPPT, F., MOLLS, M. & ZIMMERMANN, F. 2015. Stereotactic radiation therapy for liver metastases: factors affecting local control and survival. *Radiat Oncol,* 10**,** 69.

ARISTOPHANOUS, M., BERBECO, R. I., KILLORAN, J. H., YAP, J. T., SHER, D. J., ALLEN, A. M., LARSON, E. & CHEN, A. B. 2011. Clinical Utility of 4D FDG-PET/CT Scans in Radiation Treatment Planning. *Int J Radiat Oncol Biol Phys*.

ARISTOPHANOUS, M., BERBECO, R. I., KILLORAN, J. H., YAP, J. T., SHER, D. J., ALLEN, A. M., LARSON, E. & CHEN, A. B. 2012. Clinical utility of 4D FDG-PET/CT scans in radiation treatment planning. *Int J Radiat Oncol Biol Phys,* 82**,** e99-105.

BAYNE, M., HICKS, R. J., EVERITT, S., FIMMELL, N., BALL, D., REYNOLDS, J., LAU, E., PITMAN, A., WARE, R. & MACMANUS, M. 2010. Reproducibility of "intelligent" contouring of gross tumor volume

in non-small-cell lung cancer on PET/CT images using a standardized visual method. *Int J Radiat Oncol Biol Phys,* 77**,** 1151-7.

BEZJAK, A., RUMBLE, R. B., RODRIGUES, G., HOPE, A. & WARDE, P. 2012. Intensity-modulated radiotherapy in the treatment of lung cancer. *Clin Oncol (R Coll Radiol),* 24**,** 508-20.

BOELLAARD, R., DELGADO-BOLTON, R., OYEN, W. J., GIAMMARILE, F., TATSCH, K., ESCHNER, W., VERZIJLBERGEN, F. J., BARRINGTON, S. F., PIKE, L. C., WEBER, W. A., STROOBANTS, S., DELBEKE, D., DONOHOE, K. J., HOLBROOK, S., GRAHAM, M. M., TESTANERA, G., HOEKSTRA, O. S., ZIJLSTRA, J., VISSER, E., HOEKSTRA, C. J., PRUIM, J., WILLEMSEN, A., ARENDS, B., KOTZERKE, J., BOCKISCH, A., BEYER, T., CHITI, A. & KRAUSE, B. J. 2015. FDG PET/CT: EANM procedure guidelines for tumour imaging: version 2.0. *Eur J Nucl Med Mol Imaging,* 42**,** 328-54.

BOWEN, S. R., NYFLOT, M. J., HERRMANN, C., GROH, C. M., MEYER, J., WOLLENWEBER, S. D., STEARNS, C. W., KINAHAN, P. E. & SANDISON, G. A. 2015. Imaging and dosimetric errors in 4D PET/CT-guided radiotherapy from patient-specific respiratory patterns: a dynamic motion phantom end-to-end study. *Phys Med Biol,* 60**,** 3731-46.

BREEMAN, W. A., DE BLOIS, E., SZE CHAN, H., KONIJNENBERG, M., KWEKKEBOOM, D. J. & KRENNING, E. P. 2011. (68)Ga-labeled DOTA-peptides and (68)Ga-labeled radiopharmaceuticals for positron emission tomography: current status of research, clinical applications, and future perspectives. *Semin Nucl Med,* 41**,** 314-21.

BUCHMANN, I., HENZE, M., ENGELBRECHT, S., EISENHUT, M., RUNZ, A., SCHAFER, M., SCHILLING, T., HAUFE, S., HERRMANN, T. & HABERKORN, U. 2007. Comparison of 68Ga-DOTATOC PET and 111In-DTPAOC (Octreoscan) SPECT in patients with neuroendocrine tumours. *Eur J Nucl Med Mol Imaging,* 34**,** 1617-26.

BUNDSCHUH, R. A., ANDRATSCHKE, N., DINGES, J., DUMA, M. N., ASTNER, S. T., BRUGEL, M., ZIEGLER, S. I., MOLLS, M., SCHWAIGER, M. & ESSLER, M. 2012. Respiratory gated [18F]FDG PET/CT for target volume delineation in stereotactic radiation treatment of liver metastases. *Strahlenther Onkol,* 188**,** 592-8.

CALDWELL, C. B., MAH, K., SKINNER, M. & DANJOUX, C. E. 2003. Can PET provide the 3D extent of tumor motion for individualized internal target volumes? A phantom study of the limitations of CT and the promise of PET. *Int J Radiat Oncol Biol Phys,* 55**,** 1381-93.

CALLAHAN, J., BINNS, D., DUNN, L. & KRON, T. 2011a. Motion effects on SUV and lesion volume in 3D and 4D PET scanning. *Australas Phys Eng Sci Med,* 34**,** 489-95.

CALLAHAN, J., HOFMAN, M. S., SIVA, S., KRON, T., SCHNEIDER, M. E., BINNS, D., EU, P. & HICKS, R. J. 2014a. High-resolution imaging of pulmonary ventilation and perfusion with 68Ga-VQ respiratory gated (4-D) PET/CT. *Eur J Nucl Med Mol Imaging,* 41**,** 343-9.

CALLAHAN, J., KRON, T., SCHNEIDER, M. E. & HICKS, R. J. 2014b. A prospective investigation into the clinical impact of 4D-PET/CT in the characterisation of solitary pulmonary nodules. *Cancer Imaging,* 14**,** 24.

CALLAHAN, J., KRON, T., SCHNEIDER-KOLSKY, M., DUNN, L., THOMPSON, M., SIVA, S., AARONS, Y., BINNS, D. & HICKS, R. J. 2013. Validation of a 4D-PET maximum intensity projection for delineation of an internal target volume. *Int J Radiat Oncol Biol Phys,* 86**,** 749-54.

CALLAHAN, J., KRON, T., SCHNEIDER-KOLSKY, M. & HICKS, R. J. 2011b. The clinical significance and management of lesion motion due to respiration during PET/CT scanning. *Cancer Imaging,* 11**,** 224-36.

CALLAHAN, J., KRON, T., SIVA, S., SIMOENS, N., EDGAR, A., EVERITT, S., SCHNEIDER, M. E. & HICKS, R. J. 2014c. Geographic miss of lung tumours due to respiratory motion: a comparison of 3D vs 4D PET/CT defined target volumes. *Radiat Oncol,* 9**,** 291.

CHAVAUDRA, J. & BRIDIER, A. 2001. [Definition of volumes in external radiotherapy: ICRU reports 50 and 62]. *Cancer Radiother,* 5**,** 472-8.

CHIRINDEL, A., ADEBAHR, S., SCHUSTER, D., SCHIMEK-JASCH, T., SCHANNE, D. H., NEMER, U., MIX, M., MEYER, P., GROSU, A. L., BRUNNER, T. & NESTLE, U. 2015. Impact of 4D-FDG-PET/CT imaging on target volume delineation in SBRT patients with central versus peripheral lung tumors. Multi-reader comparative study. *Radiother Oncol*.

CHRISTIAN, J. A., PARTRIDGE, M., NIOUTSIKOU, E., COOK, G., MCNAIR, H. A., CRONIN, B., COURBON, F., BEDFORD, J. L. & BRADA, M. 2005. The incorporation of SPECT functional lung imaging into inverse radiotherapy planning for non-small cell lung cancer. *Radiother Oncol,* 77**,** 271-7.

CHURCH, T. R., BLACK, W. C., ABERLE, D. R., BERG, C. D., CLINGAN, K. L., DUAN, F., FAGERSTROM, R. M., GAREEN, I. F., GIERADA, D. S., JONES, G. C., MAHON, I., MARCUS, P. M., SICKS, J. D., JAIN, A. & BAUM, S. 2013. Results of initial low-dose computed tomographic screening for lung cancer. *N Engl J Med,* 368**,** 1980-91.

COLE, A. J., O'HARE, J. M., MCMAHON, S. J., MCGARRY, C. K., BUTTERWORTH, K. T., MCALEESE, J., JAIN, S., HOUNSELL, A. R., PRISE, K. M., HANNA, G. G. & O'SULLIVAN, J. M. 2014. Investigating the potential impact of four-dimensional computed tomography (4DCT) on toxicity, outcomes and dose escalation for radical lung cancer radiotherapy. *Clin Oncol (R Coll Radiol),* 26**,** 142-50.

CREACH, K. M., BRADLEY, J. D., MAHASITTIWAT, P. & ROBINSON, C. G. 2012. Stereotactic body radiation therapy in the treatment of multiple primary lung cancers. *Radiother Oncol,* 104**,** 19-22.

CRONIN, P., DWAMENA, B. A., KELLY, A. M., BERNSTEIN, S. J. & CARLOS, R. C. 2008. Solitary pulmonary nodules and masses: a meta-analysis of the diagnostic utility of alternative imaging tests. *Eur Radiol,* 18**,** 1840-56.

CUI, G., GOPALAN, S., YAMAMOTO, T., BERGER, J., MAXIM, P. G. & KEALL, P. J. 2010. Commissioning and quality assurance for a respiratory training system based on audiovisual biofeedback. *J Appl Clin Med Phys,* 11**,** 3262.

DIDIERLAURENT, D., RIBES, S., CASELLES, O., JAUDET, C., CAZALET, J. M., BATATIA, H. & COURBON, F. 2013. A new respiratory gating device to improve 4D PET/CT. *Med Phys,* 40**,** 032501.

DINKEL, J., HINTZE, C., TETZLAFF, R., HUBER, P. E., HERFARTH, K., DEBUS, J., KAUCZOR, H. U. & THIEKE, C. 2009. 4D-MRI analysis of lung tumor motion in patients with hemidiaphragmatic paralysis. *Radiother Oncol,* 91**,** 449-54.

DUAN, Y., LI, J., ZHANG, Y., WANG, W., SUN, X., FAN, T., SHAO, Q., XU, M., GUO, Y. & SHANG, D. 2015. Comparison of primary tumour volumes delineated on four-dimensional computed tomography maximum intensity projection and F-fluorodeoxyglucose positron emission tomography computed tomography images of non-small cell lung cancer. *J Med Imaging Radiat Oncol*.

DUNLEAVY, K., MIKHAEEL, G., SEHN, L. H., HICKS, R. J. & WILSON, W. H. 2010. The value of positron emission tomography in prognosis and response assessment in non-Hodgkin lymphoma. *Leuk Lymphoma,* 51 Suppl 1**,** 28-33.

DUNN, L., KRON, T., JOHNSTON, P. N., MCDERMOTT, L. N., TAYLOR, M. L., CALLAHAN, J. & FRANICH, R. D. 2012. A programmable motion phantom for quality assurance of motion management in radiotherapy. *Australas Phys Eng Sci Med,* 35**,** 93-100.

ERDI, Y. E., NEHMEH, S. A., PAN, T., PEVSNER, A., ROSENZWEIG, K. E., MAGERAS, G., YORKE, E. D., SCHODER, H., HSIAO, W., SQUIRE,

O. D., VERNON, P., ASHMAN, J. B., MOSTAFAVI, H., LARSON, S. M. & HUMM, J. L. 2004. The CT motion quantitation of lung lesions and its impact on PET-measured SUVs. *J Nucl Med,* 45**,** 1287-92.

EVERITT, S., KRON, T., LEONG, T., SCHNEIDER-KOLSKY, M. & MAC MANUS, M. 2009. Geographic miss in radiation oncology: have we missed the boat? *J Med Imaging Radiat Oncol,* 53**,** 506-9.

FARID, K., POULLIAS, X., ALIFANO, M., REGNARD, J. F., SERVOIS, V., CAILLAT-VIGNERON, N. & PETRAS, S. 2015. Respiratory-gated imaging in metabolic evaluation of small solitary pulmonary nodules: 18F-FDG PET/CT and correlation with histology. *Nucl Med Commun*.

FIN, L., DAOUK, J., MORVAN, J., BAILLY, P., EL ESPER, I., SAIDI, L. & MEYER, M. E. 2008. Initial clinical results for breath-hold CT-based processing of respiratory-gated PET acquisitions. *Eur J Nucl Med Mol Imaging,* 35**,** 1971-80.

FLETCHER, J. W., KYMES, S. M., GOULD, M., ALAZRAKI, N., COLEMAN, R. E., LOWE, V. J., MARN, C., SEGALL, G., THET, L. A. & LEE, K. 2008. A comparison of the diagnostic accuracy of 18F-FDG PET and CT in the characterization of solitary pulmonary nodules. *J Nucl Med,* 49**,** 179-85.

GAMBHIR, S. S., CZERNIN, J., SCHWIMMER, J., SILVERMAN, D. H., COLEMAN, R. E. & PHELPS, M. E. 2001. A tabulated summary of the FDG PET literature. *J Nucl Med,* 42**,** 1S-93S.

GARCIA VICENTE, A. M., CASTREJON, A. S., LEON MARTIN, A. A., GARCIA, B. G., PILKINGTON WOLL, J. P. & MUNOZ, A. P. 2011. Value of 4-dimensional 18F-FDG PET/CT in the classification of pulmonary lesions. *J Nucl Med Technol,* 39**,** 91-9.

GARCIA VICENTE, A. M., SORIANO CASTREJON, A. M., TALAVERA RUBIO, M. P., LEON MARTIN, A. A., PALOMAR MUNOZ, A. M., PILKINGTON WOLL, J. P. & POBLETE GARCIA, V. M. 2010. (18)F-FDG PET-CT respiratory gating in characterization of pulmonary lesions: approximation towards clinical indications. *Ann Nucl Med,* 24**,** 207-14.

GEETS, X. 2013. 4D PET-CT guided radiation therapy. *JBR-BTR,* 96**,** 155-9.

GOLDSMITH, C. & GAYA, A. 2012. Stereotactic ablative body radiotherapy (SABR) for primary and secondary lung tumours. *Cancer Imaging,* 12**,** 351-60.

GOULD, M. K., DONINGTON, J., LYNCH, W. R., MAZZONE, P. J., MIDTHUN, D. E., NAIDICH, D. P. & WIENER, R. S. 2013. Evaluation of individuals with pulmonary nodules: when is it lung cancer?

Diagnosis and management of lung cancer, 3rd ed: American College of Chest Physicians evidence-based clinical practice guidelines. *Chest,* 143**,** e93S-120S.

GRECO, C., ROSENZWEIG, K., CASCINI, G. L. & TAMBURRINI, O. 2007. Current status of PET/CT for tumour volume definition in radiotherapy treatment planning for non-small cell lung cancer (NSCLC). *Lung Cancer,* 57**,** 125-34.

GREGORY, D. L., HICKS, R. J., HOGG, A., BINNS, D. S., SHUM, P. L., MILNER, A., LINK, E., BALL, D. L. & MAC MANUS, M. P. 2012. Effect of PET/CT on Management of Patients with Non-Small Cell Lung Cancer: Results of a Prospective Study with 5-Year Survival Data. *J Nucl Med,* 53**,** 1007-15.

GRILLS, I. S., YAN, D., BLACK, Q. C., WONG, C. Y., MARTINEZ, A. A. & KESTIN, L. L. 2007. Clinical implications of defining the gross tumor volume with combination of CT and 18FDG-positron emission tomography in non-small-cell lung cancer. *Int J Radiat Oncol Biol Phys,* 67**,** 709-19.

GUERRA, L., DE PONTI, E., ELISEI, F., BETTINARDI, V., LANDONI, C., PICCHIO, M., GILARDI, M. C., VERSARI, A., FIORONI, F., DZIUK, M., KOZA, M., AHOND-VIONNET, R., COLLIN, B. & MESSA, C. 2012. Respiratory gated PET/CT in a European multicentre retrospective study: added diagnostic value in detection and characterization of lung lesions. *Eur J Nucl Med Mol Imaging,* 39**,** 1381-90.

GUERRA, L., MEREGALLI, S., ZORZ, A., NIESPOLO, R., DE PONTI, E., ELISEI, F., MORZENTI, S., BRENNA, S., CRESPI, A., GARDANI, G. & MESSA, C. 2014. Comparative evaluation of CT-based and respiratory-gated PET/CT-based planning target volume (PTV) in the definition of radiation treatment planning in lung cancer: preliminary results. *Eur J Nucl Med Mol Imaging,* 41**,** 702-10.

GUPTA, N. C., FRANK, A. R., DEWAN, N. A., REDEPENNING, L. S., ROTHBERG, M. L., MAILLIARD, J. A., PHALEN, J. J., SUNDERLAND, J. J. & FRICK, M. P. 1992. Solitary pulmonary nodules: detection of malignancy with PET with 2-[F-18]-fluoro-2-deoxy-D-glucose. *Radiology,* 184**,** 441-4.

HANLEY, J., DEBOIS, M. M., MAH, D., MAGERAS, G. S., RABEN, A., ROSENZWEIG, K., MYCHALCZAK, B., SCHWARTZ, L. H., GLOEGGLER, P. J., LUTZ, W., LING, C. C., LEIBEL, S. A., FUKS, Z. & KUTCHER, G. J. 1999. Deep inspiration breath-hold technique for lung tumors: the potential value of target immobilization and reduced lung density in dose escalation. *Int J Radiat Oncol Biol Phys,* 45**,** 603-11.

HANNA, G. G., HOUNSELL, A. R. & O'SULLIVAN, J. M. 2010. Geometrical analysis of radiotherapy target volume delineation: a systematic review of reported comparison methods. *Clin Oncol (R Coll Radiol),* 22**,** 515-25.

HANNA, G. G., VAN SORNSEN DE KOSTE, J. R., DAHELE, M. R., CARSON, K. J., HAASBEEK, C. J., MIGCHIELSEN, R., HOUNSELL, A. R. & SENAN, S. 2012a. Defining target volumes for stereotactic ablative radiotherapy of early-stage lung tumours: a comparison of three-dimensional 18F-fluorodeoxyglucose positron emission tomography and four-dimensional computed tomography. *Clin Oncol (R Coll Radiol),* 24**,** e71-80.

HANNA, G. G., VAN SORNSEN DE KOSTE, J. R., DAHELE, M. R., CARSON, K. J., HAASBEEK, C. J., MIGCHIELSEN, R., HOUNSELL, A. R. & SENAN, S. 2012b. Defining Target Volumes for Stereotactic Ablative Radiotherapy of Early-stage Lung Tumours: A Comparison of Three-dimensional (18)F-fluorodeoxyglucose Positron Emission Tomography and Four-dimensional Computed Tomography. *Clin Oncol (R Coll Radiol)*.

HARDCASTLE, N., HOFMAN, M. S., HICKS, R. J., CALLAHAN, J., KRON, T., MACMANUS, M. P., BALL, D. L., JACKSON, P. & SIVA, S. 2015. Accuracy and Utility of Deformable Image Registration in (68)Ga 4D PET/CT Assessment of Pulmonary Perfusion Changes During and After Lung Radiation Therapy. *Int J Radiat Oncol Biol Phys,* 93**,** 196-204.

HICKS, R. J. & HOFMAN, M. S. 2012. Is there still a role for SPECT-CT in oncology in the PET-CT era? *Nat Rev Clin Oncol,* 9**,** 712-20.

HICKS, R. J., KALFF, V., MACMANUS, M. P., WARE, R. E., HOGG, A., MCKENZIE, A. F., MATTHEWS, J. P. & BALL, D. L. 2001. (18)F-FDG PET provides high-impact and powerful prognostic stratification in staging newly diagnosed non-small cell lung cancer. *J Nucl Med,* 42**,** 1596-604.

HILL, R. P. 2005. Radiation effects on the respiratory system. *BJR Suppl,* 27**,** 75-81.

HOF, H., RHEIN, B., HAERING, P., KOPP-SCHNEIDER, A., DEBUS, J. & HERFARTH, K. 2009. 4D-CT-based target volume definition in stereotactic radiotherapy of lung tumours: comparison with a conventional technique using individual margins. *Radiother Oncol,* 93**,** 419-23.

HOFMAN, M., BINNS, D., JOHNSTON, V., SIVA, S., THOMPSON, M., EU, P., COLLINS, M. & HICKS, R. J. 2015. 68Ga-EDTA PET/CT imaging

and plasma clearance for glomerular filtration rate quantification: comparison to conventional 51Cr-EDTA. *J Nucl Med,* 56**,** 405-9.

HOFMAN, M. S., BEAUREGARD, J. M., BARBER, T. W., NEELS, O. C., EU, P. & HICKS, R. J. 2011. 68Ga PET/CT ventilation-perfusion imaging for pulmonary embolism: a pilot study with comparison to conventional scintigraphy. *J Nucl Med,* 52**,** 1513-9.

HOFMAN, M. S., CALLAHAN, J., EU, P. & HICKS, R. J. 2014. Segmental hyperperfusion in lobar pneumonia visualized with respiratory-gated four-dimensional pulmonary perfusion positron emission tomography-computed tomography. *Am J Respir Crit Care Med,* 189**,** 104-5.

HOFMAN, M. S., KONG, G., NEELS, O. C., EU, P., HONG, E. & HICKS, R. J. 2012. High management impact of Ga-68 DOTATATE (GaTate) PET/CT for imaging neuroendocrine and other somatostatin expressing tumours. *J Med Imaging Radiat Oncol,* 56**,** 40-7.

HOUTVEEN, J. H., GROOT, P. F. & DE GEUS, E. J. 2006. Validation of the thoracic impedance derived respiratory signal using multilevel analysis. *Int J Psychophysiol,* 59**,** 97-106.

HUANG, T. C., CHOU, K. T., WANG, Y. C. & ZHANG, G. 2014. Motion freeze for respiration motion correction in PET/CT: a preliminary investigation with lung cancer patient data. *Biomed Res Int,* 2014**,** 167491.

HUBNER, K. F., BUONOCORE, E., GOULD, H. R., THIE, J., SMITH, G. T., STEPHENS, S. & DICKEY, J. 1996. Differentiating benign from malignant lung lesions using "quantitative" parameters of FDG PET images. *Clin Nucl Med,* 21**,** 941-9.

HUERTAS, A., BAUMANN, A. S., SAUNIER-KUBS, F., SALLERON, J., OLDRINI, G., CROISE-LAURENT, V., BARRAUD, H., AYAV, A., BRONOWICKI, J. P. & PEIFFERT, D. 2015. Stereotactic body radiation therapy as an ablative treatment for inoperable hepatocellular carcinoma. *Radiother Oncol,* 115**,** 211-6.

JANI, S. S., LAMB, J. M., WHITE, B. M., DAHLBOM, M., ROBINSON, C. G. & LOW, D. A. 2015. Assessing margin expansions of internal target volumes in 3D and 4D PET: a phantom study. *Ann Nucl Med,* 29**,** 100-9.

JOGI, J., JONSON, B., EKBERG, M. & BAJC, M. 2010. Ventilation-perfusion SPECT with 99mTc-DTPA versus Technegas: a head-to-head study in obstructive and nonobstructive disease. *J Nucl Med,* 51**,** 735-41.

KALADE, A. V., EDDIE LAU, W. F., CONRON, M., WRIGHT, G. M., DESMOND, P. V., HICKS, R. J. & CHEN, R. 2008. Endoscopic ultrasound-guided fine-needle aspiration when combined with positron

emission tomography improves specificity and overall diagnostic accuracy in unexplained mediastinal lymphadenopathy and staging of non-small-cell lung cancer. *Intern Med J,* 38**,** 837-44.

KAYANI, I., BOMANJI, J. B., GROVES, A., CONWAY, G., GACINOVIC, S., WIN, T., DICKSON, J., CAPLIN, M. & ELL, P. J. 2008. Functional imaging of neuroendocrine tumors with combined PET/CT using 68Ga-DOTATATE (DOTA-DPhe1,Tyr3-octreotate) and 18F-FDG. *Cancer,* 112**,** 2447-55.

KEALL, P. J., MAGERAS, G. S., BALTER, J. M., EMERY, R. S., FORSTER, K. M., JIANG, S. B., KAPATOES, J. M., LOW, D. A., MURPHY, M. J., MURRAY, B. R., RAMSEY, C. R., VAN HERK, M. B., VEDAM, S. S., WONG, J. W. & YORKE, E. 2006. The management of respiratory motion in radiation oncology report of AAPM Task Group 76. *Med Phys,* 33**,** 3874-900.

KELLOFF, G. J., HOFFMAN, J. M., JOHNSON, B., SCHER, H. I., SIEGEL, B. A., CHENG, E. Y., CHESON, B. D., O'SHAUGHNESSY, J., GUYTON, K. Z., MANKOFF, D. A., SHANKAR, L., LARSON, S. M., SIGMAN, C. C., SCHILSKY, R. L. & SULLIVAN, D. C. 2005a. Progress and promise of FDG-PET imaging for cancer patient management and oncologic drug development. *Clin Cancer Res,* 11**,** 2785-808.

KELLOFF, G. J., KROHN, K. A., LARSON, S. M., WEISSLEDER, R., MANKOFF, D. A., HOFFMAN, J. M., LINK, J. M., GUYTON, K. Z., ECKELMAN, W. C., SCHER, H. I., O'SHAUGHNESSY, J., CHESON, B. D., SIGMAN, C. C., TATUM, J. L., MILLS, G. Q., SULLIVAN, D. C. & WOODCOCK, J. 2005b. The progress and promise of molecular imaging probes in oncologic drug development. *Clin Cancer Res,* 11**,** 7967-85.

KILLORAN, J. H., GERBAUDO, V. H., MAMEDE, M., IONASCU, D., PARK, S. J. & BERBECO, R. 2011. Motion artifacts occurring at the lung/diaphragm interface using 4D CT attenuation correction of 4D PET scans. *J Appl Clin Med Phys,* 12**,** 3502.

KINAHAN, P. E., TOWNSEND, D. W., BEYER, T. & SASHIN, D. 1998. Attenuation correction for a combined 3D PET/CT scanner. *Med Phys,* 25**,** 2046-53.

KIPRITIDIS, J., SIVA, S., HOFMAN, M. S., CALLAHAN, J., HICKS, R. J. & KEALL, P. J. 2014. Validating and improving CT ventilation imaging by correlating with ventilation 4D-PET/CT using 68Ga-labeled nanoparticles. *Med Phys,* 41**,** 011910.

KOIVUMAKI, T., TEUHO, J., TERAS, M., VAUHKONEN, M. & HAKULINEN, M. A. 2015. A novel respiratory gating method for oncologic positron

emission tomography based on bioimpedance approach. *Ann Nucl Med*.

KONERT, T., VOGEL, W., MACMANUS, M. P., NESTLE, U., BELDERBOS, J., GREGOIRE, V., THORWARTH, D., FIDAROVA, E., PAEZ, D., CHITI, A. & HANNA, G. G. 2015. PET/CT imaging for target volume delineation in curative intent radiotherapy of non-small cell lung cancer: IAEA consensus report 2014. *Radiother Oncol*.

KONG, F. M., RITTER, T., QUINT, D. J., SENAN, S., GASPAR, L. E., KOMAKI, R. U., HURKMANS, C. W., TIMMERMAN, R., BEZJAK, A., BRADLEY, J. D., MOVSAS, B., MARSH, L., OKUNIEFF, P., CHOY, H. & CURRAN, W. J., JR. 2011. Consideration of dose limits for organs at risk of thoracic radiotherapy: atlas for lung, proximal bronchial tree, esophagus, spinal cord, ribs, and brachial plexus. *Int J Radiat Oncol Biol Phys,* 81**,** 1442-57.

KOTZERKE, J., ANDREEFF, M. & WUNDERLICH, G. 2010a. PET aerosol lung scintigraphy using Galligas. *Eur J Nucl Med Mol Imaging,* 37**,** 175-7.

KOTZERKE, J., ANDREEFF, M., WUNDERLICH, G., WIGGERMANN, P. & ZOPHEL, K. 2010b. [Ventilation-perfusion-lungscintigraphy using PET and 68Ga-labeled radiopharmaceuticals]. *Nuklearmedizin,* 49**,** 203-8.

LAMB, J. M., ROBINSON, C., BRADLEY, J., LAFOREST, R., DEHDASHTI, F., WHITE, B. M., WUENSCHEL, S. & LOW, D. A. 2011. Generating lung tumor internal target volumes from 4D-PET maximum intensity projections. *Med Phys,* 38**,** 5732-7.

LAMB, J. M., ROBINSON, C. G., BRADLEY, J. D. & LOW, D. A. 2013. Motion-specific internal target volumes for FDG-avid mediastinal and hilar lymph nodes. *Radiother Oncol,* 109**,** 112-6.

LARSON, S. M., NEHMEH, S. A., ERDI, Y. E. & HUMM, J. L. 2005. PET/CT in non-small-cell lung cancer: value of respiratory-gated PET. *Chang Gung Med J,* 28**,** 306-14.

LEBLANC, M., LEVEILLEE, F. & TURCOTTE, E. 2007. Prospective evaluation of the negative predictive value of V/Q SPECT using 99mTc-Technegas. *Nucl Med Commun,* 28**,** 667-72.

LEE, H. Y., JEONG, J. Y., LEE, K. S., KIM, H. J., HAN, J., KIM, B. T., KIM, J., SHIM, Y. M., KIM, J. H. & SONG, I. 2012. Solitary pulmonary nodular lung adenocarcinoma: correlation of histopathologic scoring and patient survival with imaging biomarkers. *Radiology,* 264**,** 884-93.

LI, F. X., LI, J. B., ZHANG, Y. J., LIU, T. H., TIAN, S. Y., XU, M., SHANG, D. P. & MA, C. S. 2011. Comparison of the planning target volume based

on three-dimensional CT and four-dimensional CT images of non-small-cell lung cancer. *Radiother Oncol,* 99**,** 176-80.

LI, G., CITRIN, D., CAMPHAUSEN, K., MUELLER, B., BURMAN, C., MYCHALCZAK, B., MILLER, R. W. & SONG, Y. 2008. Advances in 4D medical imaging and 4D radiation therapy. *Technol Cancer Res Treat,* 7**,** 67-81.

LIN, Y. Y., CHEN, J. H., DING, H. J., LIANG, J. A., YEH, J. J. & KAO, C. H. 2012. Potential value of dual-time-point (1)(8)F-FDG PET compared with initial single-time-point imaging in differentiating malignant from benign pulmonary nodules: a systematic review and meta-analysis. *Nucl Med Commun,* 33**,** 1011-8.

LIU, C., PIERCE, L. A., 2ND, ALESSIO, A. M. & KINAHAN, P. E. 2009. The impact of respiratory motion on tumor quantification and delineation in static PET/CT imaging. *Phys Med Biol,* 54**,** 7345-62.

LUPI, A., ZAROCCOLO, M., SALGARELLO, M., MALFATTI, V. & ZANCO, P. 2009. The effect of 18F-FDG-PET/CT respiratory gating on detected metabolic activity in lung lesions. *Ann Nucl Med,* 23**,** 191-6.

MAC MANUS, M., HICKS, R. J. & EVERITT, S. 2006. Role of PET-CT in the optimization of thoracic radiotherapy. *J Thorac Oncol,* 1**,** 81-4.

MAC MANUS, M. P. 2010. Use of PET/CT for staging and radiation therapy planning in patients with non-small cell lung cancer. *Q J Nucl Med Mol Imaging,* 54**,** 510-20.

MAC MANUS, M. P., EVERITT, S., BAYNE, M., BALL, D., PLUMRIDGE, N., BINNS, D., HERSCHTAL, A., CRUICKSHANK, D., BRESSEL, M. & HICKS, R. J. 2013. The use of fused PET/CT images for patient selection and radical radiotherapy target volume definition in patients with non-small cell lung cancer: results of a prospective study with mature survival data. *Radiother Oncol,* 106**,** 292-8.

MAC MANUS, M. P., WADA, M., MATTHEWS, J. P. & BALL, D. L. 2000. Characteristics of 49 patients who survived for 5 years following radical radiation therapy for non-small cell lung cancer: the potential for cure. *Int J Radiat Oncol Biol Phys,* 46**,** 63-9.

MACMANUS, M., NESTLE, U., ROSENZWEIG, K. E., CARRIO, I., MESSA, C., BELOHLAVEK, O., DANNA, M., INOUE, T., DENIAUD-ALEXANDRE, E., SCHIPANI, S., WATANABE, N., DONDI, M. & JEREMIC, B. 2009. Use of PET and PET/CT for radiation therapy planning: IAEA expert report 2006-2007. *Radiother Oncol,* 91**,** 85-94.

MARTEL, M. K. 2004. Advanced radiation treatment planning and delivery approaches for treatment of lung cancer. *Hematol Oncol Clin North Am,* 18**,** 231-43.

MATHIAS, C. J. & GREEN, M. A. 2008. A convenient route to [68Ga]Ga-MAA for use as a particulate PET perfusion tracer. *Appl Radiat Isot,* 66**,** 1910-2.

MILESHKIN, L., HICKS, R. J., HUGHES, B. G., MITCHELL, P. L., CHARU, V., GITLITZ, B. J., MACFARLANE, D., SOLOMON, B., AMLER, L. C., YU, W., PIRZKALL, A. & FINE, B. M. 2011. Changes in 18F-Fluorodeoxyglucose and 18F-Fluorodeoxythymidine Positron Emission Tomography Imaging in Patients with Non-Small Cell Lung Cancer Treated with Erlotinib. *Clin Cancer Res,* 17**,** 3304-15.

MOLLER, D. S., KHALIL, A. A., KNAP, M. M., MUREN, L. P. & HOFFMANN, L. 2011. A planning study of radiotherapy dose escalation of PET-active tumour volumes in non-small cell lung cancer patients. *Acta Oncol,* 50**,** 883-8.

MOOREES, J. & BEZAK, E. 2012. Four dimensional CT imaging: a review of current technologies and modalities. *Australas Phys Eng Sci Med,* 35**,** 9-23.

NATH, S. K., SANDHU, A. P., JENSEN, L., KIM, D., BHARNE, A., NOBIENSKY, P. D., LAWSON, J. D., FUSTER, M. M., BAZHENOVA, L., SONG, W. Y. & MUNDT, A. J. 2011. Frameless image-guided stereotactic body radiation therapy for lung tumors with 4-dimensional computed tomography or 4-dimensional positron emission tomography/ computed tomography. *Clin Lung Cancer,* 12**,** 180-6.

NEHMEH, S. A. & ERDI, Y. E. 2008. Respiratory motion in positron emission tomography/computed tomography: a review. *Semin Nucl Med,* 38**,** 167-76.

NEHMEH, S. A., ERDI, Y. E., LING, C. C., ROSENZWEIG, K. E., SCHODER, H., LARSON, S. M., MACAPINLAC, H. A., SQUIRE, O. D. & HUMM, J. L. 2002. Effect of respiratory gating on quantifying PET images of lung cancer. *J Nucl Med,* 43**,** 876-81.

NEHMEH, S. A., ERDI, Y. E., MEIRELLES, G. S., SQUIRE, O., LARSON, S. M., HUMM, J. L. & SCHODER, H. 2007. Deep-inspiration breath-hold PET/CT of the thorax. *J Nucl Med,* 48**,** 22-6.

NEHMEH, S. A., ERDI, Y. E., PAN, T., PEVSNER, A., ROSENZWEIG, K. E., YORKE, E., MAGERAS, G. S., SCHODER, H., VERNON, P., SQUIRE, O., MOSTAFAVI, H., LARSON, S. M. & HUMM, J. L. 2004. Four-dimensional (4D) PET/CT imaging of the thorax. *Med Phys,* 31**,** 3179-86.

NYENG, T. B., KALLEHAUGE, J. F., HOYER, M., PETERSEN, J. B., POULSEN, P. R. & MUREN, L. P. 2011. Clinical validation of a 4D-CT based method for lung ventilation measurement in phantoms and patients. *Acta Oncol,* 50**,** 897-907.

OSMAN, M. M., COHADE, C., NAKAMOTO, Y. & WAHL, R. L. 2003. Respiratory motion artifacts on PET emission images obtained using CT attenuation correction on PET-CT. *Eur J Nucl Med Mol Imaging,* 30**,** 603-6.

OTANI, Y., FUKUDA, I., TSUKAMOTO, N., KUMAZAKI, Y., SEKINE, H., IMABAYASHI, E., KAWAGUCHI, O., NOSE, T., TESHIMA, T. & DOKIYA, T. 2010. A comparison of the respiratory signals acquired by different respiratory monitoring systems used in respiratory gated radiotherapy. *Med Phys,* 37**,** 6178-86.

PALMA, D. A., SENAN, S., TSUJINO, K., BARRIGER, R. B., RENGAN, R., MORENO, M., BRADLEY, J. D., KIM, T. H., RAMELLA, S., MARKS, L. B., DE PETRIS, L., STITT, L. & RODRIGUES, G. 2013. Predicting radiation pneumonitis after chemoradiation therapy for lung cancer: an international individual patient data meta-analysis. *Int J Radiat Oncol Biol Phys,* 85**,** 444-50.

PAN, T., MAWLAWI, O., NEHMEH, S. A., ERDI, Y. E., LUO, D., LIU, H. H., CASTILLO, R., MOHAN, R., LIAO, Z. & MACAPINLAC, H. A. 2005. Attenuation correction of PET images with respiration-averaged CT images in PET/CT. *J Nucl Med,* 46**,** 1481-7.

PARK, S. J., IONASCU, D., KILLORAN, J., MAMEDE, M., GERBAUDO, V. H., CHIN, L. & BERBECO, R. 2008. Evaluation of the combined effects of target size, respiratory motion and background activity on 3D and 4D PET/CT images. *Phys Med Biol,* 53**,** 3661-79.

PETERS, L. J., O'SULLIVAN, B., GIRALT, J., FITZGERALD, T. J., TROTTI, A., BERNIER, J., BOURHIS, J., YUEN, K., FISHER, R. & RISCHIN, D. 2010. Critical impact of radiotherapy protocol compliance and quality in the treatment of advanced head and neck cancer: results from TROG 02.02. *J Clin Oncol,* 28**,** 2996-3001.

PURDIE, T. G., MOSELEY, D. J., BISSONNETTE, J. P., SHARPE, M. B., FRANKS, K., BEZJAK, A. & JAFFRAY, D. A. 2006. Respiration correlated cone-beam computed tomography and 4DCT for evaluating target motion in Stereotactic Lung Radiation Therapy. *Acta Oncol,* 45**,** 915-22.

REINHARDT, M. J., WIETHOELTER, N., MATTHIES, A., JOE, A. Y., STRUNK, H., JAEGER, U. & BIERSACK, H. J. 2006. PET recognition of pulmonary metastases on PET/CT imaging: impact of attenuation-

corrected and non-attenuation-corrected PET images. *Eur J Nucl Med Mol Imaging,* 33**,** 134-9.

RIOU, O., SERRANO, B., AZRIA, D., PAULMIER, B., VILLENEUVE, R., FENOGLIETTO, P., ARTENIE, A., ORTHOLAN, C., FARAGGI, M. & THARIAT, J. 2014. Integrating respiratory-gated PET-based target volume delineation in liver SBRT planning, a pilot study. *Radiat Oncol,* 9**,** 127.

ROACH, P. J., GRADINSCAK, D. J., SCHEMBRI, G. P., BAILEY, E. A., WILLOWSON, K. P. & BAILEY, D. L. 2010. SPECT/CT in V/Q scanning. *Semin Nucl Med,* 40**,** 455-66.

ROSENZWEIG, K. E., HANLEY, J., MAH, D., MAGERAS, G., HUNT, M., TONER, S., BURMAN, C., LING, C. C., MYCHALCZAK, B., FUKS, Z. & LEIBEL, S. A. 2000. The deep inspiration breath-hold technique in the treatment of inoperable non-small-cell lung cancer. *Int J Radiat Oncol Biol Phys,* 48**,** 81-7.

ROSS, C. S., HUSSEY, D. H., PENNINGTON, E. C., STANFORD, W. & DOORNBOS, J. F. 1990. Analysis of movement of intrathoracic neoplasms using ultrafast computerized tomography. *Int J Radiat Oncol Biol Phys,* 18**,** 671-7.

SALHAB, K. F., BARAM, D. & BILFINGER, T. V. 2006. Growing PET positive nodule in a patient with histoplasmosis: case report. *J Cardiothorac Surg,* 1**,** 23.

SCHEENSTRA, A. E., ROSSI, M. M., BELDERBOS, J. S., DAMEN, E. M., LEBESQUE, J. V. & SONKE, J. J. 2013. Local dose-effect relations for lung perfusion post stereotactic body radiotherapy. *Radiother Oncol,* 107**,** 398-402.

SEPPENWOOLDE, Y., SHIRATO, H., KITAMURA, K., SHIMIZU, S., VAN HERK, M., LEBESQUE, J. V. & MIYASAKA, K. 2002. Precise and real-time measurement of 3D tumor motion in lung due to breathing and heartbeat, measured during radiotherapy. *Int J Radiat Oncol Biol Phys,* 53**,** 822-34.

SHI, X., MENG, X., SUN, X., XING, L. & YU, J. 2014. PET/CT imaging-guided dose painting in radiation therapy. *Cancer Lett,* 355**,** 169-75.

SHIELDS, A. F., GRIERSON, J. R., DOHMEN, B. M., MACHULLA, H. J., STAYANOFF, J. C., LAWHORN-CREWS, J. M., OBRADOVICH, J. E., MUZIK, O. & MANGNER, T. J. 1998. Imaging proliferation in vivo with [F-18]FLT and positron emission tomography. *Nat Med,* 4**,** 1334-6.

SIVA, S., CHESSON, B., CALLAHAN, J. W., HARDCASTLE, N., CRAWFORD, L., ANTIPPA, P., WRIGHT, G., MACMANUS, M. P.,

HICKS, R. J., KRON, T. & BALL, D. L. 2015a. Dosimetric Consequences of 3D Versus 4D PET/CT for Target Delineation of Lung Stereotactic Radiotherapy. *J Thorac Oncol,* 10**,** 1112-5.

SIVA, S., DEVEREUX, T., BALL, D. L., MACMANUS, M. P., HARDCASTLE, N., KRON, T., BRESSEL, M., FOROUDI, F., PLUMRIDGE, N., STEINFORT, D., SHAW, M., CALLAHAN, J., HICKS, R. J. & HOFMAN, M. S. 2015b. Ga-68 MAA Perfusion 4D-PET/CT Scanning Allows for Functional Lung Avoidance Using Conformal Radiation Therapy Planning. *Technol Cancer Res Treat*.

SIVA, S., HARDCASTLE, N., KRON, T., BRESSEL, M., CALLAHAN, J., MACMANUS, M., SHAW, M., PLUMRIDGE, N., HICKS, R., STENFORT, D., BALL, D. & HOFMAN, M. 2015c. Ventilation/Perfusion (VQ) PET based assessment of radiation injury to lung. *International Journal of Radiation Oncology*Biology*Physics*.

SIVA, S., THOMAS, R., CALLAHAN, J., HARDCASTLE, N., PHAM, D., KRON, T., HICKS, R. J., MACMANUS, M. P., BALL, D. L. & HOFMAN, M. S. 2015d. High-resolution pulmonary ventilation and perfusion PET/CT allows for functionally adapted intensity modulated radiotherapy in lung cancer. *Radiother Oncol,* 115**,** 157-62.

SLOTMAN, B. J., LAGERWAARD, F. J. & SENAN, S. 2006. 4D imaging for target definition in stereotactic radiotherapy for lung cancer. *Acta Oncol,* 45**,** 966-72.

STELZMUELLER, I., HUBER, H., WUNN, R., HODOLIC, M., MANDL, M., LAMPRECHT, B., SCHINKO, H., FELLNER, F., SKANJETI, A., GIAMMARILE, F., COLLETTI, P. M., RUBELLO, D. & GABRIEL, M. 2015. 18F-FDG PET/CT in the Initial Assessment and for Follow-up in Patients With Tuberculosis. *Clin Nucl Med*.

STOELBEN, E. & LUDWIG, C. 2009. Chest wall resection for lung cancer: indications and techniques. *Eur J Cardiothorac Surg,* 35**,** 450-6.

SUGA, K., YASUHIKO, K., ZAKI, M., YAMASHITA, T., SETO, A., MATSUMOTO, T. & MATSUNAGA, N. 2004. Assessment of regional lung functional impairment with co-registered respiratory-gated ventilation/perfusion SPET-CT images: initial experiences. *Eur J Nucl Med Mol Imaging,* 31**,** 240-9.

SURA, S., GRECO, C., GELBLUM, D., YORKE, E. D., JACKSON, A. & ROSENZWEIG, K. E. 2008. (18)F-fluorodeoxyglucose positron emission tomography-based assessment of local failure patterns in non-small-cell lung cancer treated with definitive radiotherapy. *Int J Radiat Oncol Biol Phys,* 70**,** 1397-402.

TEO, B. K., SABOURY, B., MUNBODH, R., SCHEUERMANN, J., TORIGIAN, D. A., ZAIDI, H. & ALAVI, A. 2012. The effect of breathing irregularities on quantitative accuracy of respiratory gated PETCT. *Med Phys,* 39**,** 7390-7.

TER-POGOSSIAN, M. M., PHELPS, M. E., HOFFMAN, E. J. & MULLANI, N. A. 1975. A positron-emission transaxial tomograph for nuclear imaging (PETT). *Radiology,* 114**,** 89-98.

TEWSON, T. J., WELCH, M. J. & RAICHLE, M. E. 1978. [18F]-labeled 3-deoxy-3-fluoro-D-glucose: synthesis and preliminary biodistribution data. *J Nucl Med,* 19**,** 1339-45.

VAN ELMPT, W., DE RUYSSCHER, D., VAN DER SALM, A., LAKEMAN, A., VAN DER STOEP, J., EMANS, D., DAMEN, E., OLLERS, M., SONKE, J. J. & BELDERBOS, J. 2012. The PET-boost randomised phase II dose-escalation trial in non-small cell lung cancer. *Radiother Oncol,* 104**,** 67-71.

VICENTE, A. M., CASTREJON, A. S., MUNOZ, A. P., WOLL, P. P. & GARCIA, A. N. 2010. Impact of 18F-FDG PET/CT with retrograde filling of the urinary bladder in patients with suspected pelvic malignancies. *J Nucl Med Technol,* 38**,** 128-37.

WAGNER, H. N., JR., SABISTON, D. C., JR., IIO, M., MCAFEE, J. G., MEYER, J. K. & LANGAN, J. K. 1964. Regional Pulmonary Blood Flow in Man by Radioisotope Scanning. *JAMA,* 187**,** 601-3.

WANG, Y., BAO, Y., ZHANG, L., FAN, W., HE, H., SUN, Z. W., HU, X., HUANG, S. M., CHEN, M. & DENG, X. W. 2013. Assessment of respiration-induced motion and its impact on treatment outcome for lung cancer. *Biomed Res Int,* 2013**,** 872739.

WANG, Y. C., HSIEH, T. C., YU, C. Y., YEN, K. Y., CHEN, S. W., YANG, S. N., CHIEN, C. R., HSU, S. M., PAN, T., KAO, C. H. & LIANG, J. A. 2012. The clinical application of 4D 18F-FDG PET/CT on gross tumor volume delineation for radiotherapy planning in esophageal squamous cell cancer. *J Radiat Res,* 53**,** 594-600.

WARBURG O, P. K., NEGELEIN E. 1924. Uber den stoff-wechsel der carcinomzelle. *Biochem Zeitschrift,* 152**,** 302-35.

WERNER, M. K., PARKER, J. A., KOLODNY, G. M., ENGLISH, J. R. & PALMER, M. R. 2009. Respiratory gating enhances imaging of pulmonary nodules and measurement of tracer uptake in FDG PET/CT. *AJR Am J Roentgenol,* 193**,** 1640-5.

WESTER, H. J., HERZ, M., WEBER, W., HEISS, P., SENEKOWITSCH-SCHMIDTKE, R., SCHWAIGER, M. & STOCKLIN, G. 1999. Synthesis

and radiopharmacology of O-(2-[18F]fluoroethyl)-L-tyrosine for tumor imaging. *J Nucl Med,* 40**,** 205-12.

WOLTHAUS, J. W., VAN HERK, M., MULLER, S. H., BELDERBOS, J. S., LEBESQUE, J. V., DE BOIS, J. A., ROSSI, M. M. & DAMEN, E. M. 2005. Fusion of respiration-correlated PET and CT scans: correlated lung tumour motion in anatomical and functional scans. *Phys Med Biol,* 50**,** 1569-83.

YAKOUMAKIS, N., WINEY, B., KILLORAN, J., MAYO, C., NIEDERMAYR, T., PANAYIOTAKIS, G., LINGOS, T. & COURT, L. 2012. Using four-dimensional computed tomography images to optimize the internal target volume when using volume-modulated arc therapy to treat moving targets. *J Appl Clin Med Phys,* 13**,** 3850.

YAMAMOTO, T., KABUS, S., VON BERG, J., LORENZ, C. & KEALL, P. J. 2011. Impact of four-dimensional computed tomography pulmonary ventilation imaging-based functional avoidance for lung cancer radiotherapy. *Int J Radiat Oncol Biol Phys,* 79**,** 279-88.

YANG, D. J., WALLACE, S., CHERIF, A., LI, C., GRETZER, M. B., KIM, E. E. & PODOLOFF, D. A. 1995. Development of F-18-labeled fluoroerythronitroimidazole as a PET agent for imaging tumor hypoxia. *Radiology,* 194**,** 795-800.

YANG, J., YAMAMOTO, T., CHO, B., SEO, Y. & KEALL, P. J. 2012. The impact of audio-visual biofeedback on 4D PET images: results of a phantom study. *Med Phys,* 39**,** 1046-57.

YIP, S., MCCALL, K., ARISTOPHANOUS, M., CHEN, A. B., AERTS, H. J. & BERBECO, R. 2014. Comparison of texture features derived from static and respiratory-gated PET images in non-small cell lung cancer. *PLoS One,* 9**,** e115510.

YORKE, E. D., JACKSON, A., ROSENZWEIG, K. E., MERRICK, S. A., GABRYS, D., VENKATRAMAN, E. S., BURMAN, C. M., LEIBEL, S. A. & LING, C. C. 2002. Dose-volume factors contributing to the incidence of radiation pneumonitis in non-small-cell lung cancer patients treated with three-dimensional conformal radiation therapy. *Int J Radiat Oncol Biol Phys,* 54**,** 329-39.

YOUNG, H., BAUM, R., CREMERIUS, U., HERHOLZ, K., HOEKSTRA, O., LAMMERTSMA, A. A., PRUIM, J. & PRICE, P. 1999. Measurement of clinical and subclinical tumour response using [18F]-fluorodeoxyglucose and positron emission tomography: review and 1999 EORTC recommendations. European Organization for Research and Treatment of Cancer (EORTC) PET Study Group. *Eur J Cancer,* 35**,** 1773-82.

ZHAN, P., XIE, H., XU, C., HAO, K., HOU, Z. & SONG, Y. 2013. Management strategy of solitary pulmonary nodules. *J Thorac Dis,* 5**,** 824-829.

ZHANG, H. Q., YU, J. M., MENG, X., YUE, J. B., FENG, R. & MA, L. 2011. Prognostic value of serial [18F]fluorodeoxyglucose PET-CT uptake in stage III patients with non-small cell lung cancer treated by concurrent chemoradiotherapy. *Eur J Radiol,* 77**,** 92-6.

ZHANG, J., MA, J., ZHOU, S., HUBBS, J. L., WONG, T. Z., FOLZ, R. J., EVANS, E. S., JASZCZAK, R. J., CLOUGH, R. & MARKS, L. B. 2010. Radiation-induced reductions in regional lung perfusion: 0.1-12 year data from a prospective clinical study. *Int J Radiat Oncol Biol Phys,* 76**,** 425-32.

CHAPTER 10 - APPENDICES

10.1 PUBLISHED ABSTRACTS AND CONFERENCE PRESENTATIONS

The following is a list of publications and presentation giving arising from work presented in this thesis.

PUBLICATIONS

Callahan J, Kron T, Schneider-Kolsky M, Hicks RJ: **The clinical significance and management of lesion motion due to respiration during PET/CT scanning**. *Cancer Imaging* 2011, **11**:224-236.

Callahan J, Binns D, Dunn L, Kron T: **Motion effects on SUV and lesion volume in 3D and 4D PET scanning**. *Australas Phys Eng Sci Med* 2011, **34**(4):489-495.

Callahan J, Kron T, Schneider-Kolsky M, Dunn L, Thompson M, Siva S, Aarons Y, Binns D, Hicks RJ: **Validation of a 4D-PET Maximum Intensity Projection for Delineation of an Internal Target Volume**. *Int J Radiat Oncol Biol Phys* 2013.

Callahan J, Kron T, Siva S, Simoens N, Edgar A, Everitt S, Schneider ME, Hicks RJ: **Geographic miss of lung tumours due to respiratory motion: a comparison of 3D vs 4D PET/CT defined target volumes**. *Radiat Oncol* 2014, **9**(1):291.

Callahan J, Kron T, Schneider ME, Hicks RJ: **A prospective investigation into the clinical impact of 4D-PET/CT in the characterisation of solitary pulmonary nodules**. *Cancer Imaging* 2014, **14**(1):24.

Callahan J, Hofman MS, Siva S, Kron T, Schneider ME, Binns D, Eu P, Hicks RJ: **High-resolution imaging of pulmonary ventilation and perfusion with 68Ga-VQ respiratory gated (4-D) PET/CT**. *Eur J Nucl Med Mol Imaging* 2014, **41**(2):343-349.

PRESENTATIONS 2011-2015

2011

- **Management of Respiratory motion in PET/CT** – APSEM Annual scientific meeting, Darwin, August (invited Speaker)
- **4D PET/CT in Radiotherapy** – William Buckland Radiotherapy centre monthly scientific meeting, Alfred Hospital, Melbourne, April (invited Speaker)
- **4D PET/CT workshop** – Nuclear Medicine Monthly Scientific meeting, Peter MacCallum Cancer Centre, October
- **Emerging Pet Technologies –** VSNM Annual day Seminar, Royce Hotel, Melbourne, October (invited Speaker)

2012

- **20 years of PET in Australia: Present perspectives** – ANSZNM Annual Scientific meeting Technologist symposium, Melbourne convention Centre, Melbourne April (invited Speaker)
- **Management of Respiratory motion in PET/CT –** Radiotherapy monthly Scientific meeting, Peter MacCallum Cancer Centre, Melbourne, February (invited Speaker)
- **4D PET/CT MIP for delineation of RT target volumes –** Radiotherapy Technical implementation group, Peter MacCallum Cancer Centre, Melbourne, June (invited Speaker)
- **Clinical indication for 4D-PET/CT** – Translational Research Lab, Peter MacCallum Cancer Centre, Melbourne, July (invited Speaker)
- **Respiratory Gating in PET –** RAINS annual workshop, Sydney, October (invited Speaker)
- **Technical and Practical considerations of Gallium-68 Ventilation and Perfusion (VQ) 4D-PET/CT in radiation oncology** – Molecular Imaging in Radiation Oncology Meeting, Vienna, Austria, April (Poster presentation)

2013

- **RT Planning and 4D PET/CT** – International conference on computing in radiotherapy, Melbourne convention Centre, Melbourne, May (invited Speaker)
- **Research in PET –** RAINS annual workshop, Sydney, July (invited Speaker)
- **Research in PET and PhD in Nuclear Medicine** – Nuclear Medicine Intern Workshop, St Vincent's hospital, Melbourne, September (invited Speaker)

- **Clinical Indications for 4D-PET/CT** – Post Graduate Research Seminar, Monash University, Melbourne, November
- **Advances in PET/CT** – 3rd Year Nuclear Medicine, RMIT University, May (guest Lecturer)

2014

- **A prospective investigation into the clinical impact of 4D-PET/CT in the characterisation of SPNs** – Post Graduate Research Seminar, Monash University, Melbourne, August
- **Technical perspectives on PET in radiotherapy planning** – Annual combine scientific meeting, Melbourne convention Centre, Melbourne, September (invited Speaker)
- **Research in PET and PhD in Nuclear Medicine** – Nuclear Medicine Intern Workshop, St Vincent's hospital, Melbourne, October (invited Speaker)

2015

- **Radiotherapy PET at PeterMac including 4D-PET/CT** – ANZSNM Physics SIG, University of Sydney, Sydney, February (invited Speaker)
- **Advances in PET/CT** – 3rd Year Nuclear Medicine, RMIT University, May (guest Lecturer)
- **Research in PET and PhD in Nuclear Medicine** – Nuclear Medicine Intern Workshop, St Vincent's hospital, Melbourne, September (invited Speaker)

10.2 APPENDIX 1: DECLARATION FOR THESIS

Declaration for Thesis Chapter 2

Declaration by candidate

In the case of Chapter 2, the nature and extent of my contribution to the work was the following:

Nature of contribution	Extent of contribution (%)
The clinical significance and management of lesion motion due to respiration during PET/CT scanning.	80% of concept and 90% of manuscript writing

The following co-authors contributed to the work. If co-authors are students at Monash University, the extent of their contribution in percentage terms must be stated:

Name	Nature of contribution	Extent of contribution (%) for student co-authors only
Tomas Kron	Concept and Manuscript Writing	
Michal Schneider-Kolsky	Concept and Manuscript Writing	
Rodney J Hicks	Concept and Manuscript Writing	

The undersigned hereby certify that the above declaration correctly reflects the nature and extent of the candidate's and co-authors' contributions to this work*.

Candidate's Signature		**Date**
Main Supervisor's Signature		**Date**

*Note: Where the responsible author is not the candidate's main supervisor, the main supervisor should consult with the responsible author to agree on the respective contributions of the authors.

Declaration for Thesis Chapter 3

Declaration by candidate
In the case of Chapter 3, the nature and extent of my contribution to the work was the following:

Nature of contribution	**Extent of contribution (%)**
A prospective investigation into the clinical impact of 4D-PET/CT in the characterisation of solitary pulmonary nodules	90% of concept, design, data interpretation and manuscript writing, 100% of study conduct, data generation and data collection

The following co-authors contributed to the work. If co-authors are students at Monash University, the extent of their contribution in percentage terms must be stated:

Name	**Nature of contribution**	**Extent of contribution (%) for student co-authors only**
Tomas Kron	Concept and Manuscript Writing	
Michal Schneider-Kolsky	Concept and Manuscript Writing	
Rodney J Hicks	Concept and Manuscript Writing	

The undersigned hereby certify that the above declaration correctly reflects the nature and extent of the candidate's and co-authors' contributions to this work*.

Candidate's Signature		**Date**
Main Supervisor's Signature		**Date**

*Note: Where the responsible author is not the candidate's main supervisor, the main supervisor should consult with the responsible author to agree on the respective contributions of the authors.

Declaration for Thesis Chapter 4

Declaration by candidate
In the case of Chapter 4, the nature and extent of my contribution to the work was the following:

Nature of contribution	Extent of contribution (%)
Validation of a 4D-PET Maximum intensity projection for delineation of an internal target volume.	90% of concept, design, data interpretation and manuscript writing, 100% of study conduct, data generation and data collection

The following co-authors contributed to the work. If co-authors are students at Monash University, the extent of their contribution in percentage terms must be stated:

Name	Nature of contribution	Extent of contribution (%) for student co-authors only
Tomas Kron	Concept and Manuscript Writing	
Michal Schneider-Kolsky	Concept and Manuscript Writing	
Leon Dunn	Study conduct	
Michael Thompson	Concept and Analysis	
Siva Shankar	Concept and Manuscript Writing	
Yolanda Aarons	Concept and Study Conduct	
David Binns	Concept and Analysis	
Rodney J Hicks	Concept and Manuscript Writing	

The undersigned hereby certify that the above declaration correctly reflects the nature and extent of the candidate's and co-authors' contributions to this work*.

Candidate's Signature		**Date**
Main Supervisor's Signature		**Date**

*Note: Where the responsible author is not the candidate's main supervisor, the main supervisor should consult with the responsible author to agree on the respective contributions of the authors.

Declaration for Thesis Chapter 5

Declaration by candidate

In the case of Chapter 5, the nature and extent of my contribution to the work was the following:

Nature of contribution	Extent of contribution (%)
Geographic miss of lung tumour due to respiratory motion: a comparison of 3D vs 4D PET/CT defined target volumes	90% of concept, design, data interpretation and manuscript writing, 100% of study conduct, data generation and data collection

The following co-authors contributed to the work. If co-authors are students at Monash University, the extent of their contribution in percentage terms must be stated:

Name	Nature of contribution	Extent of contribution (%) for student co-authors only
Tomas Kron	Concept and Manuscript Writing	
Michal Schneider-Kolsky	Concept and Manuscript Writing	
Siva Shankar	Concept and Manuscript Writing	
Nathalie Simoens	Study Conduct and Analysis	
Amanda Edger	Study Conduct and Analysis	
Sarah Everitt	Concept	
Rodney J Hicks	Concept and Manuscript Writing	

The undersigned hereby certify that the above declaration correctly reflects the nature and extent of the candidate's and co-authors' contributions to this work*.

Candidate's Signature		**Date**
Main Supervisor's Signature		**Date**

*Note: Where the responsible author is not the candidate's main supervisor, the main supervisor should consult with the responsible author to agree on the respective contributions of the authors.

Declaration for Thesis Chapter 6

Declaration by candidate
In the case of Chapter 6, the nature and extent of my contribution to the work was the following:

Nature of contribution	**Extent of contribution (%)**
High resolution imaging of pulmonary ventilation and perfusion with 68Ga-VQ respiratory gated (4-D) PET/CT	90% of concept, design, data interpretation and, data generation and data collection 80% of study conduct and manuscript writing

The following co-authors contributed to the work. If co-authors are students at Monash University, the extent of their contribution in percentage terms must be stated:

Name	**Nature of contribution**	**Extent of contribution (%) for student co-authors only**
Michael Hofman	Study Conduct, Concept and Manuscript Writing	
Siva Shankar	Study Conduct, Concept and Manuscript Writing	
Tomas Kron	Concept and Manuscript Writing	
Michal Schneider	Concept and Manuscript Writing	
David Binns	Study Conduct and Analysis	
Peter Eu	Study Conduct and Manuscript Writing	
Rodney J Hicks	Concept and Manuscript Writing	

The undersigned hereby certify that the above declaration correctly reflects the nature and extent of the candidate's and co-authors' contributions to this work*.

Candidate's Signature		**Date**

Main Supervisor's Signature		**Date**

*Note: Where the responsible author is not the candidate's main supervisor, the main supervisor should consult with the responsible author to agree on the respective contributions of the authors.

10.3 APPENDIX 2: APPROVAL TO CONDUCT STUDY REPORTED IN CHAPTER 4

Peter MacCallum Cancer Centre
Ethics Committee Secretariat
Level 4, #10 St Andrews Place
East Melbourne Victoria
[redacted]
Postal Address:
Locked Bag 1 A'Beckett Street
Victoria 8006 Australia

PETER MACCALLUM CANCER CENTRE AUTHORISATION TO CONDUCT A RESEARCH PROJECT

Peter Mac Project No: 10/102

Project Title:
A pilot study to investigate the impact of respiratory gated PET scanning in patients with solitary pulmonary nodules

Principal Investigator: Mr Jason Callahan

Approval Date: 22 November 2010 **Approval Expiry:** 22 November 2015

I am pleased to advise that the above project has received ethical approval and satisfies Peter Mac research governance requirements and may now be conducted at Peter MacCallum Cancer Centre. Conduct of the project is subject to compliance with the conditions set out below.

Approved Documents:

- *Protocol version 3.0, dated 22 November 2010*
- *Participant Information and Consent Form version 3, dated 22 November 2010*

In order to comply with the National Statement on Ethical Conduct in Human Research (2007), Guidelines for Good Clinical Research Practice and local research policies and guidelines, you are required to notify the Peter MacCallum Cancer Centre Ethics Committee Secretariat of:

- The actual start date of the project at Peter MacCallum Cancer Centre;
- Any amendments to the project after these have been approved by the reviewing HREC;
- Any adverse events involving patients of Peter MacCallum Cancer Centre, in accordance with the Peter MacCallum Cancer Centre Guidelines for Safety Reporting.
- Any unexpected developments in the project with ethical implications;
- Your inability to continue as Principal Investigator and any other change in research personnel involved in the project at Peter MacCallum Cancer Centre;
- Any proposed extension to the duration of the project, past the above stated approval date;

- Any decision taken to end the project prior to the expected date of completion or of withdrawal of Peter MacCallum Cancer Centre as a site participating in the project.

You are also required to submit to the Ethics Committee Secretariat:

- An Annual Progress Report every 12 months for the duration of the project. This report is due on the anniversary of HREC approval. *Note: Continuation of ethics approval is contingent on submission of an annual report in a timely manner;;* and
- A comprehensive Final Report upon completion of the project.

MONASH University

Monash University Human Research Ethics Committee (MUHREC)
Research Office

Human Ethics Certificate of Approval

Date:	**7 December 2010**
Project Number:	**2010001755**
Project Title:	**Respiratory gated PET scanning in solitary pulmonary nodules**
Chief Investigator:	**Dr Michal Schneider-Kolsky**
Approved:	**From: 7 December 2010 To: 7 December 2015**

Terms of approval

1. The Chief investigator is responsible for ensuring that permission letters are obtained, if relevant, and a copy forwarded to MUHREC before any data collection can occur at the specified organisation. **Failure to provide permission letters to MUHREC before data collection commences is in breach of the National Statement on Ethical Conduct in Human Research and the Australian Code for the Responsible Conduct of Research.**
2. Approval is only valid whilst you hold a position at Monash University.
3. It is the responsibility of the Chief Investigator to ensure that all investigators are aware of the terms of approval and to ensure the project is conducted as approved by MUHREC.
4. You should notify MUHREC immediately of any serious or unexpected adverse effects on participants or unforeseen events affecting the ethical acceptability of the project.
5. **Complaints:** The researchers are required to inform MUHREC promptly of any complaints made about the project, whether the complaint was made directly to a member of the research team or to the primary HREC.
6. **Amendments to the approved project (including changes in personnel):** Requires the submission of a Request for Amendment form to MUHREC and must not begin without written approval from MUHREC. Substantial variations may require a new application.
7. **Future correspondence:** Please quote the project number and project title above in any further correspondence.
8. **Annual reports:** Continued approval of this project is dependent on the submission of an Annual Report. This is determined by the date of your letter of approval.
9. **Final report:** A Final Report should be provided at the conclusion of the project. MUHREC should be notified if the project is discontinued before the expected date of completion.
10. **Monitoring:** Projects may be subject to an audit or any other form of monitoring by MUHREC at any time.
11. **Retention and storage of data:** The Chief Investigator is responsible for the storage and retention of original data pertaining to a project for a minimum period of five years.

[redacted]

Professor Ben Canny
Chair, MUHREC

cc: Mr Jason Callahan

Postal – Monash University, Vic 3800, Australia
Building 3E, Room 111, Clayton Campus, Wellington Road, Clayton
[redacted] www.monash.edu/research/ethics/human/index/html
ABN 12 377 614 012 CRICOS Provider #00008C